UNIVERSITÀ
DEGLI STUDI
DI PADOVA

Sede Amministrativa: Università degli Studi di Padova

Dipartimento di BIOLOGIA

SCUOLA DI DOTTORATO DI RICERCA IN : BIOTECNOLOGIE E BIOSCIENZE

INDIRIZZO: BIOTECNOLOGIE

CICLO: XXIV

STRUCTURAL AND FUNCTIONAL STUDIES ON HUMAN DNA TOPOISOMERASE IB: INTERATION WITH SUPERCOILED DNA AND THE ANTITUMOUR DRUG CAMPTOTHECIN

Direttore della Scuola : Ch.mo Prof. GIUSEPPE ZANOTTI

Coordinatore d'indirizzo: Ch.mo Prof. GIORGIO VALLE

Supervisore :Ch.mo Prof. PIETRO BENEDETTI

Dottorando : STEFANIA RODIO

ABSTRACT

DNA Topoisomerases are essentials enzymes in biological process involving the relaxation of the superhelical tension of the DNA molecules. Human DNA topoisomerase I (hTop1p) is a monomeric conserved enzyme of 91 KDa, subdivided into four domains: the N-terminal; the core constituted by three subdomains; the C-terminal domain containing the catalytic residue Tyr723; the linker connecting the core with the C-terminal domain, locating the active site in the catalytic pocket, and characterized by two protruding coiled coil α-helices. DNA relaxation occured with a mechanism of DNA strand rotation in a multiple step process where the 5'-OH end is free to rotate around the intact strand. Two conformational changes are involved in this dynamic process: the enzyme binding the DNA through an open shape, then closed clamp that completely embraces the DNA. No external energy source occurred, but arises from the release of the superhelical tension. In addition hTop1p is of great interest since is the cellular target of the antitumor drug camptothecin (CPT). The reversible binding of the drug to the covalent complex DNA-Top1p brings to lethality due to religation inhibition and double strand breaks formation in a S-phase dependent manner. Different data supported the "controll rotation mechanism" to explain how this enzyme can relax both positevely and negatevely supercoiled substrates. First of all crystal structures [17] of human Top1 with a 22 bp oligonucleotide reported no sufficient space inside the clamp for a free rotation. Moreover a mutant isoform of the protein with 2 cysteines produced opposetely to the lips domains, locked the clamp through a disulfide bridge and reported that an opening conformation was not required for the relaxation activity [21] [135]. Also single-molecule experiments suggested that friction and torque are necessary for the relaxation process and the number of supercoils removed per cleavage-religation cycle is strictly dependent from the number of supercoils of the DNA substrate. The aim of this project is focused on the contribute of key residues located al the level of the *hinge* and involved in the control rotation mechanism during DNA relaxation. In my experiments *Saccharomyces cerevisiae* strains were used as a model organism to investigate a series of topoisomerase IB mutants:

Pro431Gly; Arg434Ala; Arg434Cys; Trp205Cys. These substitutions are interesting because of their position in the enzyme three-dimensional structure. The flexible *hinge* (429-436 residues) facilitating clamp opening by a stretching or bending motion pivoting around Pro-431 and the cluster of large aromatic residues around the top of the *hinge,* probably are involved in controlling the movements of the α-helix and the proper closing of the clamp. In 2005 Sari and Andricioaei simulation analyses reported the possible role of the *lips* for the relaxation of the positive supercoils and the strechting of the *hinge* for the negative supercoils removal. Yeast strains lacking for endogenous topoisomerase I gene were transformed with YCpGAL1-hTOP1, YCpGAL1-hTOP1Pro431Gly, YCpGAL1-hTOP1Arg434Cys, YCpGAL1-hTOP1Arg434Ala, YCpGAL1-hTOP1Trp205Cys plasmids and viability was verified in a drug yeast sensitivity assay. Transformants were spotted in presence and absence of camptothecin at different concentrations. Moreover CPT sensitivity for each mutant was analyzed through measures of the stability of the covalent complex formation. Results are congruents and are also supported by Frohlich and Knudsen data, in 2007, suggesting a role for the Trp-205 and surrounding residues in the control of strand rotation during negative but not positive supercoiled removal, and reported a more CPT sensitivity during relaxation of positively versus negatevely supercoils. EKY3 strains expressing *htop*1W205Cp showed a partial resistance phenotype, and *top1*R434A, *top1*R434C mutants are not sensitive to lower drug dose (0.01<ug/ml<0.5). Processivity and distributivity of the catalytic activity for purified proteins was also tested at low (50mM), optimal (150mM) and high (500 and 1000 mM) salt concentration with both negative and positive supercoils. This allowed revealing mutant behaviors and its DNA affinity under stressed non-physiological conditions. The *top1*R434A mutant showed an interesting relaxation activity also in presence of high salt concentration up to 1000 mM KCl and reported a faster ability in realeasing positevely than negatevely supercoiled if compared to the wild-type and other mutants. The association/dissociation is rate limiting for DNA relaxation but the mutation R434 showed residue a stronger affinity for DNA. This data was obtained by the ability of the mutant to relax two topologically

different DNAs in a two step relaxation experiment. Dynamic modeling simulation analyses for the *top1*R434A mutant in comparison with the WT enzyme was performed to better understand the real contribute of the protein domains in the mechanism of supercoils relaxation.

RIASSUNTO

Le DNA topoisomerasi sono enzimi essenziali in tutti i processi biologici in cui è necessario un riarrangiamento topologico della doppia elica. La DNA topoisomerasi IB umana (hTop1p) è una proteina monomerica di 91KDa, caratterizzata da 4 domini: uno N-terminale; uno "core" costituito a sua volta da 3 subdomini; un C-terminale contenente il residuo catalitico in posizione Tyr723 e una regione linker costituita da 2 α-eliche sporgenti e che connette il dominio core con il C-terminale. Il meccanismo di rilassamento del DNA è un processo multiplo attraverso il quale un filamento di DNA con un'estremità libera al 5'-OH è in grado di ruotare intorno a quello rimasto intatto. L'enzima lega la doppia elica dapprima assumendo una conformazione aperta, e successivamente si richiude attorno al substrato, in questo modo l'energia necessaria per la reazione di topoisomerizzazione è fornita dallo srotolamento della superelica e il rilascio di energia torsionale. hTop1p è anche target specifico di un farmaco antitumorale noto come camptotecina (CPT). Il legame reversibile tra CPT e il complesso DNA-enzima è dipendente dalla fase S del ciclo cellulare e porta ad apoptosi in seguito all'inibizione della fase di riligazione e alla formazione di frammenti a doppio filamento (noti come DSBs *double strand breaks).* Il meccanismo che spiega come questo enzima sia in grado di rilassare sia superavvolgimenti positivi che negativi è definito "meccanismo di controllo della rotazione" e vi sono diversi dati a suo supporto. La struttura cristallografica della hTop1p in complesso con un frammento di DNA di 22pb, ottenuta nel 1998 da Stewart e i suoi collaboratori ha evidenziato che non vi è spazio sufficiente per una rotazione libera all'interno della "tasca enzimatica". Inoltre mediante un mutante della hTop1p con 2 residui terminali delle regioni delle *"lips"* sostituiti da 2 cisteine in modo da ottenere un ponte disolfuro, è stato possibile bloccare l'enzima nella conformazione chiusa e dimostrare comunque l'attività di rilassamento da parte della proteina [21] [135]. Vi sono inoltre esperimenti di "single-molecule" che evidenziano come il numero di superavvolgimenti rimossi per ciclo di taglio e riligazione sia direttamente proporzionale al numero di avvolgimenti del DNA substrato e che durante la topoisomerizzazione si registrano attriti e forze rotatorie

derivanti dal meccanismo di rotazione del DNA durante il suo rilassamento. Lo scopo di questo progetto di ricerca verte sull'indagine di residui chiave localizzati nella regione *hinge* (residui 429-436) e coinvolti in tale meccanismo. Negli esperimenti è stato utilizzato l'organismo modello *Saccharomyces cerevisiae*, nel quale sono state introdotte le seguenti mutazioni: Pro431Gly; Arg434Ala; Arg434Cys; Trp205Cys. Tali sostituzioni risultano di grande interesse per quanto concerne la struttura tridimensionale: il residuo 431 caratterizzato da una prolina si è ipotizzato essere coinvolto in movimenti flessori e di stretching dell'*hinge* attraverso cui l'enzima medierebbe l'apertura/chiusura e l'interazione con i residui aromatici situati nel suo intorno. Sari e Andricioaei nel 2005 attraverso studi di dinamica molecolare evidenziarono il contributo della regione delle *lips* nel rilassamento dei superavvolgimenti positivi, mentre riportarono uno stretching dell'*hinge* per quelli negativi. Dapprima sono stati utilizzati ceppi di lievito deleti della topoisomerasi I endogena per trasfettare i plasmidi con all'interno la sequenza di espressione per la hTop1p mutata ed è stata analizzata la capacità di formare colonie nonché la loro vitalità in presenza di camptotecina a diverse concentrazioni. La sensibilità al farmaco è stata inoltre analizzata mediante saggio di equilibrio taglio-riligazione e valutando la formazione dei complessi di taglio per ciascun mutante in presenza e assenza di camptotecina. I risultati si sono rivelati congruenti con quanto già riportato nel 2007 dal laboratorio di Knudsen, secondo cui il residuo Trp205 e l'intorno aromatico regolano il meccanismo di rotazione durante il rilassamento di superavvolgimenti negativi e riportando una maggior sensibilità al farmaco durante la rimozione di substrati positivi piuttosto che del segno opposto. Il mutante *htop1*W205Cp nei miei esperimenti ha mostrato un fenotipo parzialmente resistente mentre per i mutanti *top1*R434A e *top1*R434C si è riportata una maggior sensibilità e capacità di formare colonie a dosi inferiori a 0.5ug/ml. Per ciascuna proteina è stata misurata la sua attività catalitica nel rilassare superavvolgimenti positivi e negativi, in condizioni di processività e distributività a forza ionica bassa (50 mM), a 150 mM (condizione ottimale) e a forza ionica elevata (500 mM e 1000 mM). In questo modo è stato possibile valutare l'affinità di legame di

ciascun mutante per il DNA ed evidenziare aspetti biochimici funzionali legati alla mutazione specifica. Per quanto riguarda il mutante *top1*R434A è stata riportata attività catalitica ad alte concentrazioni saline, fino a 1000 mM KCl, ed è stata misurata una velocità maggiore nel rilassare substrati positivi piuttosto che negativi, e in ogni caso più performanti sia rispetto l'enzima wild type che gli altri mutanti. La sostituzione dell'arginina (R434) con un'alanina ha migliorato l'affinità di legame per il DNA dell'enzima e questo è stato ancor più evidenziato da saggi di rilassamento in cui *top1*R434A mostrava capacità di rilassamento, a basse e alte forze ioniche, di due DNA topologicamente diversi, ma contemporaneamente presenti nella miscela di reazione. L'enzima è perciò in grado di staccarsi e riassociarsi ad una nuova molecola di DNA. Inoltre tramite analisi di modelling molecolare è stato possibile indagare il contributo reale dei diversi domini della proteina wild type a confronto con quella mutata nel residuo R434, durante il processo di topoisomerizzazione.

CONTENTS

1. INTRODUCTION

1.1 DNA TOPOLOGY

DNA in all organisms is well described in a supercoiled state. Supercoiling literally means the coiling of a coil, imaging an axis as a line down the center of the molecule between helical curves of the two strands, so refering to the coiling of the axis of the double helix in space [1].

DNA metabolism such as DNA synthesis, recombination and transcription generates torsional stress resulting in a underwinding or overwinding of the double helix. A covalently closed double-strand DNA (dsDNA) is the most frequent shape in bacterial cells where the two strands are linked. In eukaryotic cells genomes are linear DNA molecules, but the overall organization is highly complex and the chromosomes are organized in large loops that can be considered as circular DNA domains that behave as bacterial chromosomes, from a topology point of view.

The major storage form of supercoiling is *solenoidal* or *toroidal* (fig. 1.1.1 down). The term toroidal comes from imaging DNA as winding about a torus (doughnut shape surface).

Its shape is generated by the interaction on the surface with proteins to which it is bound. In eukaryotic cells this DNA structure winds nucleosomes, facilitating the packing inside the cells.

The second form is the *plectonemic* or *interwound* one (fig.1.1.1 up), resulting from the supertwisting of the double helix around its axis.

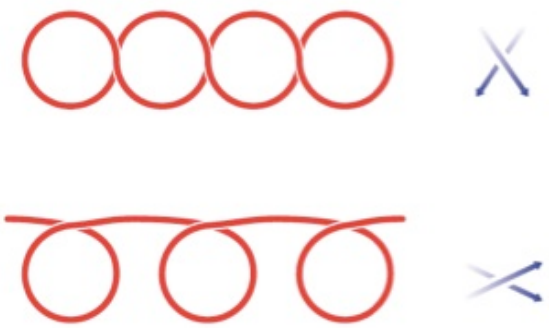

Fig.1.1.1: Plectonemic (up) versus **solenoidal** (down) DNA supercoils. In this case both molecules are negatevely supercoiled and arise from costrained DNA, as indicated by blue arrows. [2]

In prokaryotic cells no regular DNA packaging has been identified as in the case of eukaryotic chromatin condensation, but half of the supercoiled remains costrained by binding proteins [3] [4] [5] [6].

DNA supercoiling obeys to the mathematical rules of topology for ribbons. Glaubiger and Hearst in 1967 introduced the mathematical concept of a ***linking number*** (**L_k**) describing the supercoiled DNA [7]. Then White in 1969 formulated mathematically the "space curves concept" but the linking number was definetely parametrized in the "*Fuller equation*" (see Eq.1 Fuller 1971):

$$L_k = T_w + W_r \qquad \text{[Eq.1]}$$

The twist (T_w) representes the number of base pairs per helix turn related to the local winding of the DNA helix. This parameter strictly correlates with temperature and ionic conditions and summerize the total twist of the space curves about the central axis. The write (W_r) describes how the axis of the DNA passes through space depending on the supercoiling of the DNA. The write is refering to the global winding of the DNA considering the central axis. Each cross of DNA axis with itself give rise to a number +1 or -1 assegned to the writhe (figure 1.1.2) according to the "right-hand rule".

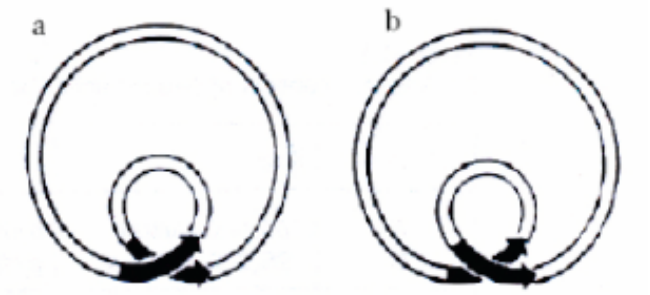

Fig.1.1.2 Definition of writhe. Circular DNA double strand showed as a ribbon a) negative node with W_r= -1 and b) positive node with W_r= +1

The *linking number* is a mathematical quantity and it's no altered by DNA distortions or breaking to one or both strands, is one-half the sum of signed crossing of DNA single strands (fig.1.1.3).

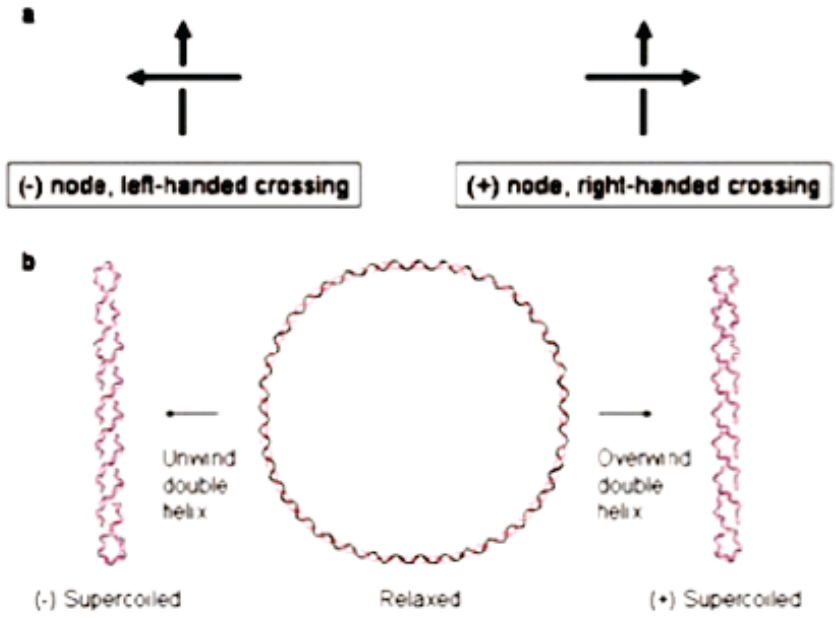

Figure 1.1.3: Closed circular DNA and topology a) convention for DNA crossings, a left-handed crossing is counted as negative and a right-handed crossing is counted as positive. b) conversion of relaxed DNA into a negatively and positively supercoiled DNA.

A linear DNA in which the ends can rotate freely represents the lowest energy form of the molecule and when exists in a covalently closed molecule the relaxed DNA has no writhe (fig. 1.1.3 b). As a conseguence the linking number results equal to the twist.

Linking number can be calculated according to its surface and orientation. When stressed, the entire double helix leads to a change in the number of base pairs per helix turn in a closed circular DNA and eventually produce regular spatial deformation. The axis of the double strand DNA then forms a helix of a higher order called the superhelix or **supercoiled**.

Because the linking number is a costant for each topologically closed DNA domain, the writhe must changes according to the twist compensation of the double helix. In negatively supercoiled DNA reduction of linking number is due to the negative writhe resulting in right-handed interwound supercoils. Left-handed interwound supercoils are generated by positive writhe producing positively supercoiled and an increased linking number.

$\mathbf{L_{ko}}$ indicates absence of torsional stress.

Lk is defined as the number of times the helix axis crosses the spanning surface of the ribbon. By convention Lk of a closed circular DNA formed by a right-handed double helix is positive, otherwise is negative.
The helical repeat is about 10,5 bp per helical turn so linking number can also been defined as (equation 2):

$$Lk_o = N/10{,}5 \qquad \text{[Eq.2]}$$

Where *N* is the number of base pairs in the DNA molecule.

Following, the DNA topology can be subdivided in:

- *relaxed* DNA if Lk = Lk_0, W_r = 0 and Lk= T_w;

- *negatevely* supercoiled DNA if Lk < Lk_0 or underwound becouse each helical turns contains more base pairs than 10,5 as in the relaxed form;

- *positevely* supercoiled DNA if Lk> Lk_o or overwound;

the **linking difference (ΔLk**) can be defined as (equation 3):

$$\Delta Lk = Lk - Lk_o \qquad \text{[Eq.3]}$$

The ΔLk is the most used descriptor of supercoiling and allows to describe also the **superhelix density** (σ) as follow (equation 4):

$$\sigma = \frac{\Delta Lk}{Lk_o} \qquad \text{[Eq.4]}$$

Superhelix density is a lenght-indipendent descriptor and is easily measured in a experimentally way becouse of Lk_o changes according to conditions such as temperature [8] [9], ionic strenght [8] and kind of DNA ligand concentration [10].

ΔLk, σ, together with Wr and N the number of superhelical turns around the superhelix axis, all are the most commonly descriptors of topological and geometric properties of DNA.

Topological properties remain costant under continous deformations as conformational changes resulting from thermal motion or the binding of proteins, RNA or drugs. While discontinous deformations are those produced by strand breakage mediated by nucleases or other physical forces. The torsional stress frequently occured during biological processes thereby removal of supercoils becomes a limiting step, unable to proceed in its absence. The enzymology of supercoiling was originally investigated by J. C. Wang, discovering a member of a class of enzymes capable to introduce and remove supercoils, these enzymes were called DNA topoisomerases [11].

1.2 DNA topoisomerases

DNA topoisomerases were first isolated for their ability to relax closed circular, negatevely supercoiled DNA. This was clear because of the changing in the topological property and the persisting relaxed structure of the closed DNA after the protein removal.

Topoisomerases emerging interest, beside the discovery of their essential biological functions is due to the wide variety of drugs, both antimicrobials and antitumor, identified in these recent years and used currently in clinical treatment.

1.2.1 Classification of topoisomerases

Topoisomerases can be divided according both structural considerations and mechanism of action. Nevertheless all kind of topoisomerases catalyze the interconversion of topological states of DNA loops by breaking and rejoining DNA strands and DNA cleavage is mediated by the formation of a transient phosphodiester bond between a tyrosine residue located in the protein that remain attached at the ends of the broken strand.

Type I enzymes cleave one DNA strand while type II cleave both strands of a dsDNA. Indeed type I subfamily is further distinguished in **type IA,** if the protein attaches to 5' phosphate, or **type IB** if this occurs to a 3' phosphate.
Type II enzymes act in different manner, they need ATP to catalyze the topoisomerizzation process and were subdiveded in **type IIA** and **type IIB** after the recent discovery of a novel type II enzyme of the *Sulfolobus shibatae*, a hyperthermophilic archean organism.
Following in table 1.2.1 the various subfamilies of both prokaryotic and eukaryotic topoisomerases are reported.

SUBFAMILY	IA	IB	IIA	IIB
DNA cleavage	Single strand	Single strand	Double strand	Double strand
Cleavage polarity	5'	3'	5'	5'
ATP dependent	no	no	yes	yes
Representative members	- Bacterial DNA topoisomerase I and III - Yeast DNA topoisomerase III - *Drosophila melanogaster* DNA topoisomerase IIIα and IIIβ -Mammalian DNA topoisomerases IIIα and IIIβ	-Eukaryotic DNA topoisomerase I -Mammalian mitochondrial DNA topoisomerase I - Pox virus topoisomerase	-Bacterial gyrase -DNA topoisomerase IV -Phage T4 DNA topoisomerase -Yeast DNA topoisomerase II -*Drosophila* DNA topoisomerase II -Mammalian DNA topoisomerase IIα and IIβ	- *Sulfolobus shibatae* DNA topoisomerase VI

Table 1.2.1: Classification and characteristics of topoisomerases

Besides those topoisomerases listed in table 1.2.1, it has also been described a number of viral encoded topoisomerases, as the vaccinia virus type IB topoisomerase and plasmid-encoded type IA in Gram-negative as well as Gram-positive bacterial genera [12] but their functions remains unclear.

1.2.2 Type I enzymes

Type IA topoisomerases share commons properties: they are all monomeric enzymes with the only exception for the reverse gyrase *Methanopyrus kandleri* [13]; require Mg(II) and an exposed single stranded region in the

DNA substrate for the relaxaction activity. They catalyzed the cleavage reaction by covalently attached one of the DNA ends to the enzyme through a 5' phosphodiester bond to the active site tyrosine, and are capable to relax plasmid containing negative supercoils but not positive [13]. Inside the type I subfamily, enzymes can be also divided depending the negative supercoiling degree preferred as DNA substrate: eukaryotic topoisomerases III require a hypernegatively supercoiling, others distinguished DNA catenation or decatenation. The mechanism of DNA relaxation for typeI enzymes was defined as "*enzyme-bridging model"* and suggested by the crystal structure of the *E. coli* enzyme (figure 1.2.2.1).

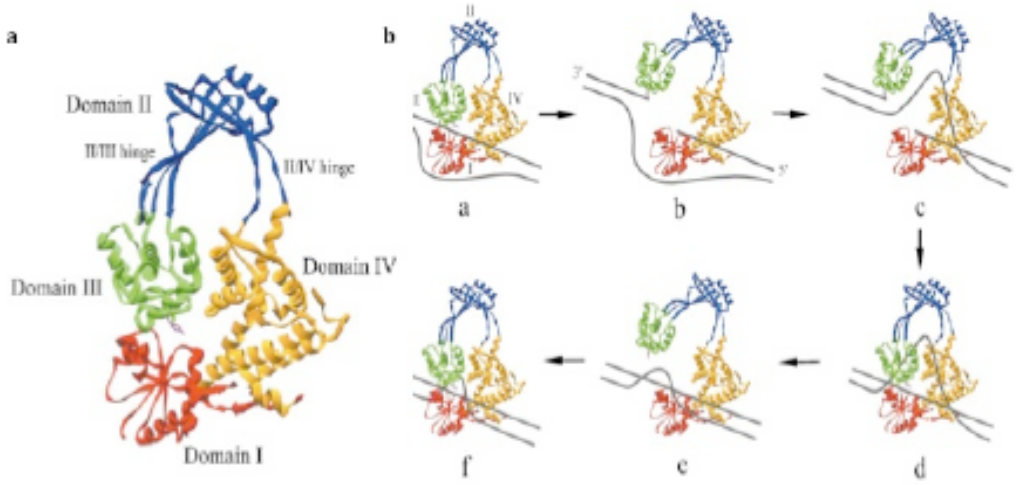

Fig. 1.2.2.1: Type I *E. coli* topoisomerase I structure a) and its possible mechanism of DNA relaxation b). *E.coli* structure (aa32-509, pdb entry 1ECL) is represented by domain I in red, II in blue, III in green and IV in orange. The two DNA strands are shown in dark gray and the mechanism of action is characterized by the conformational change between DNA and enzyme opening and closing structure [13].

Crystal structure of a 67KDa N-terminal fragment of *E.coli* topoisomerase I showed a toroidal shape and corresponding to the cleavage/strand passage domain. This allows to suppose a multiple step process as shown in fig. 1.2.2.1 b where a single strand of DNA was cleaved (fig. 1.2.2.1 b step a and b), then enzyme keeping both DNA ends at the breaking sites (fig. 1.2.2.1 step c), bridges the gap passing around the intact strand. Then the clamp closure occured (fig. 1.2.2.1 b step d) and religation of the cleaved strand is permetted. Finally to ensure the dissociation between DNA and enzyme,

protein should be opening and closing again (fig. 1.2.2.1 b step e and f). As already explained, no ATP is needed as external energy source, but the driving force derives from negative supercoiling relaxation mechanism and protein-DNA interactions.

1.2.3 Type II enzymes

Type II enzymes catalyze the topoisomerization process by binding both strands of DNA and cleaving the opposing strands. The covalent attachment is ensured by a pair of catalytic active tyrosines attacking dsDNA and performing a phosphotyrosine linkage with 5' ends. Linking number changes in steps of two because of the changing in the supercoiling substrate. Subfamily II despite to type I enzymes need ATP hydrolysis as external energy source. The ATP hydrolysis is used to induce major conformational changes in the enzyme structure to allow the strand passage.

Type II subclasses have similar structures with flexible regions linking catalytic domains, but type IIA enzymes (fig. 1.2.3.1 a) are characterized by two inter-connected rings and type IIB (fig. 1.2.3.1 b) show a single clamp shape. In figure 1.2.3.1 c is reported the hypothetic model of the DNA strand-passage reaction [14] in both type II subclasses.

To better understand the mechanism of action, this model imagines dsDNA as two segments, the intact double helix or T-segment in green and the G-segment in red costituting a kind of a gate (figure 1.2.3.1 c). Enzymes acts as a clamp capturing and releasing T-segment passing trought the G-segment permanently linked to the DNA cleavage/religation domain. ATP hydrolysis allows the conformational changes in the protein structure and the release of the T-segment in the solvent. This model was recently confirmed by crystallographic studies in bacterial typeII enzymes [14].

The mechanism of type II protein is manifest in several topological transformations including catenation and decatenation and the relaxation of positive or negative supercoiled DNA [15].

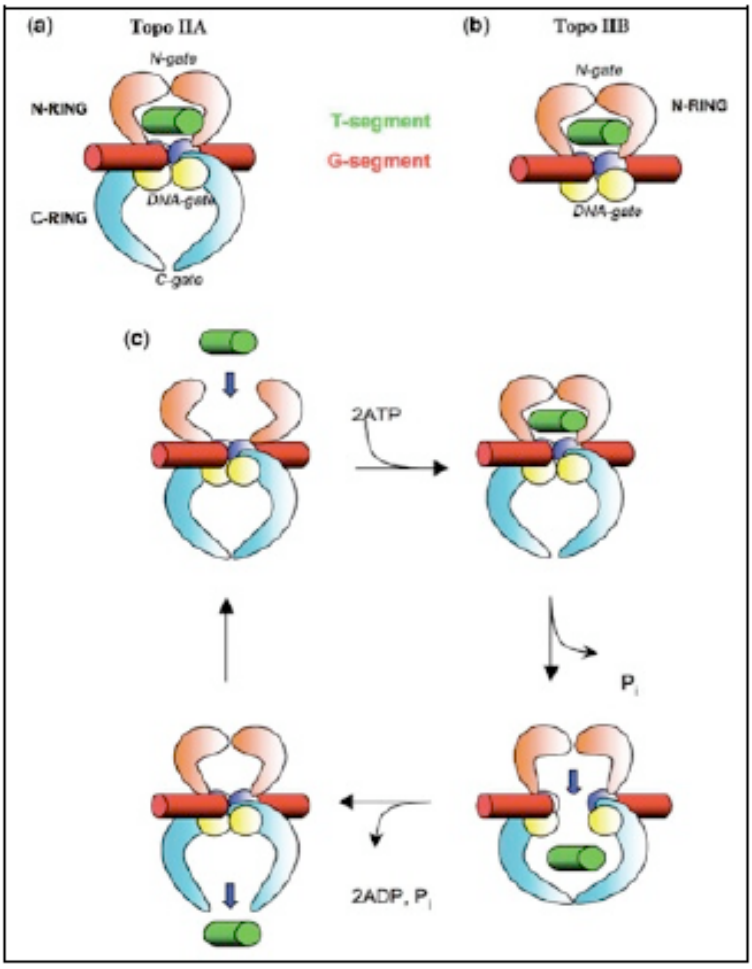

Fig. 1.2.3.1 Type II topoisomerases and mechanism of action: the schematic structure of typeIIA and type IIB are shown in figure a) and b) respectevely. In section c) the topoisomerization process is presented trought the strand-passage model in which the movement of T-segment in green is mediated by the transition in the G-segment gate in red. In orange and cyan are respectevely shown the N-ring and the C-ring [14].

1.3 Human DNA Topoisomerase I

Belonging to type IB subfamily, human DNA topoisomerase I (figure 1.3.1) is one of the best known among the six human topoisomerases.

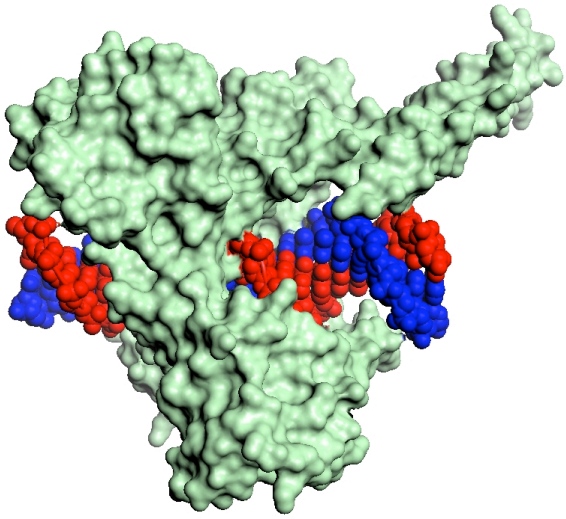

Figure 1.3.1: Human DNA topoisomerase I structure. Enzyme (light grey) was structured together with a 22 pb DNA fragment, double helix are showed in blue and red. The figure was prepared using the PyMol Molecular graphics system. Pdb entry 1A36 (aa 636-640 are missing).

In the last few years several crystallographic structures have been produced and all are obtained in a co-crystals with a 22 base pairs DNA fragment: enzyme constituted by the C-terminal and the core domains (pdb entries 1A31 and 1A35), or the structure including the linker in non-covalent complex with DNA as shown in figure 1.3.1 (pdb entries 1A36 and 1EJ9).

The enzyme structure was also solved in a ternary complex with inhibitors in pdb entries 1SC7, 1SEU and 1T8I.

The most complete crystal structure remains that showing aa 201 to aa 765.

All available structures lack in the N-terminal domain because of its difficulty in crystallization, it has been proposed that this portion is high flexible and not so stable for crystal formation.

Crystal structure together with limited proteolysis analyses, conservation of sequences and hydrodynamic properties, allowed to identify the human topoisomerase I as a 91-KDa monomeric enzyme [765 aminoacids] constituted by four structural domains (fig. 1.3.2): the C-terminal, the linker, the core and the N-terminal.

Figure 1.3.2: Crystal structure of 70KDa form of human topoisomerase I complexed with 22 bp DNA fragment. Core domain is subdivided in sub domain I (yellow), sub domain II (blue) and sub domain III (red). Moreover linker domain is shown in orange and the C-terminal is in green [16]. Intact DNA strand is represented in cyan and at the level of the cleavage site other strand is shown in magenta upstream and pink downstream.

1.3.1 HtopIB structure insight

- **The N-terminal** is a 24 KDa domain (Met1-Ile215), poorly conserved and protease-sensitive, is considered highly charged because of its 72% of charged and 90% polar residues. This region has no defined spatial organization [17] and suggesting to be unstructured in the final folded form of the protein. It also contains five nuclear localization signals (NLS) [18] contributing to the interaction with nuclear proteins as nucleolin [19]. The most complete structure domain is that Ile215 to Gly201 residues. Indeed *in vitro* study has been demonstrated that DNA relaxation occurs also in its absence [20] [21], yet it has been implicated in mediating protein interactions *in vivo* without modify Top1 protein binding of DNA [21]. However protein interactions with this domain have been reported to alter the intracellular localization of the enzyme [22].

The N-terminal in combination with the linker domain affects protein clamp dynamics [21].

- **The core** (Ile215-Ala635) is about 54KDa conserved domain, is a globular region subdivided into three subdomains, the I and II costitute the so called "upper lobe" or "cap" of the protein, moreover the III together with the C-terminal domain compose the "lower lobe". Thus the three-dimensional structure revealed a bi-lobed protein as a clamp opening and closing around the DNA substrate. The opposite faces of the double helix are implicated in the binding but the upper lobe has no direct interaction, while the lower one contains the catalytic residues involving the DNA phosphate groups. Indeed the cap domain contains two helices (302-339 aa) protuding from the main body of the protein, posetively charged and poising in the DNA major groove as a v-shaped motif, called "nose-cone".

Moreover the two lobes are linked by a long α-helix, called ***hinge*** and on the other hand two loops from Lys 369 to Glu497 called ***lips*** interact through six amino acids and one salt bridge.

Structural data [17] shown that region from Trp204 to Gly214 interacts with several residues at the level of subdomain I, the C-terminal and the *hinge* portion of subdomainIII producing an hydrofobic amino acid cluster (Trp205, Trp206, Trp441, Trp754, fig. 1.3.1.1).

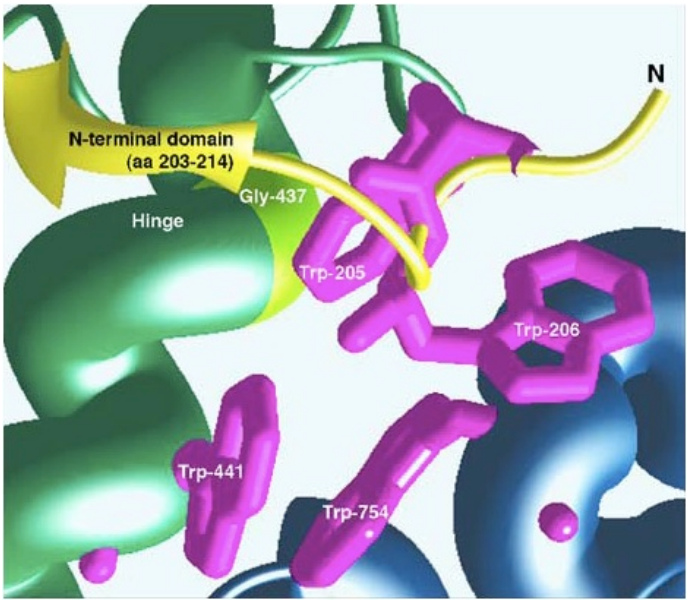

Fig. 1.3.1.1: Hydrofobic cluster between N-terminal domain (yellow), **the core domain** (green) and **C-terminal domain** (blue). The top of the *hinge* contributes to the opening and closing of the clamp around the DNA, image adapted from [23].

This suggests the residue Pro431 at the top of the *hinge*, mediates the clamps movements thanks to the strechting or the bending of the flexible α-helix [24]. Oppositely lips contact each others during closed clamp conformation at residues Lys369-Gly497, Asp366-Asn500 [25] and with a salt bridge Arg364-Asp533 [26].

- **The C-terminal domain** (Gln713-Phe765) 6,3KDa highly conserved, contains the catalytically active Tyr723. Protein-DNA interactions in this region occur five base pairs upstream the cleavage site 5'-3' direction of the scissile strand.

Five conserved residues Arg488, Lys532, Arg590, His632 and Tyr723 are involved in the cleavage reaction: excepted Tyr723 performing the nucleophilic attack by its O-4 oxigen, others four amino acids allocate the scissile phosphate entering in the DNA minor groove (fig. 1.3.1.2).

Then a phosphodiester link is generated between the tyrosine and the 3' phosphate realeasing a 5'hydroxyl.

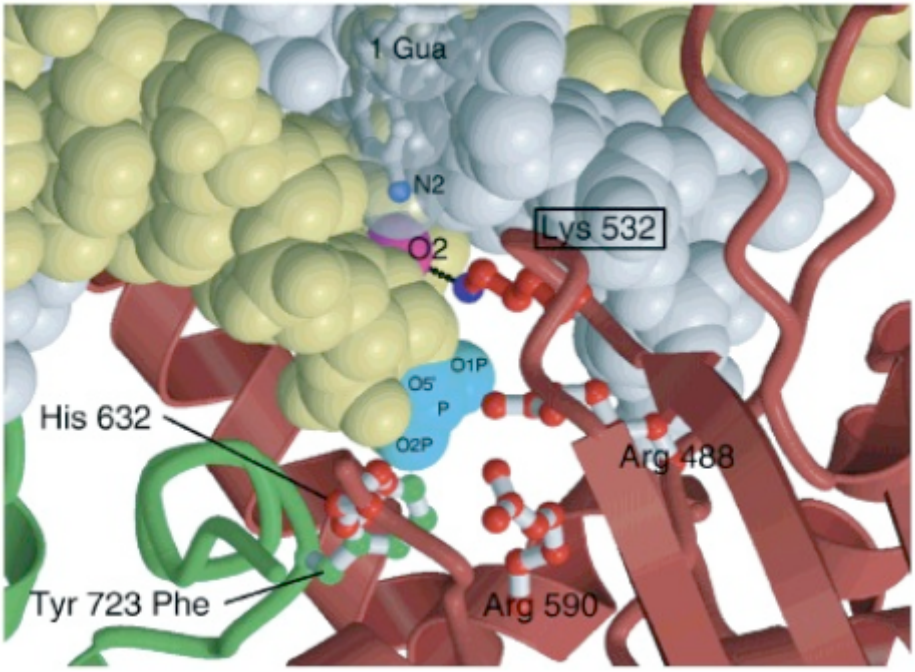

Fig. 1.3.1.2: Active site residues representation The scissile and intact strands are shown in yellow and light gray respectevely. The active site residues Arg488, Arg590 and His 632 were represented in white and red or in white and green (Tyr-723-Phe). Lys532 in red is shown making the hydrogen bond with O2, in magenta, of the cytosine base in the scissile -1 position of the C-G base pairing in minor groove. The figure is adapted from [24].

- **The linker domain** (Pro636-Lys712) 7KDa posetively charged and protease sensitive is constitued by two α-helices connected by a short turn forming an anti-parallel coiled-coil structure and links together the C-terminal with the core domain. Nine lysine and arginine residues composed the side in front of the DNA helix, but linker contacts DNA only two times with Lys650 and Arg708 [17]. Lacking of this domain it has been reported to bring the topoisomerization equilibrium to the religation and to an increased rate [27] or a decreased one [28]. Moreover has been reported that mutation of Ala653Pro changes in the cleavage/religation equilibrium and confers resistance to camptothecin (CPT) [29], [30]. Furthermore following molecular dynamics simulation study of double mutation Ala653Pro-Thr718Ala showed flexibility of the linker and a strong influence to the catalytic site according to CPT resistance and activity maintenance [31].

Human topoisomerase IB has also structural similarity with a family of tyrosine recombinase allowing to better understand its catalytic reaction.

1.3.2 The topoisomerization process

As already explained by crystallographic data in the topoisomerization process only one base-specific, enzyme-DNA interaction occurs, involving a hydrogen bond between Lys532 and O-2 atom of the preferred thymine/cytosine residue. Even if the reaction is known to be a multiple step process in which two transesterification reactions lead to the cleavage and to the religation reactions, mechanistic details of DNA relaxation for human TopoIB still remains unclear.
Crystallographic data highlighted a possible role to a water molecule in activating base of the catalytic Tyr [32].
To date, two different models have been proposed for the catalytic mechanism, the most attractive is the "**controlled rotation**" (figure 1.3.2.1) [33].

This terminology was first used by Champoux and coworkers and indicates a costrained mechanism, based on the tension energy derived from the supercoiling substrate and driving the rotation of the broken strand around the intact one. Binding event involved the surface and the charge complementation between DNA and protein in a non covalent manner, thus an opening conformation has to be the preliminary state.

Then the active site residues reached the right position performing the cleavage through the nucleophilic attack to the scissile phosphate.

Now enzyme is covalently attached to the 3' end of the DNA as shown in the figure 1.3.2.1 and releasing a 5' hydroxyl. The covalent intermediate has been formed and controlled rotation of the DNA downstream the break for one or more cycles occured to release the superhelical tension.

The release of the Tyr723 from the end of the DNA allows the religation reaction and DNA molecule with a different linking number is generated.

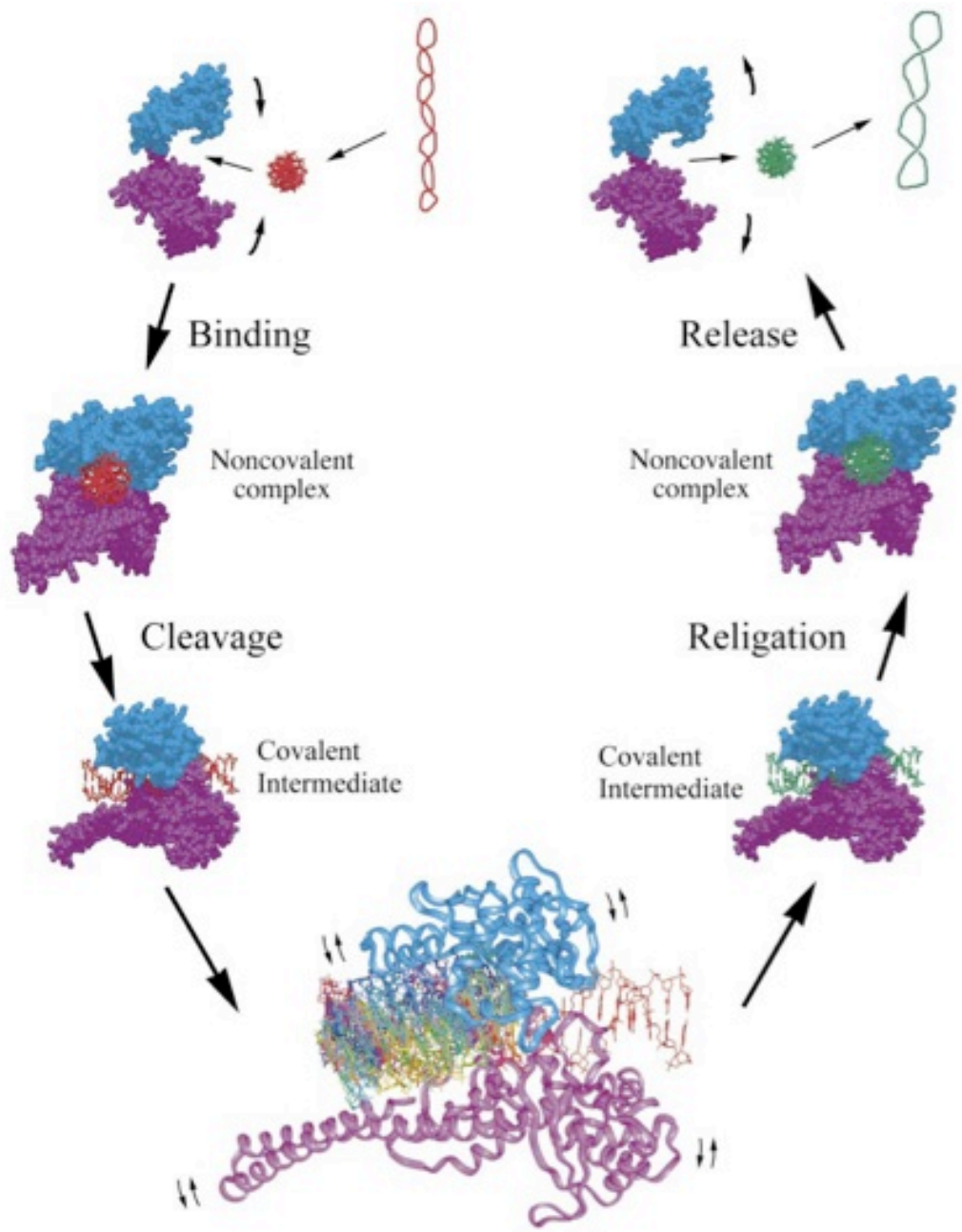

Fig. 1.3.2.1 The controlled rotation model for human topo I catalysis: DNA substrate shown in red, first, non covalently bind the enzyme (represented with two colours indicating the upper in cyan and lower lobe in magenta), then cleavage reaction produces intermediate of the reaction during which controlled rotation movements occured in order to release superhelicity tension. Religation step finally release the DNA molecule with a reduced superhelicity (light grey) and the enzyme are ready for a new relaxation cycle [33].

Co-crystal structures of topoisomerase I bound to DNA reported no sufficient space for a free DNA rotation, the cap and the linker domain should interact one or more time in order to allow the rotation mechanism [33]. Indeed the initial open conformational state is facilitated by a hinge-bending motion located at the top oh the *hinge* between subdomains I and III, residues Pro431 and Lys452, while the closure state brings together the opposable lips of core subdomains I and III.

The alternative model proposed for the relaxation is the "**free rotation**" mechanism. In this case an additional opening of the clamp is hypothesized after the DNA cleavage, but this also needs the domain flexibility [34]. Elegant experiments of real-time single-molecule (figure 1.3.2.2) showed that human topoisomerase IB releases the superhelical tension trought a pivoting mechanism between enzyme clamp and rotating DNA [35].

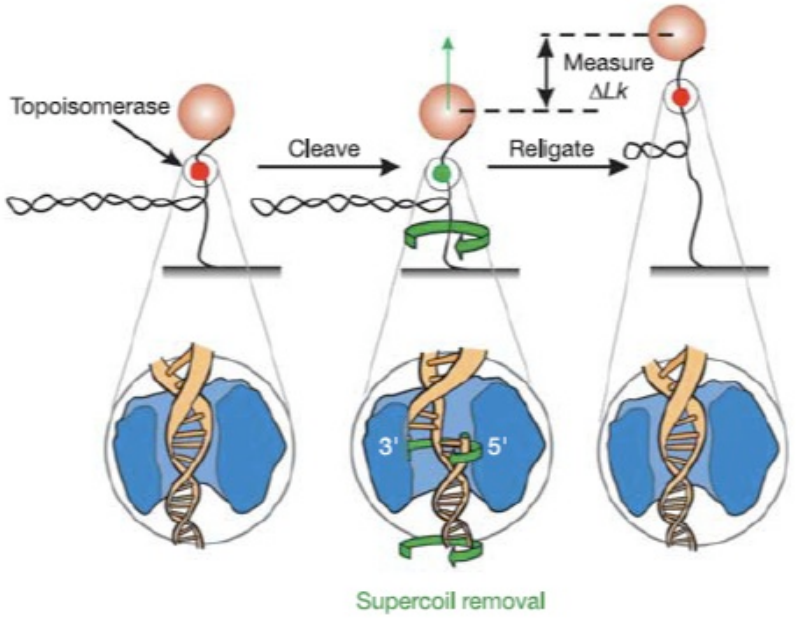

Fig. 1.3.2.2: Real-time single molecule analyses dsDNA is covalently attached to a paramagnetic bead (in red) at one strand, and to a glass surface on the other. Topoisomerase from left to right follow the relaxation process, beginning from a non covalently link, then binds the DNA resulting in the supercoil removal and last relegates the DNA molecule. The distance between the bead and the glass surface was measured at the begin and at the end of the reaction (ΔLk) and this was directly linked to the supercoil removed. The figure is adapted from [35].

The approach gives a value, of the twisting and stretching movements of the rotating DNA, proportional to the supercoil removal. One DNA strand is anchored to a glass surface, while the other was attached to a paramagnetic

bead (1-4.5 μm in diameter). A magnet positionated above the apparatus is necessary to control and rotate the beads in the right orientation, according to the stretch and twist of the DNA molecules. During the topoisomerization process, cleavage and religation release superhelical tension, and this began proportional to the changing of the height of the beads from the glass surface. This measured value, increases as the number of the removed supercoils. Enzyme cannot relaxes all the supercoils in a single cleavage and religation event, but friction and torque drive the DNA rotation following an exponential distribution. This was the first evidence supporting the controlled rotation model.

In addition has been reported that a salt bridge between Lys369 and Glu497 contributes to close the enzyme around the DNA [17] and this was also confirmed by mutation in cysteine of His367 and Ala499, respectevely located each to one opposable lips, that covalently close the clamp. All these features suggest that the free rotation model is quite impossible considering the steric clashes between DNA strand rotation and protein structure.

1.4 Reverse gyrase

In 1984 Kikuchi and Asai described a new topoisomerase, with the ability to introduce positively supercoils into DNA molecules and named this enzyme reverse gyrase. It's a large protein of about 1050-2000 amino-acid residues with two distinct domains, a C-terminal typeIA topoisomerase module and an N-terminal region containing conserved sequences of the SF2 family helicases-like [36]. As SF2 family also reverse gyrase sequences contain the ATP-binding domain thus the ATP hydrolysis is essential for the positive supercoiled relaxation [37]. The C-terminal domain have 30% of sequence identity with type IA topoisomerases. As in human topoisomerase I this domain contains a conserved tyrosine residue required for the catalytic activity. From sequence prediction analyses a zinc-finger domain has been reported in the N-terminal domain [38].

Its relevance was claryfied when highly positive supercoiled DNA were observed in a hyperthermophilic virus, the *Sulfolobus shibatae* Virus 1 (SSV1)

[39]. Reverse gyrase activity was identified in all hyperthermophilic organism: in Archaea as well as in Bacteria [40] [41]. Since reverse gyrase cleaves one DNA strand and transiently forms a phosphotyrosil link with the 5' end of the cleaved DNA strand is considered a type IA subfamily topoisomerase [42].

The unique three-dimensional structure known for this enzyme is from *A. fulgidus* (fig. 1.4.1), resolved bound and unbound to an ATP analog, non-hydrolysable analog (ADPNP) [43].

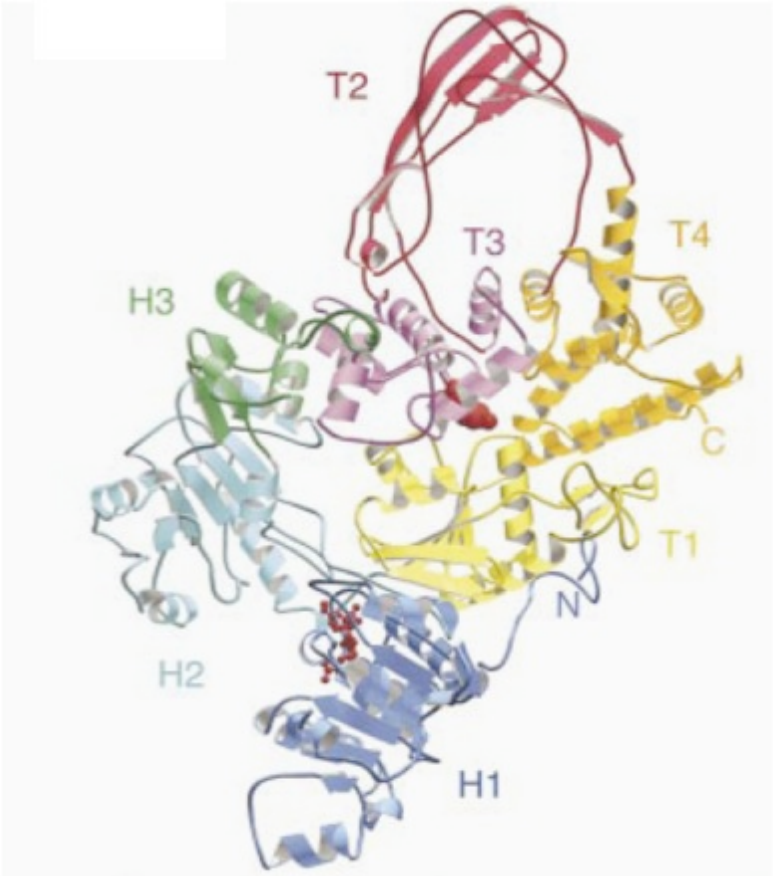

Fig. 1.4.1 Reverse Gyrase structure of a *Archaeoglobus fulgidus* the C-terminal domain is shown in red and the Zn-finger motif in yellow at the final part of the N-terminal domain in dark-blue, figure adapted from [43].

The two distinct domains were analyzed in the *Sulfolobus acidocaldarius* in separately manner [44]. The single C-terminal domain is able, in an ATP-dependent reaction, to relax the DNA substrate, while the N-terminal alone doesn't.

Helicase-like and topoisomerase domains are unique and specifically cooperate to induce positive supercoils, if substitution of one of them occured, no positive supercoiling accumulation is observed [44] [45].
Indeed reverse gyrase is a thermophilic sensor, its activity in the relaxation of supercoils is maximal at temperatures close to that of the optimal growth of the organism from which it was purified [46]. For the hyperthermophiles is reported an optimal growth temperature above 80^0C.

The function of this enzyme in life cell remains still unclear and it's possible to argue that it could prevent DNA denaturation and degradation induced by high temperature. For sure, it has a certain role in hyperthermophiles organisms in which DNA exists in positively supercoiled state. Its ability to stabilize genome seems to be the key for understanding its contribute in living cells.

1.5 Topoisomerases biological functions

Controlling DNA supercoiling is an essential process in all cells, local changes or excessive supercoiling in the DNA template could impede movement of RNA or DNA polymerases. Human topoisomerase I resolves the torsional stress associated in DNA replication, transcription and chromatin condensation. It has been demonstrated that topoisomerase I is a nuclear protein, enriched in the nucleolus (figure 1.5.1).
The N-terminal domain contains nuclear localization signals allowing the protein to localize in both subcellular compartments and moreover to associate with RNA polymerase I holoenzyme [47].
Nucleus accumulation has been reported to be associated with rDNA transcription, the central machinery for the nuclear organizer regions (NORs).

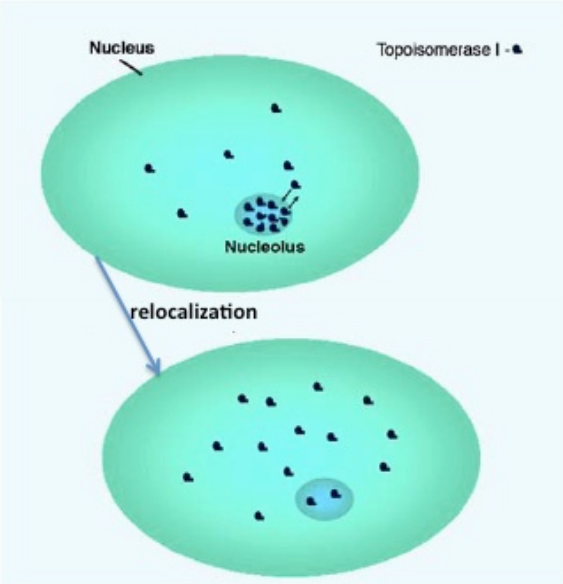

Fig. 1.5.1: Topoisomerase I localization and dynamic variation Enzyme dominantly localizes in the nucleolus where associated processes with ribosomal DNA occured. Otherwise inhibition of trascription or drug treatment leads to a relocalization of topoisomerase I, figure adapted from [48].

The N-terminal and the C-terminal domains have been identified as the *in vivo* topoisomerase I acting portions, influencing the nucleolar re-localization of the enzyme and also contributing to the double cleavable complex formation [49] [50] [51].

It has been demonstrated by Christensen and collaborator (2004) that DNA topoisomerase I colocalizes with RNA polymerase if the N-terminal is present, during rRNA transcription at the level of fibrillar center of the nucleolus, then migrates in the outer perimeter during the disruption of the molecular transcription machinery. In addition they observed a dynamic migration of the enzyme from the nucleoplasm and nucleolus.

Still remains unclear if the N-terminal domain is necessary for the nucleolar localization of the topoisomerase I. In truncated mutants (1-190 residues) enzyme accumulates in the nucleolus, contrast to Y723F mutants in which a nucleus uniform distribution is observed [52].

These controversial results suggest the protein-protein interactions as a key role for the enzyme localization during transcription and DNA replication, so the human protein transiently associated.

In human cells it has been found that colocalized with RNA polymerase I [47], indeed the N-terminal fragment of human topoisomerase I colocalized with RNA polymerase II in *Drosophila melanogaster* [53].

It is well known that human topoisomerase IB solves topological tension on a duplex DNA of both positive and negative signs, but it's also strongly associated with mRNA and rRNA transcription, DNA synthesis, repair and recombination through distinct unclear mechanisms.

Genome-wide analysis in yeast shows that topoisomerase I and II act together in close proximity to a replication forks and are required for its progression [54], and in addition has been reported that protein interacts with the human lamin B2 origin in a cell-cycle dependent manner [55] [56]. Moreover a number of factors has been demonstrated to interact with topoisomerases in *S.cerevisiae* [57] and the large T antigen helicase from Simian Virus 40 (SV40) directly interacts with Topo1 stimulating DNA synthesis [58].

All these data suggests that topoisomerase I is an integral component of the "Replication Progression Complex", the large macromolecular assembly with helicase activity. In eukaryotic cells functional coupling between helicase and topoisomerase I has been proposed [59] and in the case of *papillomavirus* (PV) has been reported the binding beetween E1 helicase and the E2 origin binding protein, allowing topoisomerase activity and origin interaction [60] [61].

During replication there is a continous separation of the parental DNA strands mediated by the helicase activity as reported in the upper part of figure 1.5.2 as the replication fork proceeds DNA becomes overwound in front of its and positive supercoils accumulate.

Topological variations are locally and transiently observed during transcription due to the separation of the duplex DNA strands. In front of the "transcription machinery" accumulated positive supercoils and the negative are localized behind it (lower part of the figure 1.5.2).

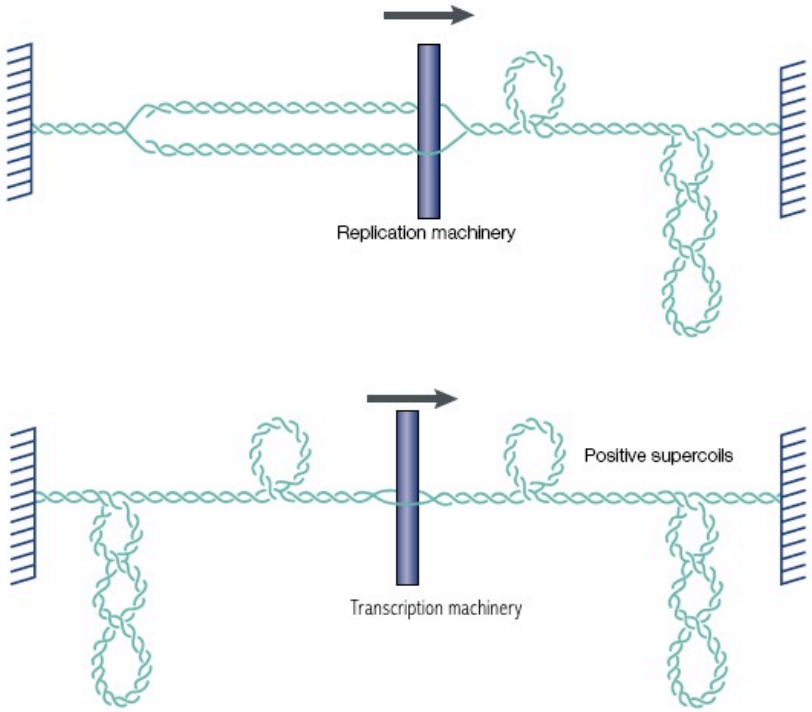

Fig. 1.5.2 Human topoisomerase I during replication and transcription: during replication positive supercoils accumulate in front of the progressing replication fork, while in the transcription process positive supercoils are generated ahead and negative supercoils behind the RNA polymerase and associated proteins (transcription apparatus). The figure was adapted from [15].

This model was also called "twin supercoil domain" model [62] [63].

In the replication process it has been reported an accumulation of DNA strand breaks follow to treatment with the topoisomerase I inhibitor [64], supporting that enzyme acts in front of the replication fork redistributing the topological strains.

In addition *S.cerevisiae* studies also demonstrated the contribution of DNA topoisomerase IIα in the replication fork [65], its role may be related to its ability to relax positively supercoiled DNA faster than negative [66].

It could be possible that topoisomerase I needs a protein partner for the interaction with DNA template [67].

It's also important to notice that human topoisomerase IB was isolated from a mammalian multiprotein DNA replication complex containing PCNA, *proliferating cell nuclear antigen* in the Werner syndrome [68].

For what concerns the transcription process, the topoisomers relaxation is required for the elongation step [69], indeed it has been reported that human topoisomerase I activates gene containing TATA box in their promoter

region, involving TATA-box binding protein (TBP) and TATA-binding protein-associated factors (TAFs) [70].

1.6 Other Human topoisomerase I contributes in cell

Topoisomerase IB showed also kinase activity, contributing to transcription and splicing coordination [71]. In addition has been reported that dephosphorylation of the enzyme leads to the inhibition of the relaxation activity, this suggests a possible role of the Protein Kinase C (PKC) and c-Abl tyrosine kinase [72] [73].

A recombination activity has also been recognized according to the close similarity between the conserved catalytic domain of the human topoisomerase IB and that of the site-specific recombinases. It has been reported the ability of topoisomerases to insert and excise viral DNA into cellular DNA [74] [75]. Since topoisomerization is similar to that carried out by DNA strand transferase, it has been found that a strand transferase can act as a topoisomerase and a topoisomerase can act as a DNA transferase, generating "illegitimate recombination" [76] [77].
One exception from the topoisomerase reaction is that the DNA strand transferase attachs the 3' end of a transiently broken strand to the 5' end of another one broken end. Interestingly recombination also mediated the lambda prophage excision by the vaccinia virus topoisomerase I.
Moreover in yeast a correlation between increased topoisomerase I activity and increased levels of illegitimate recombination it has been observed [78].
Since the highly supercoiled DNA generated by replication or transcription reactions could become substrate for recombination, hyper-recombination phenotypes may arise from the deletion of topoisomerases.

Eukaryotic DNA topoisomerase I has also been proposed to have a role in chromosome condensation [15]. In yeast double mutants *trf4-top1* of DNA topoisomerase I and the product gene of TRF4, are defective in chromosome

condensation, nuclear segregation thus suggesting a function of these enzymes during mitosis [79].

Variation in DNA topology during chromatin related process is consistent with DNA topoisomerase mediating condensation or decondensation. Recently condensins, ubiquitous ATP-dependent protein complexes, were identified for the requirement of DNA topoisomerase in chromosome condensation [80].

1.7 Topoisomerase I inhibitors

DNA topoisomerases are the targets of many antimicrobial and anticancer drugs. Topoisomerase I inhibitors can be divided into four classes: camptothecin derivatives, polyheterocyclic aromatic inhibitors, benzimidazoles and minor groove ligands [81], DNA damaging agents. These drugs covalently bind the reaction intermediate (enzyme linked to the DNA), leads to generation of double strand breaks and DNA damage during S-phase of the cell cycle. The most selective inhibitor group for the human topoisomerase IB are the “camptothecins” or also called CPT derivatives.

Camptothecin, the leader compound, was originally isolated from the Chinese bush Camptotheca acuminata in 1966. CPT, extracted from the tree native of China and Tibet, was used in traditional Chinese medicine (Wall American chimica society: Washington DC ’93), and only in 1985 was identified as the unique target for the topoisomerase I [82]. Camptothecin is a lactone compound (top left of the figure 1.7.1) and its extreme low solubility disables the parental administration, thus the sodium salt of camptothecin carboxylate was the first to be validated for clinical treatment.

Since its controindications as myelosuppression, diarrhea and hemorraghic cystitis [83] [84], a second generation analogs was formulated, this includes the topotecan (TTC), (9-(dimethylamino)methyl-10-hydroxy-camptothecin) and Irinotecan (CPT-11), (7-thyl-10-(4-(1-piperidino)-1-piperidino)carbonyloxycamptothecin) (top right and bottom of the figure 1.7.1).

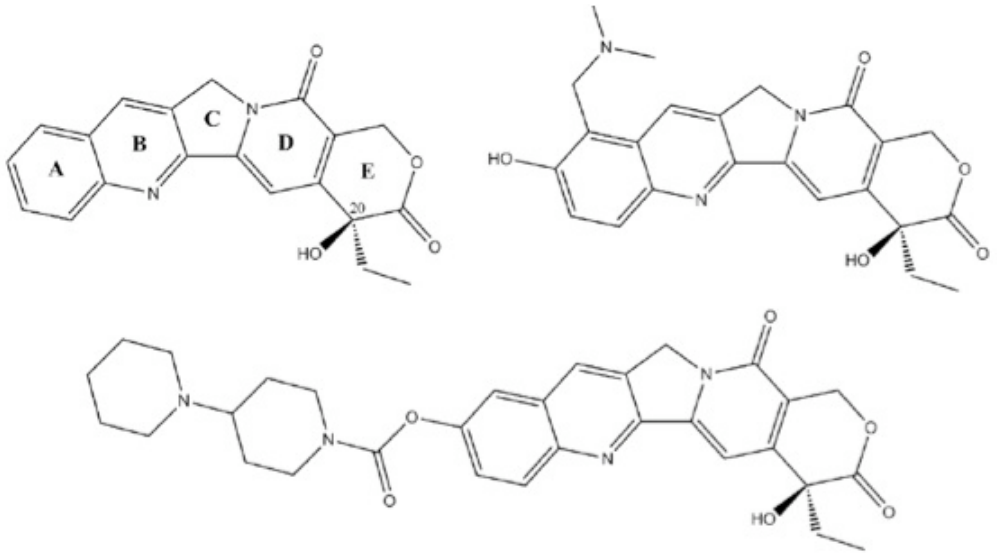

Figure 1.7.1: Camptothecin structures top left is shown the camptothecin CPT, top right the topotecan TTC and bottom irinotecan CPT-11. Figure adapted from [85].

The equilibrium between hydroxy acid (hydrolyzed A ring) and lactone type is responsible for cytotoxicity, if this shifted versus the lactone forms [86]. Modifications of A and B rings with a 10 hydroxy camptothecin with functional groups (phosphates, sulphates and carbamates) were demonstrated to be tolerated and more water soluble [87]. The Irinotecan (Camptosar® Yacult Honsha KK), among carbamates, showed the substitution of the 4-(1-piperidino)-1-piperidino carbonyloxy group at position 10 of the A ring with an ethyl group at position 7 of the B ring.

In 1991 Tsujii and collaborators, demonstrated that the pharmacology activity was exerted by its 10-hydroxy metabolite (SN-38) enzymatic hydrolysis of carbamate was required. Topotecan (Hycamtin®, Glaxo SmithKline) was produced by substituting 10 hydroxy camptothecin with a positively charged dymethyl-aminomethyl group at position 9 [88].

Today, topotecan and Irinotecan, are used clinically, in solid tumours therapy, but there are limitations for the chimical instability of the hydroxylactone ring, multidrug-resistance and dose-limiting side-effects [89] [85]. Indeed this family of anti-cancer drugs showed also antiviral activity [90] allowing active efforts in developping new topoisomerase I inhibitors.

1.7.1 Mechanism of resistance to camptothecin and DNA damage

Biochemical data suggests that CPT binds at interface beetween topoisomerase I and DNA, inhibiting the religation step in the cleavage/religation reaction (fig. 1.7.1.1).

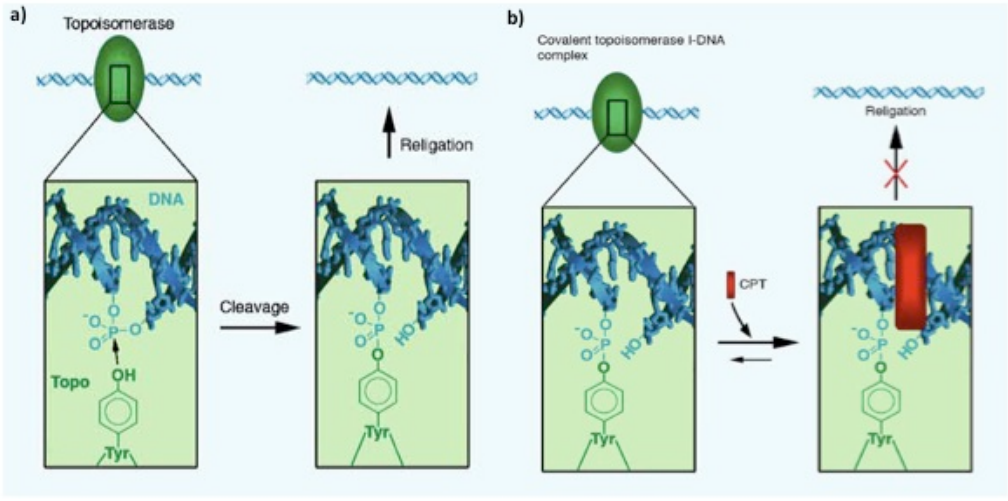

Figure 1.7.1.1: Camptothecin intercalation during cleavage/religation reaction. The figure adapted from [48].

The drug directly binds the enzyme-DNA complex producing a reversible bond and preventing the dissociation of the two macromolecules. In figure 1.7.1.1 a, the nucleophilic attack from the catalytic tyrosine (Tyr723) of the human topoisomerae I producing a Top1-mediated DNA break is showed.

The resulting covalently Top1-cleaved DNA intermediates are also defined "**cleavable complexes**" and are not detectable because of the fast religation step in normal condition [91]. There are a variety of exogenous and endogenous factors that may alter the cleavage/religation equilibrium with an increase in the cleavable complexes formation and the religation inhibition. A higlhy selective and specific agent are the anticancer drugs camptothecins (fig. 1.7.1.1 b). Top1 cleavable complexes are normally reversibles after camptothecin removal, and it has been reported that exposure for less than 1 hour is relatively non-cytotoxic [92] [93].

Long exposure is required for effective cell killing and cleavable complexes were converted in DNA damages by cellular metabolism [91].

Crystallographic studies of topoisomerase I with and without DNA substrate (figure 1.7.1.2) reported multiple interactions in both the cleavable and non-cleavable complex [17]. The resolution of a co-crystal structure of the clinically approved CPT analog, topotecan (Hycamtin®) with the Top1-DNA complex by Staker and co-workers in 2002 clarify these interactions. The whole structure (fig. 1.7.1.2 c) appears to mimic a DNA base pairs allowed by the unwinding of the DNA and the traslation downstream of the cleavage site, occupying the same space as +1 base pair in absence of the inhibitor (fig. 1.7.1.3 a and enlarged view in fig. 1.7.1.3 b).

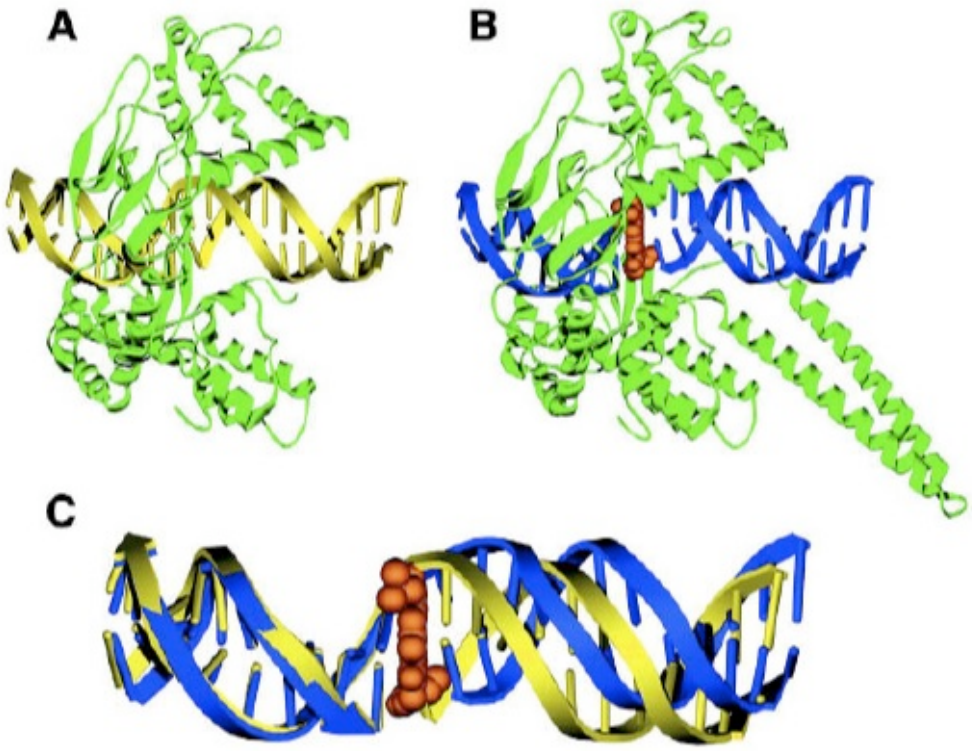

Figure 1.7.1.2: TopI-DNA complex a), bound to topotecan b) and dsDNA interactions with the drug (orange) were represented. Protein was shown in green, when DNA is unbound is coulored in yellow a) and c), while is in blue when it's bound with the topotecan b) and c). The binding pocket for drug-DNA interaction revealed 36 direct contacts and 6 others water mediated. The figure adapted from [95].

The binding is generated by minimal protein conformational changes and at the phosphodiester bond between the +1 and -1 base pairs of the uncleaved strand [94]. Indeed the ternary complexes trapped by camptothecin (fig. 1.7.1.3) are located at the base pairs at a thymine to -1 position and at a guanine at the +1 position.

The intercalated conformation is stabilized by 36 direct contacts and 6 additional water-mediated protein-DNA interactions.

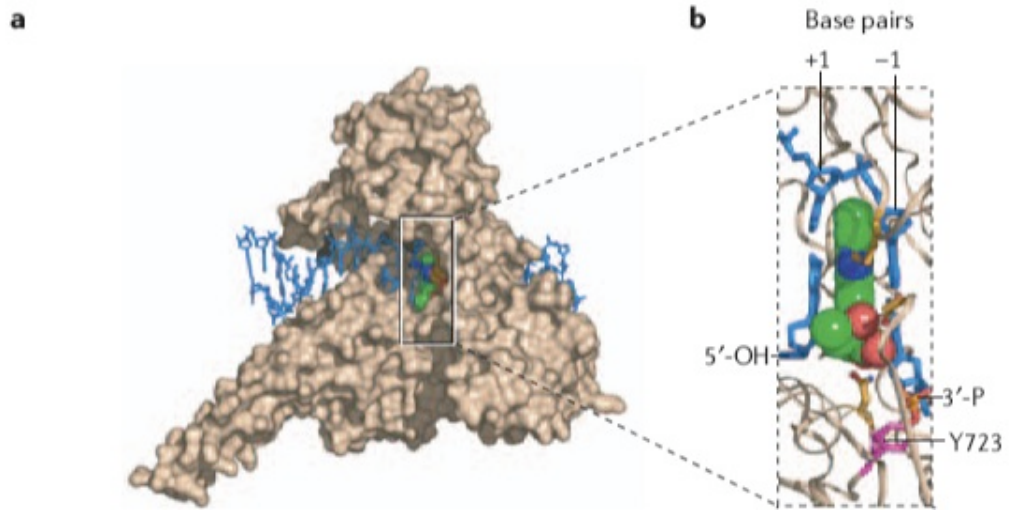

Fig. 1.7.1.3: a) TOP1 ternary complex at the cleavage site and b) enlarged view of the intercalation with camptothecin. Inhibitor is shown in green for almost carbon atoms, and oxygen and nitrogen are respectevely in red and blue, enzyme surface in brown and dsDNA in blue. The catalytic tyrosine Y723 in magenta linked to TOP1 in -1 position and the 5'-OH end is referred to +1 as shown in **b)**. The 5'-end of the nicked strand is occupied by the drug intercalated in the cleavage site. The blue sticks represented base pairs closed to TOP1 cleavage site. The figure is adapted from [96].

This model explains how the drug stopped the relegation process, the ternary complex (DNA-TopoI-drug) is shifted 3.4 Å downstream, dislocating 10 Å far the free 5'-OH group from the phosphotyrosine.

Co-crystal structures of the ternary complexes with camptothecins analogs as indenoisoquinolines and indolocarbazole [94] [97] showed the intercalator configuration between the -1 and +1 base pairs flanking the cleavage site, moreover only the 20-S CPT enantiomer is active, all data suggested a stereo-specific binding site for the drug [96].

It has also been reported that point mutations in camptothecin-resistant cells are localized at the level of residues involved in H-bonds beetwen the drug and the enzyme [98]. Analyzing the crystal structures of these camptothecin-resistant enzymes was possible to argue that single point mutations don't interfere with the crystallization process and drug orientations were not changed; moreover the lack of a single H-bond don't preclude the binding, suggesting a weakest drug retention for the resistance mechanism [26] [96].

Camptothecin cytotoxicity is reported to be primarily related to replication-mediated DNA DAMAGE in budding yeast and in most tumour cells [99] [100] [101].

Indeed microarray analysis showed dose dependent effects in the transcriptional regulation. In the cell cycle a lower drug concentration produces reversibile delay of G2 while a higher dose leads to an S-phase delay and G2 arrest [102].

The drug cytotoxicity comes out from the collision of the replication machinery at the fork with the Top1-DNA cleavage complexes, on the leading strand [100] [101] [103], thus single strand DNA breaks became irreversibile double strand breaks (DSB figure 1.7.1.4).

Replication proceed according to "replication run-off" mechanism (figure 1.7.1.4), up to the 5'-end of the Top1-cleaved DNA, and the 5'-termini of the DSBs are rapidly phosphorylated *in vivo* by the kinase activity of polynucleotide kinase phosphatase PNKP [104] [91].

In figure 1.7.1.4 d, has been represented a "suicide complex" or "dead-end covalent complex", as the result of the DNA damage. It's characterized by a covalently-linked Top1 enzyme at the 3'-end of the break, while the 5'-end of the gap is associated with the complementary strand, exceptions from this are the base lesions and single strand removal [91]. In nicked DNA a staggered double strand break represents a suicide complex (fig. 1.7.1.4 d).

The collision has also been demonstrated because of the p53 expression alteration and for the NKkB activation or phosphorylation of Chk1 and RPA, other essential molecoles in the DNA repair pathway. A persistent inhibition of DNA synthesis is observed for up to 8 hours after CPT removal, probably due to activation of an S-phase checkpoint [105].

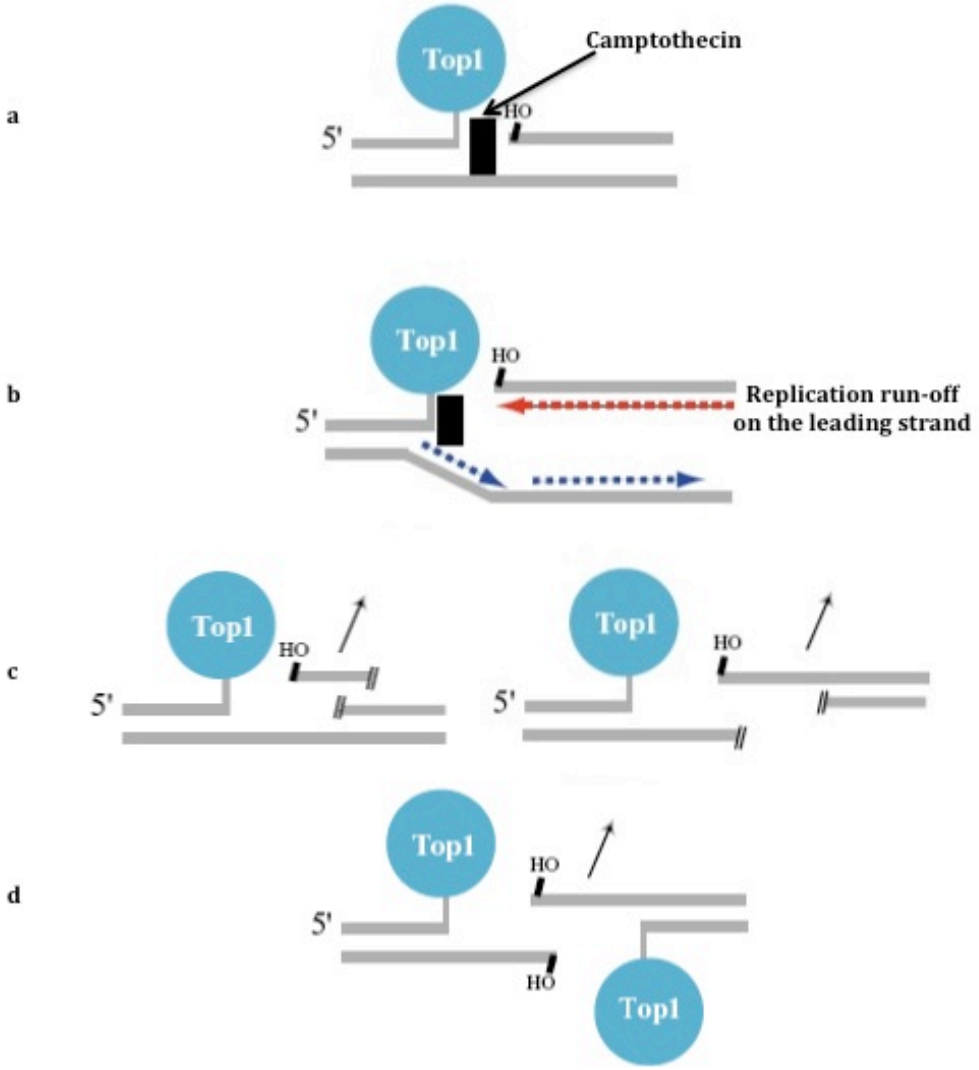

Fig. 1.7.1.4 Schematic rappresentation of Top1 mediated DNA damage: Top1 covalently linked to the 3'end of the broken DNA is shown **a)**. The other strand is a 5'-OH (hydroxyl). Collision beetween replication fork on the leading strand (in red) and camptothecin (black rectangular) generated cleavage complex (Top1-DNA). Lagging strand is represented in blue. Red arrow also showed the proceeding of the replication machinery **b)**. Then a suicide complex results from a single-strand break on the same strand or on the opposite **c)**. Formation of a double-strand break at two Top1 cleavage sites occured **d)**. Figure was edited from [91].

Even if checkpoint activation could prevent DNA damage the replication fork arrests avoid the risk of an other collision. It obvious that DNA repair process has to involve the removal of the Top1 covalent complex, the repair of the double strand breaks and replication fork has to restart.

Several mechanisms have been explained: a tyrosyl DNA phosphodiesterase (Tdp1) and a 3'-flap endonucleases could remove the topoisomerase I (figure 1.7.1.5).

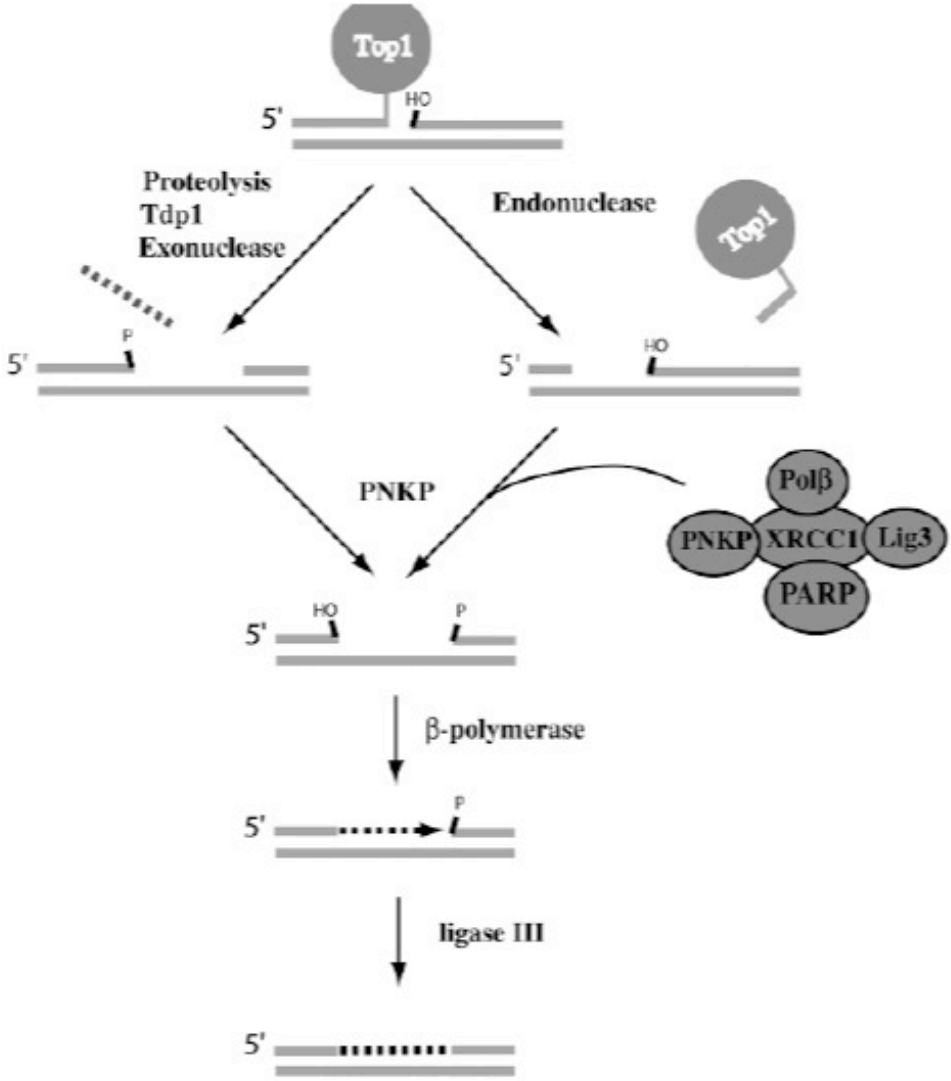

Figure 1.7.1.5 Top1 poison involving in the base exciption repair pathway: Suicide substrate can be processed by both the Tdp1 or an endonuclease. After the Tdp1 action, an exonuclease activity is required for the DNA ends. In either cases a polynucleotide kinase phosphatase (PNKP) produces 3'-hydroxyl and 5'-phosphate ends. PNKP activity is exploited in complex with XRCC1, poly(ADP-ribose) polymerase (PARP), β-polymerase (Polβ) which estended and completed the gap and ligase III (Lig3) binding the DNA ends The figure is adapted from [95].

Although Tdp1 produces a 3'-phosphate end, then the removal of the phosphate is required in the proceeding repair substrate. Thus a polynucleotide kinase phosphatase (PNKP) activity is suggested for processing the 3' phosphate lesions (figure 1.7.1.5).

Moreover it has been observed after CPT treatment, 5'-end of the DSBs during replicating cells a rapidly phosphorylation occured [104]. In figure 1.7.1.5 a, revisited of the well-known base exciption repair (BER) mechanism is reported for the DSBs repair mediated by topoI. Several data suggests the

contribute of PNKP in concert with the poly(ADP-ribose)polymerase (PARP) complex which includes β-polymerase (Polβ) and ligaseIII (Lig3). PARP activity increased in CPT-treated cells and in a CPT-resistant cell-line, indeed Tdp1 co-immunoprecipitates with XRCC1 [106] [107] [108]. PARP has a zinc finger motif allowing to bind both ssDNA and dsDNA breaks, while XRCC1 may functions as a scaffold, no enzymatic activity has been reported, thus the Top1-DNA adduct were processed by PNKP, then β-polymerase replaces the missing DNA segment and LigIII seals the DNA ends.

An other mechanism as topoisomerase ability to religate a non-homologous DNA strand mediated by a bear formation at the 5'-hydroxyl end has been reported [109].

The non-homologous recombination was first reported for the Vaccinia Top1 [110] and to data Vaccinia Top1-mediated DNA religation is commercially used for cloning (Invitrogen Life TEchnology®, Carlsbad, CA).

Indeed extensive DNA damage also followed by CPT treatment could also activates apoptosis involving several biochemical changes leading to cell death [111].

Several parameters controlling cellular sensitivity versus resistance to CPT remain still unclear, and the different rate of the drug accumulation in cell or the level of the cleavage complexes are not strictly related [112]. Downstream events from the cleavable complex have been identified and appear to be more dependent.

The enzyme degradation confers cellular tolerance to CPT treatment and contributes to the repair pathway of Top1-DNA adducts [95]. Moreover CPT treatment reduces the intracellular content of Top1 in several tissue culture cells suggesting to be DNA replication-indipendent [113] [114] [115].

CPT has been observed to induce specific down-regulation of TOP1 via an ubiquitin/26S proteasome pathway [114] and stimulates SUMO-1 conjugation to TOP1 [116] [117], moreover in various culture cell lines has been observed a correlation between Top1 downregulation and CPT resi stance [118]. TOP1 cellular localization, function and activity could be modulated by SUMOylation and contribute to cellular response pathways

[119]. Christensen and collaborators in 2004 demonstrated that sumoylation occured on trapped topoisomerase I-DNA intermediates.

Cell resistance to camptothecin has been reported in both yeast and human cells and this involves several mechanisms in the drug uptake and its regulation. The Multi-Drug Resistance phenotype (MDR) cells reported a reduction in the drug activity, the overexpression of the ABC protein Mdr1 allows the drug efflux. Thus energy-dependent transport processes appears to be dispansable for the drug uptake [120] even if camptothecin metabolism is not well defined yet.

1.8 *top1* mutants in the yeast model organism

TOP1 gene is not essential in budding yeast *Saccharomyces cerevisiae* [121], this feature is only one of the main advantages making this organism a useful tool for genetic and biological studies on topoisomerases. It's a unicellular genetically modifiable eukaryotic and its genome is made of 6000 genes and 16 chromosome fully sequenced (*Saccharomyces* Genome Database [SGD]). The extensive literature refering to gene functions allows investigations at several cellular levels. *S. cerevisiae* has two, type I and type II topoisomerases, thus yeast cells deleted TOP1 (*top1Δ*) are viable because of other DNA topoisomerase II compensation activity [121]. In addition type II enzyme is not CPT sensitive and *top1* strains has been used to demonstrate the selective target of the drug for topoisomerase I. The yeast genome can stably maintain plasmid in low or high copy number, respectevely ARS/CEN and 2μm-based vectors. These also allowed gene expression, because of the well-characterized costitutive or inducible promoters and the presence of selectable markers ensuring the maintenance in yeast cells and in sequence for amplification in bacteria [122]. "pGAL1" promoter is repressed in media containing dextrose, but induced in presence of galactose at high levels. The yeast relatively high rate of homologous recombination, allows also site specific integration of a DNA sequence in its genome. The introduction of plasmid-encoded yeast TOP1 or human TOP1-cDNA sequence restores CPT

sensitivity in *top1Δ* yeast cells, the expression of a catalitically active enzyme is required for drug citotoxicity [123] [124] [86]. Isogenic strains of opposite mating type could be separated and combinated after the meiotic aploide products, allowing to identified unknown alterations in cellular processes after drug treatment, a survey of isogenic strains defective in a specific repair pathway provide useful informations as in the case of *rad52Δ* yeast strains.

Yeast strains have been used in specific amino acid substitution analyses in the topoisomerase I reaction and drug interaction.

In topoisomerase I enzyme the core domains involved in the active site are highly conserved between yeast and human, and N-terminal domain, for which no structure informations are available, diverged in sequence, but not in the basic charged residues and it's required for the catalytic activity [34] [125]. Also for what concern the linker domains, both form are represented by two alpha helices, but are different in lenght and sequences. As already reported, the enzyme surface related to DNA interactions is the main region where CPT sensitive amino acid substitutions occured [17]. Reduced enzyme sensitivity to CPT was observed in human Top1 mutant in linker domain [30] according to the domain flexibility reported in binding topotecan from the crystallografic data. Several mutations have been identified around the active site tyrosine, both in human and yeast Top1, Top1Y723F mutation abolish the catalytic activity. Counterwise Top1N726S mutation showed CPT resistance without changes in the activity.

In Top1T722A mutant enzyme, acts as a CPT mimetic, reducing the rate of DNA religation, without any observed alteration in DNA binding or cleavage [126].

Other several mutations have been reported to affect camptothecin citotoxicity *in vitro*, six residues localized in a cluster in the *lip* region, Phe361Ser, Gly363Ser (also substitutions with Val and Cys showed same effect), Arg364His, Glu418Lys, Gly503Ser, Asp533Gly lead to resi stance [26]. Asp533 mutation is the only for which is reported a direct DNA-enzyme-topotecan interaction from crystallographic data. In addition Asn722 residue is located adjacent to the catalytic Tyr723 and contribute to a water mediated hydrogen bond with the drug in the ternary complex [127].

Flexibility of the linker domain has been showed by Ala653Pro mutation, which leads to an increased religation rate, and CPT binding is unpermitted [30]. One interesting mutation is represented by Thr729Ala, already pointed as resistant to the CPT analog, irinotecan, in a human lung cancer cell line [128] and from crystallographic data could impacte the contact with camptothecin because of its water-mediation function. Benedetti and co-workers demonstrated in yeast CPT resistance, when this residue is mutated in Glu, Lys or Pro [129] [130].
Single residue mutations can dramatically alter the Top1 enzymology and drug sensitivity suggesting also to induce similar DNA lesions pathway as CPT, according to the increasing stability of the covalent complex.

1.9 Distinct mechanism for positive and negative relaxation.

As already reported human topoisomerase I is able to relax supercoils of both signs and the direction of rotation will depend on the sign of the supercoils to be removed according to the controlled rotation model.
Real-time dynamics, in a single molecule approach may facilitate the understanding of positive supercoils accumulation and mechanism. Koster et al. in 2007 provided a direct determination of the increased life-time of the covalent ternary complex (DNA-protein-drug) using single molecules magnetic twezers method. In addition it has been demonstrated that topotecan interferes with DNA uncoiling resulting in a better relaxation of negatively supercoiled than positively [131]. As reported two models have been proposed for strand passage for the topoisomerization reaction in type I subfamily. The *enzyme-bridging model* in which enzyme stabilized a gate through the nick and the *strand rotation model* in which one end of the nick is driven to rotate around the intact strand by the supercoiling free energy [132]. Energy of the supercoils are necessary and allowed the DNA rotation in a driving torque dependent manner (fig.1.9.1).

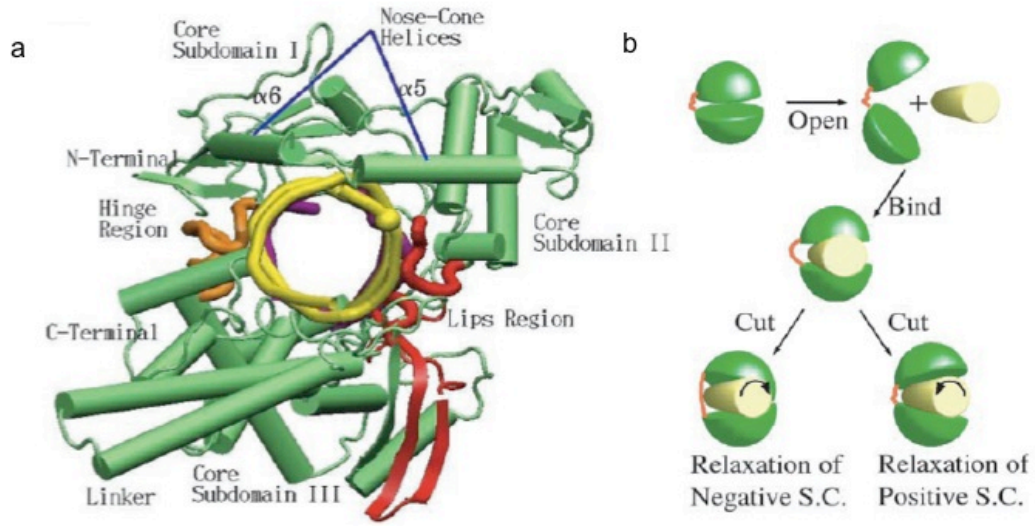

Fig. 1.9.1 a)DNA-hTop1 covalent complex, b)mechanism of relaxation of negative and positive supercoils. Different rotation is indicated by the arrows and the flexible *hinge* (represented with a red line connecting upper and lower lobe) by strechting and bending motion allows opened and closed protein conformation. The figure is adapted from [132].

From Champoux and co-workers crystallographic data, appears that when the upper and lower lobes are closed they bring together the two opposable lips localized on the other side respect to the *hinge* region fig. 1.9.1 [132].

The strand rotation model for both positive and negative supercoils is explained imaging that protein widely opens up its lips, while getting hinged on the *hinge* side, and binds the incoming DNA duplex. Then lips are closed and cleavage of one strand occured. The resulting cut allows the rotation of the DNA duplex downstream of the nick. The number of time of rotation correspond to the DNA linking number variation. Moreover if DNA is overwound, rotation for relaxing positive supercoils occured, otherwise if underwound the negative DNA substrate is preferred. Enzyme again opens up the lips after religation step and the product of reaction is realesed less-supercoiled.

The *controlled rotation model* probably is driven by charge residues of the nose-cone and the linker flexibility that interacts electrostatically with the downstream DNA strand. The accomodation of the duplex inside the enzyme structure should allow the rotation and requires high flexibility of the structure.

Sari and Andricioei simulations proposed that the removal of positive supercoils requires opening of the lips by 10-14 Å, while removal of negative supercoils involves the *hinge* region stretching by 12 Å. The *hinge* involved amino-acids beetween Leu429 and ends with Lys436.

This model proposes that the enzyme is not a symmetrical bolt around the DNA molecule, but depending from sense of rotation, the double helix will hits different residues. This observation is also based on two different experiments that analyzed strand rotation. Residues of the lips region where substituted by opposing cysteines, to covalently block the enzyme in a closed clamp conformation. When the clamp was tighter the strand rotation would not occur and oppositely when the two cysteines where positioned to form a more flexible clamp, strand rotation could still occur.

The linker domain and the nose-cone helices are also involved in the relaxation of positive and negative substrate respectevely.

Moreover crystallographic data of the human TOP1 in the region between 201 and 205 residues showed no interactions with the DNA substrate nevertheless coordinates DNA rotation or clamp movement. In addition several interactions between residues were reported, as the Trp-203 and Trp-205 with the His-346 and Gly-437 at the level of the *hinge* [24].

Simulation analyses of the 203-214 residues showed a significant flexibility and a correlated movement between 203-208 aminoacids with the helix 8 in core subdomail III; a N-terminal portion in the linker domain; the catalytic region around the Tyr723 and 22-23 helices of the C-terminal domain [133].

Bjornsti and Dekker collaborators in 2007 demonstrated with the single molecule approach that positive supercoils accumulate in yeast cells upon CPT-induced inhibition of topoisomerase I relaxation activity. Positive supercoils accumulated during transcription and replication suggesting a direct link with the CPT poisoning of the enzyme withouth altering its catalytical activity [131]. These data together with Sari& Andricioei studies suggested a different drug responses of the mutated enzymes when relaxing positive or negative supercoils. These also reflected different mechanism of strand rotation in order to remove supercoils of opposite sign.

Several mutations at N-terminal human topoisomerase I has been reported to be more sensitive to CPT during relaxation of positively versus negatevely supercoils [134]. In particolar human topoisomerase I enzymes reported Trp205Gly mutation, and deletion of 191-206 residues suggest a role for the Trp-205 and surrounding residues in the control of strand rotation during negative supercoiled removal, but not positive [134]. The absence of 191-206 residue allows to underline the constitutively stretched conformation of the *hinge* region leading to an uncontrolled clockwise strand rotation for removing negative substrate. According to Sari& Andricioei model the *hinge* region may have no relevant influences on the *lips* domain and the involvement in the positive supercoiled relaxation.

All these data suggest that a topology sensor could exist in this correlated movements between the linker and the N-terminal domains resulting in the active site recruitment. The changing in the clamp conformation appears to be driven by the Trp205 *hinge*-pivot mechanism.

2. AIM OF THE PROJECT

The human DNA topoisomerase I (hTopoIB) plays a key role in DNA topology regulation associated with transcription, replication and recombination. This enzyme introduce a transient break in a single strand of the DNA duplex, and allows strand rotation at the site of DNA scission and the release of the superhelical tension. In this way hTopoIB is able to relax both negative and positive supercoils, respectively before rejoining the cleaved DNA strand. Human topoisomerase IB acts as a clamp around the DNA, performing the opening and then the closure for the release of the substrate. This can occur thanks to key residues in the protein structure. To date these features remain unclear, even if 30 years are passed since the protein discovery. The most complete crystal structure showed the enzyme together with a 22 bp dsDNA as a bilobed molecule where domain movements are necessary to bind and rotate the DNA. Recent studies suggested the N-terminal domain to be involved in controlling strand rotation together with the linker domain. Other evidences based on Sari et Andricioaei data [132] gave informations about the possible role of the *lips* concerning the relaxation of the positive supercoils and about the strechting of the *hinge* for the negative DNA substrate. The enzyme could wraps the DNA from one side bringing together the upper and lower lobe through the two opposable *lips* and on the other side with the *hinge*.

The crystal structure of the enzyme shows 14 residues located in the N-terminal domain but close to the *hinge* region, suggesting that these residues could interact with the subsequent α-helix and in particular with the first residue Pro431. Staker and collaborators crystallographic data [127] show that this proline can act as a pivot allowing the changing in conformation of the protein from an open to a closed structure.

In order to investigate the involvement of the *hinge* region in controlling the rotation, Pro431 was substituted by a glycine (Gly). This amino acid lacks in a side chain and is the smallest residue because of its two hydrogen

substituents. Alteration of the catalityc activity after mutation was investigated.

Furthermore Arg434 residue is located at the top of the *hinge* in proximity of the Trp205 (N-terminal domain) as reported in figure 2.1. Indeed molecular modeling suggested mutations at 434 residue could also be crucial for changing in the electrostatic interations with the surronding and in particular with the proximal Trp205.

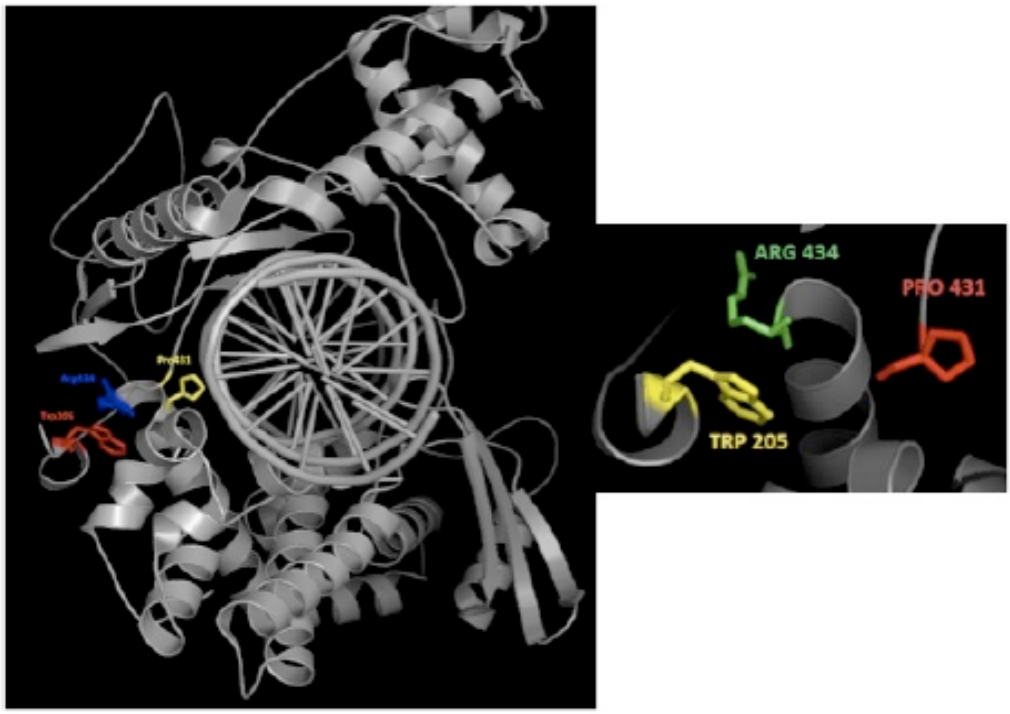

Figure 2.1: Top1 structure to the left protein is represented together with the DNA substrate and residues of interest were coloured in red (trp205), blue (arg434) and yellow (pro431). To the right a zoom at the top of the *hinge* region and amino acids interactions were showed.

The substitutions of Arg434 with an alanine (R434A), and with a cysteine (R434C) are of great interest to valuate the change in the structure and interaction with the DNA substrate. Furthermore the cysteine could performe a disulfide bond if an other cysteine locally occurred. Using the *Saccharomyces cerevisiae* the effect of these mutations was analyzed. Levels of their catalytic activity were measured *in vitro* and sensitivity to the camptothecin inhibitor was also tested. relaxation.

In order to valuate the contribute of the *hinge* and the suspected key residues, relaxation activity of positive and negative supercoils of these mutants was also investigated.

The relaxation ability was performed at low and high ionic strength condition, revealing interesting mutant behavior in non-physiological condition.

3. MATERIALS AND METHODS

3.1 Media

All reported procedures are for 1 liter solutions and were autoclaved at 121^0C for 15 minutes before use.

Ura- selective liquid/solid media

yeast nitrose base: 1.7 g (no aminoacid and ammonium sulphate inside);
ammonium sulphate: 5.0 g;
ura – drop out (composition: adenine 4 g, tryptophan 4g, histidine 2g, arginine 2g, methionine 2g, tyrosine 3g, leucine 6g, lysine 3g, phenylalanine 5g, threonine 20g, aspartate 10g): 0.7 gr;
NaOH 2N: 1 ml;
1M Hepes pH 7.5: 24 ml (only in presence of camptothecin in the mixture);
Agar: 20 g only for solid media;
Before use, sterile 20% sugar solutions (as reported in the procedures: glucose, galactose or raffinose were prepared with 20 g of powder sugar in 100 ml of milliQ dH_2O and sterilized by filtration) were added to a final 2% concentration.

YPD dex liquid/solid media

Bacto™ yeast extract: 10 g;
Bacto™ peptone: 20 g;
Glucose: 20% w/v;
Agar: 20 g only for solid media.

Luria-Bertani (LB) medium

Bacto™ tryptone: 10 g;
Difco™ yeast extract: 5 g;
NaCl: 10 g;
Agar: 20 g only for solid media.
LB-amp medium: 4 ml of ampicillin (25 mg/ml) were added to 1 liter of LB medium.

NZY+ pH 7.5

NZ ammine: 10 g;

Difco™ yeast extract: 5 g;

NaCl: 5 g.

Before use were added: $MgCl_2$ 1M (12,5 ml)

$MgSO_4$ 1M (12,5 ml)

Glucose 20% w/v (20 ml)

3.2 Buffers

10X TBE pH 8.3 1 liter solution

Tris: 6,05 g;

Boric Acid: 3,9 g;

EDTA: 0,37 g.

10X TE 1 liter solution

10mM Tris-HCl pH 7.5;

1mM EDTA.

Tris-HCl

0.5 M Tris pH 6.8 adjusted with HCl;

or

3 M Tris pH 8.9 adjusted with HCl.

1X TEEG pH 7.5 1 liter solution

1M Tris: 50 ml;

0.5 M EDTA: 2ml;

0.5 M EGTA: 2ml;

100% glycerol: 100 ml;

NaOH to adjust pH.

10X G-Buffer Topoisomerase reaction buffer

20 mM Tris pH 7.5;

0.1 mM Na_2EDTA;

10mM $MgCl_2$;

50 μg/ml acetylated BSA.

3.3 Drugs

Ampicillin (AMP) provided by Sigma® was dissolved in 50% distilled water, 50% absolute etanol and 25 mg/ml aliquots were stored at -20^{0}C.

Camptothecin (CPT) provided by Sigma® was dissolved in DMSO and 4 mg/ml aliquots were prepared and stored at -20^{0}C.

3.4 Yeast strains

Saccharomyces cerevisiae strain EKY3 (MATα, ura3-52, his3Δ200, leu2Δ1, trpΔ63, top1::TRP1), wild-type like yeast strain.

Used yeast strain lacks of the yeast topoisomerase I gene (yTOP1) allowing to be trasformed with an expression vector containing an inducible promoter. In addition URA and TRP genes, involved in the uracil and tryptophan metabolism respectevely, are deleted to reach two selective markers.

3.5. Plasmids

Yeast strain was transformed with inducible expression vector YCp, containing the human topoisomerase I gene (hTop1) under the control of the GAL1 promoter. The gene was engineered at the N-terminal with a 24 nucleotide sequence expressing a positevely charged octa-peptide, called Flag epitope: Asp-Tyr-Lys-Asp-Asp-Asp-Asp-Lys (Sigma®).

The construct allowed the analysis and purification of the enzyme to be more efficient.

-YCpGAL1-flag-hTop1

Single copy plasmid YCpGAL1-hTop1 [136] is a 12,000bp vector (fig.3.1) carrying a bacterial replication origin (oriC), a bacterial cells growth selective marker URA3 (gene for uracil production), a bacterial cells growth selective marker (Amp^r, ampicillin resistance), a yeast replication origin (ARS, *Autonomous Replicating Sequence*), a yeast derivatived centromeric sequence (CEN4) and a yeast inducible expression promoter GAL1 (galactose).

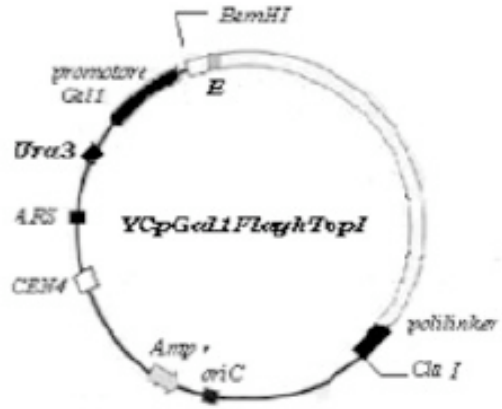

Fig. 3.1: YCpGAL1*Flag*hTop1 Single copy plasmid 12,000bp.

-pBS-SK

Plasmid lenght 3000 bp with a pUC origin, a lac promoter (817-938), a multiple cloning site (653-760) with a EcoRI restriction site and a bacterial cells growth selective marker (Amp^r, 1976-2833).

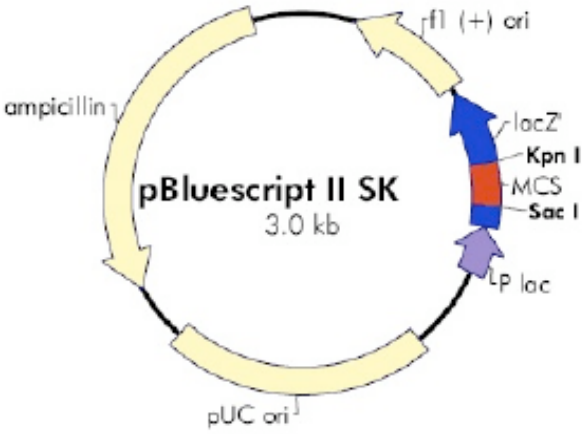

Fig.3.2: pBS plasmid 3,000 bp, MCS multiple cloning site 653-760 bp, http://image.hudsonalpha.org/html/libs/pBluescriptIISK+map.pdf

-pAk3-1

negatively supercoiled plasmid DNA, above 2300 pb in lenght. It's the pUC plasmid engeneered with a sequence containing the preferential site of binding for the topoisomerase.

3.6 Site direct mutagenesis

Mutations at P431, R434 and W205 were generated throught QuikChange® Lightning Site-Directed Mutagenesis Kit (MMedical®). Plasmids reported the insertion for the topoisomerase gene were subcloned into YCpGal1-hTop1 plasmid, in a fragment with *BamHI – ClaI* restriction sites. All the constructs used reported also the recognizable sequence: " DYKDDDDK ", the epitope don't modify the enzyme activity and drug sensitivity both *in vivo* and *in vitro.*

3.6.1 Procedures (fig. 3.3):

1) Mutant strand synthesis throught the performance of the thermal cycling (denaturation, annealing of the primer containing mutation of interest and final extension);
2) Faster *DpnI* digestion of template (metilated sequence were recognized and digested);
3) Transformation (ultracompetent cells XL10-Gold allowed the repair on the mutated plasmid).

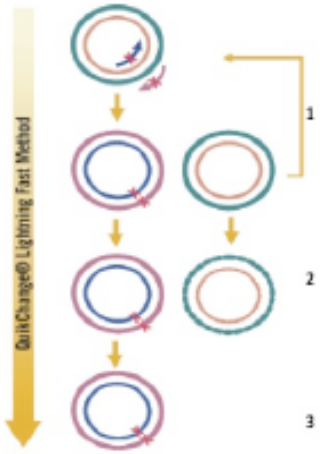

Fig.3.3: Site direct mutagenesis procedure
http://www.qcbio.com/stratagene/210518.pdf

3.6.2 Preparation of chemo-competent bacteria

Materials:

15 ml falcon tubes;

E. coli XL10 Gold® Ultracompetent cells (Agilent Stratagene);

β-mercaptoethanol;

plasmid DNA;

NZY$^+$ broth;

LB Ampicillin agar plates.

Oligonucleotides cointaining interested mutations were synthesized according the informations provided by the mutagenesis protocol kit. Primers were obtained by Eurofins mwg (fig. 3.4): https://ecom.mwgdna.com/services/home.tcl.

Mutations at level of the ***hinge*** region: Pro431Gly, Arg434Cys, Arg434Ala

Mutation at the level of the ***N-terminal*** domain: Trp205Cys

These are shown below:

N.	Primer Name	[Conc.]	Purify	Sequence
1	P431GFw	0.01 µmol	Hypur	CCA TTA AAT ACA TCA TGC TTA ACG GTA GTT CAC GAA TCA AGG GTG AG (47 bp)
2	P431GRw	0.01 µmol	Hypur	CTC ACC CTT GAT TCG TGA ACT ACC GTT AAG CAT GAT GTA TTT AAT GG (47 bp)
3	R434AFw	0.01 µmol	Hypur	CAT GCT TAA CCC TAG TTC AGC AAT CAA GGG TGA GAA GGA C (40 bp)
4	R434ARw	0.01 µmol	Hypur	GTC CTT CTC ACC CTT GAT TGC TGA ACT AGG GTT AAG CAT G (40 bp)
5	R434CFw	0.01 µmol	Hypur	CAT GCT TAA CCC TAG TTC ATG CAT CAA GGG TGA GAA GGA CT (41 bp)
6	R434CRw	0.01 µmol	Hypur	AGT CCT TCT CAC CCT TGA TGC ATG AAC TAG GGT TAA GCA TG (41 bp)
7	W205CFw	0.01 µmol	Hypur	GAA CAG AAG TGG AAA TGC TGG GAA GAA GAG CGC TA (35 bp)
8	W205CRw	0.01 µmol	Hypur	TAG CGC TCT TCT TCC CAG CAT TTC CAC TTC TGT TC (35 bp)

Fig. 3.4: Overview of primer sequences and residue mutated.

Preparation of the sample reactions:

10x reaction buffer;

10-100 ng dsDNA template;

125 ng oligonucleotide primer FW;

125 ng oligonucleotide primer RW;

1μl of dNTPs mix;

1,5 μl of QuikSolution reagent;

dH_2O to a final volume of 50 μl.

Finally 1 μl of QuikChange® Lightning Enzyme was added to the mixture.

The thermal cycler was performed at these parameters (tab. 3.1):

Step	Number of cycles	Temperature	Time
Denaturation	1	95 ^{0}C	2 min
Annealing	18	95 ^{0}C	20 sec
		60 ^{0}C	10 sec
		68 ^{0}C	30sec/Kb = 6 min
Extension	1	68 ^{0}C	5 min

Tab. 3.1: Thermal cycle parameters, plasmid lenght considered was 12,000bp.

At the end of the amplification process 2 μl of the provided *DpnI* restriction enzyme were directly added to each amplification reaction and incubated for 5 min at 37^{0}C, obtaining the digestion of the parental nonmutated supercoiled dsDNA.

3.7 Transformation of the ultracompetent cells

All procedures were performed on ice. Firstly ultracompetent cells were added into a 15 ml falcon tube, then 2 μl of *β*-mercaptoethanol were gently added and swirled for 2 min.

DpnI-treated DNA from each sample was transfered and incubated for 30 min.

Then the tubes were heat-pulsed in a 42^{0}C water bath for 30 sec, this is the most critical step, and incubated on ice for 2 min.

Finally 0,5 ml of NZY+ broth, pre-heated in a 42^{0}C water bath , were added and incubated for 1 hour at 37^{0}C with shaking at 200 rpm.
An appropriate volume of the sample was plated for each transformation on LB-ampicillin and incubated for at least 16 hours at 37^{0}C.

3.8 Plasmids extraction and enzymatic digestion

MATERIALS:
LB liquid medium;
Ampicillin 25 mg/ml;
DNAs plasmid of interest;
Quiagen Kit DNA extraction;
10X Buffer Enzyme;
restriction enzyme (BamHI- EcoRI- ClaI);
10X TBE buffer: 0.89 M Tris-borate, 20 mM EDTA, pH 8.0;
6X Loading Buffer: 30% Ficoll (type 400), 0,1% bromophenol blue, 0,1% xylene cyanol;
gel electrophoresis apparatus;
Ethidium Bromide (EtBr): 10 mg/ml dissolved in dH_2O.

1) 1 colony for sample was picked and added to 5 ml LB plus ampicillin liquid medium for more then 16 hours at 37^{0}C and 220 rpm.
2) The day after Dna extraction was carried out with Quiagen Kit starting from grown cell culture.
3) Then 500 ng obtained DNAs, were incubated with 10X enzyme buffer, 20u/μl enzyme and dH_2O to a final volume of 20 μl for 30 min at 37^{0}C.
Then samples, treated with loading buffer, were loaded in 1% agarose gel. Results were analyzed with UV transilluminator.

3.9 Yeast strain transfection with YCp plasmids: lithium acetate method

MATERIALS:
10X TE (100mM Tris pH 7.5, 10 mM EDTA);

1M Lithium acetate (LiOAc);
50% (w/v) PEG 3350 sterilized and filtrated;
Sigma® salmon sperm (10ng/μl);
YPD-2% glu liquid medium and plates;
YPD-2% gal liquid medium and plates;
YCp plasmids carrying the interested mutation.

4-5 yeast colonies were picked up and grown in YPD 2% gal liquid medium overnight at 30^0C. The day after $O.D._{600}$ was measured, and if it was more than 1, it was diluted to $O.D._{600}$ 0.7 in YPD 2% glu. For each transfection 10 ml of cell culture was calculated and set up. When reaching the $O.D._{600}$ in a range 0.9 - 1.1, cells were centrifuged for 10 minutes at 2800 rpm. The supernatant was discarded and pellet resuspended in TE-LiOAc solution (1/100 of the original culture volume).
100 μl of cell suspension were aliquoted for each sample, then 100 ng denaturated salmon sperm DNA and 1000 ng plasmid DNAs of interest were added on.
After a resuspension by pipetting, 350 μl of TE-LiOAc-40% PEG solution were added. Samples were then incubated by slow-shaking at 24^0C for 30 minutes, following by 42^0C for 15 minutes.
200 μl of each cell culture were spread on selective plates and incubated at 30^0C until the yeast colonies growth.

3.10 *In vivo* viability assay: spot test

MATERIALS:
Transfected yeast cells;
ura- 2% glucose liquid medium;
ura- 2% glucose plates;
ura- 2% glucose plates added with camptothecin (concentration from 0,01 μg/ml to 5 μg/ml);
ura- 2% galactose plates;

ura- 2% galactose plates with camptothecin (concentration from 0,01 μg/ml to 5 μg/ml).

Single yeast strain transformant, previously transfected by lithium acetate tratment with YCp construct containing the different mutated Top1 gene, were picked from ura- 2% glucose plates and grown overnight in 5 ml of ura- 2% glucose liquid medium at 30^0C.

The second day culture were diluted to an $O.D._{595}$ value of 0.3. Three 10-fold serial dilutions were calculated and for each yeast suspension 5 μl were spotted on the selected plates.

The number of cells forming colonies were scored following incubation at 30^0C for 72 hours.

3.11 Whatman® P11 phosphocellulose resin preparation and activation

MATERIALS:

1 M K_2HPO_4;

0,5 M KPO_4 added with 1mM EDTA pH 7;

Whatman® P11 phosphocellulose resin;

1 liter Buchner funnel;

3 MM® filter paper.

First day:

250 grams of phosphocellulose resin were slowly poured into a 2 liters graduated cylinder, where 1,5 liters of 1mM EDTA were previously added on. Mixed and incubated overnight at room temperature.

Second day:

The resin was slowly resuspended by inverting the cylinder and let settle for 5-10 min at time and repeated until getting a visible layer in the lower part of cylinder. With a vacuum pump the upper layer cointaining fine particles and watery solvent was removed.

Then fresh distilled water was added to the residual lower layer, mixed and let settle again, this was repeated until getting a clear and homogeneus lower layer.

When the resin was ready to use, 2 layers of 3MM filter paper were prepared and put on the Buchner funnel inserted in a 4 liters vacuum flask, then the resin was added on, allowing through the vacuum filtration the clearing of the liquid suspension.

0,5M NaOH was added into the funnel and in order to avoid the filter pores obstructions the suspension was stirred by hands. pH was constantly mesured and constantly kept to value 9 adding NaOH.

Finally was checked on filtered liquid, NaOH was removed and resin was let settle for 5 min.

Suspension was washed with distilled H_2O once and then 0,5 M HCl was added in order to get a pH solution above value of 3. Resuspension and filtration steps were repeated.

After 5 minutes and one wash with distilled water, K_2HPO_4 was added and final pH of 7 has to be reached.

Finally the resin was washed two times and resuspended in 0,5 M KPO_4 – 1mM EDTA pH 7 solution.

3.12 Human DNA topoisomerase purification from yeast

MATERIALS

Complete Protease Inhibitor cocktail (Roche®) 1 tablet in 50 ml of TEEG 1X buffer;

50X Sodium Fluoride;

100X Sodium Bisulfite;

Saturated ammonium sulphate solution;

1X TEEG buffer;

S. cerevisiae EKY3 strain;

“oak ridge” tubes;

2 ml Biorad® Poly-prep® columns;

Glass beads, acid-washed, Sigma® (diameter 425- 600 μm);

Activated Whatman® P11 phosphocellulose resin;

Potassium chloride;

Ammonium sulphate;

Ura-2% glucose liquid medium;

Ura-raffinose 2% liquid medium;

20% (w/v) galactose solution;

Protein Assay solution Biorad®;

Bovine Serum Albumin (BSA) Sigma® 10 mg / ml.

Individual colonies (4-6) of transformed EKY3 cells containing plasmid encoding human Top1 protein (wild type and mutants isoforms) no more than 2 week old were grown in 15 ml of drop out media overnight at 30^0C at 180 rpm.

The day after cultures $O.D._{595}$ was measured and diluted 1:100 in ura-raffinose 2% medium and grown to an $O.D._{595}$ value of 0,8-1. Incubated overnight at 30^0C at 180 rpm.

Cells were then induced by the addition of 2% galactose w/v, for 6-8 hours. Then cultures were centrifuged for 15 min at 3,200 rpm at 4^0C and precipitated cells were washed with dH_2O and centrifuged again. Then pellets were resuspended in 1X TEEG buffer added with a protease inhibitor cocktail tablet (final concentration 100 μg/ml, Roche®), 50X sodium fluoride (NaF), 100X sodium bisulfite ($NaHSO_3$). 2ml per gram of cells of inhibitor coctail solution were used. Cells were stored at -70^0C.

Cultures were poured into pre-chilled and sterile 250 ml centrifuge bottles, and glass beads for a half volume were added. In cold room, breakage of the cells was mechanically performed by vortexing for 30 sec, followed by 30 sec of standing on ice to a total of 30 min. Then tubes were centrifuged for 30 min at 14,350 rpm at 4^0C allowing cellular debris precipitation.

After the centrifugation, bottles were placed on ice and supernatants were moved to clean tubes. Those are the crude extracts kept for the Bradford test.

3.12.1 BRADFORD TEST

To measure total protein content of crude cell extract "Protein Assay Solution" Biorad® and bovine serum albumin (BSA) Sigma® for the standars preparation, were used. The BSA standard concentrations interpolated the sample concentrations. Five, 1 ml solution, diluitions: 1mg/ml, 2 mg/ml, 4 mg/ml, 6 mg/ml, 8 mg/ml, were prepared and the protein sample was measured after 1:5 diluition.

For each standard and aliquot of crude extract, 1 ml of diluted dye was added to the disposable cuvet, mixed and let settle at room temperature for 5 minutes. For the crude extract 2 μl sample was added to the mix and $O.D._{595}$ was determined by spectrophotometry. Total protein concentration for each sample was measured and above 6 mg/ml purification can proceed.

3.13 Ammonium sulphate purification procedure

In order to reach a saturated solution of ammonium sulphate (80% w/v) precipitation was performed. For each ml of supernatant volume previously obtained, 0,516 g of ammonium sulphate were added. The suspension was rocked overnight in cold room.

The day after samples were centrifuged at 15000 rpm, 4^0C for 30 minutes. Pellets obtained were resuspended in 1X TEEG added with the protease inhibitor cocktail solution in a equal volume to that of the starting extract.

Electrical conductivity for each sample was measured and compared to that of a 0,2 M KCl 1X TEEG solution.

In order to reach the binding of the protein to the resin, conductivity value must be lower or equal, otherwise the final volume was diluted with 1X TEEG added with protease inhibitor cocktail solution.

Activated resin was equilibrated in cold room, in a 50 ml falcon tube with 1M KCl-5X TEE – 1X glycerol, then buffer was removed and an equal volume of 0,2M KCl 1X TEEG was added. For 2 liter of starting yeast culture 2 ml of the resin were used, poured into column and washed 5 times with 0,2 M KCl 1X

TEEG. Then resin was equilibrated with 5 volumes of 0,2 M KCl 1X TEEG added with inhibitors and washed again.
Sample was now loaded in the column, elution occured with increasing KCl-1X TEEG buffer, from 0,2- 0,4- 0,6- 0,8 – 1 mM KCl. Fractions from 0,2 to 0,4 M KCl were collected in 50 ml Falcon tubes and samples from 0,6 - 0,8 to 1 M KCl were aliquoted in 2 ml Eppendorf® tubes, in a 1:1 mixture with 100% glycerol previously added. After homogenization, samples were stored at -20^{0}C.
All fractions were tested with a relaxation activity assay as followed described and positive samples were collected together and diluted with 1X TEEG with inhibitors protease solution to obtain a conductivity close to that of 150 mM KCl 1X TEEG buffer.

3.14 Affinity Chromatography procedure

To avoid contaminants in purified proteins samples were loaded on anti-flag column (3X FLAG PEPTIDE Sigma®), the binding was ensured by the flag peptide located to the N-terminal of protein structure as previous described.
The affinity chromatography procedure was performed in cold room, first column was set up and a drainage tube was attached to control the flow rate. Then a vial of ANTI-FLAG M2 (Sigma®) affinity gel was suspended to make a uniform gel beads mixture in the column. the sample previously washed, was loaded onto the column under gravity flow and binding can occured. Then washing the column, elution of 3X FLAG Fusion Proteins was carried on through the competition with 100 μg/ml 3X FLAG Peptide (Sigma®) diluted in 1X TEEG-150 mM KCl. Eluated samples were fractioned in 1 ml aliquots added with 100% glycerol.

3.15 SDS-Polyacrylamide Electrophoresis Gel (SDS-PAGE)

MATERIALS:
Biorad® 30% bisacrylamide / acrilamide (37.5:1);
1,5 M pH 6.8 Tris HCl;

1,5 M pH 8.8 Tris HCl;

60% w/v Sucrose Sigma®;

10% w/v SDS Biorad® solution;

N,N,N',N'-Tetramethylethylenediamine (TEMED Biorad®);

100 mg/ml Ammonium Persulfate (Sigma® > 98%);

Promega Broad range protein marker;

4X sample buffer (composition: 20% SDS; bromophenol blue traces; 125 mM Tris HCl pH 6,8; 50 mM DTT);

10X RUNNING BUFFER: (250 mM Tris, 250 mM Glycine, 1% SDS).

10% acrilamide gels were prepared as reported in the table 3.2:

2 gels	Running gel	Stacking gel
Distilled H_2O	3,19 ml	2,58 ml
30% bisacrylamide/ acrilamide	2,76 ml	433 µl
1,5 M pH 8.8 Tris HCl	2,5 ml	
1,5 M pH 6.8 Tris HCl		1 ml
10% w/v SDS	50 µl	20 µl
60% w/v Sucrose	1,5 ml	
APS 100mg/ml	100 µl	40 µl
Temed	4 µl	4 µl
Total volume (ml)	10 ml	4 ml

Tab. 3.2: schematic procedure for 10% acrilamide gels

The sample migration was performed at 100 volts in the stacking and 150 volts in the running of the gel.

3.16 Colloidal coomassie staining

www.jove.com/index/details.stp?ID=1431 [137]

STAINING SOLUTION:

Coomassie solution:

0.02% (w/v) CBB G-250;

5% (w/v) aluminum sulfate-(14-18)-hydrate;
10% (v/v) ethanol (96%);
2% (v/v) orthophosphoric acid (85%).

Aluminium sulfate was dissolved in Milli-Q water, then ethanol was added and CBB G-250 mixed to the solution. When completely dissolved phosphoric acid was added, allowing Coomassie molecole aggregating into their colloidal state.
Finally Milli-Q water was added to the desidered volume.

DESTAINING SOLUTION:
10% (v/v) ethanol (96%);
2% (v/v) orthophosphoric acid (85%);
After the removal of the gel from the glass of the electrophoretic apparatus, this was washed three times with Milli-Q water for 5 minutes on a horizontal shaker.
Then Coomassie solution was shaked and put on the gel overnight at room temperature.
After the staining procedure Coomassie was removed and gel was rinsed twice with Milli-Q water.
Destaining solution was added on the gel and let for more then 4 hours.

3.17 Western blot

MATERIALS:
polyacrylamide gel;
3MM Whatman® paper;
transfer apparatus;
nitrocellulose membrane Amersham®;
1X transfer buffer (reagents needed for 2Lt: 28,8 g glycine, 6,04 g Tris base, 200 ml methanol 100%, 1,6 L dH_2O);
1X TBS (50 mM pH 7.6 Tris, 150 mM NaCl);
Ponceau S solution Sigma®;

TBS-Tween 20 (50mM pH 7.6 Tris, 150 mM NaCl, 0,1% v/v Sigma® Tween 20);
3% milk solution Fluka® biochemika (1,5 g skim milk powder in 50 ml TBS);
ANTI-FLAG M2-Alkaline Phosphatase Conjugate Sigma® (1mg/ml);
Sodium azide;
BCIP/NBT- blue liquid substrate system Sigma®.

Nitrocellulose membrane and six 3MM Whatman® sheets were cut to completely cover the gel surface. All components were soaked in the 1X transfer buffer previously put into a basin. The transfer apparatus was made up of one sponge, three 3MM sheets, then the nitrocellulose membrane, the gel, the other three 3MM sheets and finally an other sponge. The transfer process was carried out at 300 mA for 1 hour. At the end of the transfer, nitrocellulose membrane was incubated with Ponceau S solution in order to directly visualize proteins on the membrane. If the blot successfully occurs membrane was firstly washed docking in a 3% milk solution for more then 1 hour and after 3 x 15 min TBS-TWEEN 20 washes was incubated in M2 ANTI-FLAG antibody solution (1:200 dilution in TBS-Tween 20. Added with antibacterial agent sodium azide) overnight at 4^0C. The day after, 3 x 15 min TBS-TWEEN 20 washes were applied to membrane, then BCIP/NBT solution was added on. BCIP/NBT contains 5-Bromo-4-Chloro-3-Indolyl sodium Phosphate (BCIP), the substrate for alkaline phosphatase and Nitro-Blue Tetrazolium (NBT) chloride, allowing hydrolization of BCIP and the visualization of dark blue precipitate. These precipitates appear at the level of the FLAG epitope located at the N-terminal domain of the human topoisomerase I protein.

3.18 Generation of positively supercoiled plasmids: Reverse Gyrase activity assay

Materials:
plasmid of interest (200 ng);

reverse gyrase buffer (composition: 35mM Tris-HCl pH 7.0; 0.1 mM Na_2EDTA; 30 mM $MgCl_2$; 2 mM DTT; 1mM ATP);
purified reverse gyrase (40-100 ng and kindly provided by Valenti A., Ciaramella M. CNR NAPLES).

All reagents were added to a final 20 μl of mixture and incubated at 70^0C for 5 min. Reaction was stopped by adding 20% SDS. For the control sample plasmid alone and plasmid with reverse gyrase but withouth ATP were used.
The reaction products were analyzed by bidimensional agarose gel electrophoresis (2D gels) figure 3.5, with ethidium bromide (0.01 μg/ml) in the second dimension. After both electrophoresis, gels were stained with ethidium bromide (1μg/ml), and sample were quantified and visualized by UV light with a Chemi-doc apparatus (Bio-Rad, Hercules, CA. USA)

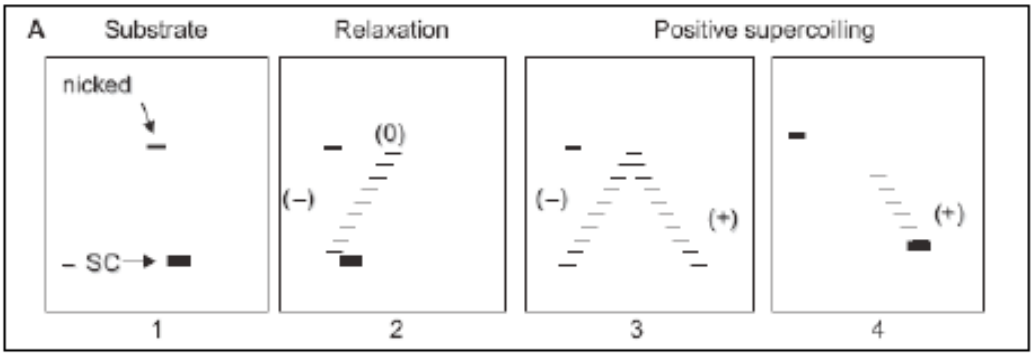

Fig. 3.5 Diagram of 2D gels: 1) migration of a negative supercoiled (-SC) and nicked forms of the plasmid substrate, 2) negatevely to relaxed topoisomers, 3) migration of negative (left side) and positive (right side) topoisomers, 4) migration of only positive topoisomers. [138]

As shown in figure 3.5, reverse gyrase has the ability to induce positive supercoiling from less negative to highly positive. After the incubation of the reverse gyrase with a negatevely supercoiled plasmid DNA, topoisomers with an increased linking number were produced (fig. 3.5 3).

3.19 2D gel in the topoisomers analysis

MATERIALS
10X TBE (108 gr Tris; 55 gr Boric Acid; 40 ml EDTA 0,5 M pH 8.0);
Etidium Bromide (EtBr 1mg/ml);

Electrophoresis apparatus;

Two-dimensional agarose gel electrophoresis are consisted by two steps electrophoresis carried out in orthogonal directions in a single agarose gel (fig. 3.6).

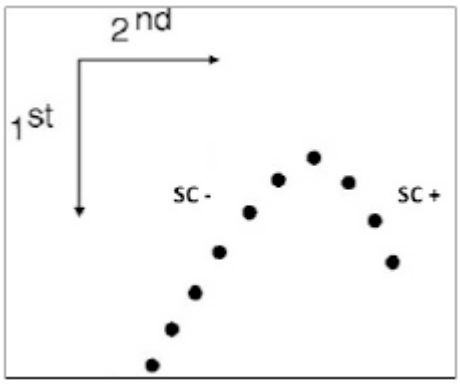

Fig. 3.6 Separation of supercoiled topoisomers by 2-D gel Topoisomers represented by dots were electrophoresed in two dimensions as indicated by the arrows [139].

This assay allowed to analyze the real overall shape of a supercoiled DNA, becouse of the addition of intercalating as ethidium bromide, altering the shape of the DNA and the electrophoretic mobility of single topoisomers. In the second dimension ethidium bromide was added to the electrophoresis buffer inducing positively migration to be faster than negatively supercoiled topoisomers.

Products were analyzed by 2D gel electrophoresis in 1,2% agarose in 1X TBE buffer at room temperature. Gel was run with no intercalators in the first dimension and 10 ng/ml ethidium bromide in the second. First dimension was carried out at 25 mA for 16 hours, then gel was soaked for 1 hour in dark with electrophoresis buffer treated with ethidium bromide (10 ng/ml).

This buffer was used for the second dimension electrophoresis at 60 mA for 4 hours, in dark condition. Then gel was stained for 1 hour in ethidium bromide (10 mg/ml) and destained in distilled water before visualization at the Chemidoc apparatus.

3.20 DNA relaxation assay

To evaluate protein activity for each aliquot, DNA relaxation assays were performed. The topoisomerization process (fig. 3.7) is visualized in an agarose-gel electrophoresis, allowing to separate DNA molecole on basis of size and shape.

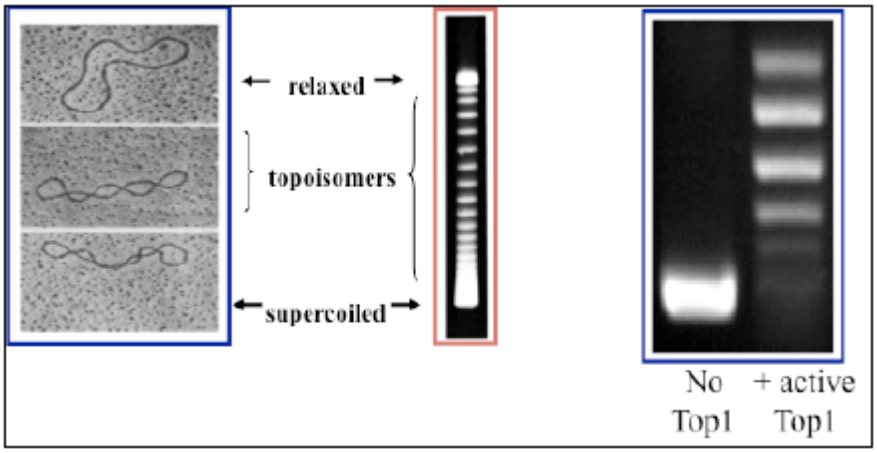

Figure 3.7: DNA relaxation assay. From the right, different shape of DNA are visualized at electron microscopy and on agarose gel electrophoresis. Supercoiled plasmid migrates faster than relaxed. If DNA is incubated with an active enzyme topoisomers were produced as reported in left side of the figure.

According to their nature, supercoiled DNA topoisomers migrate faster compared to linear DNA or relaxed DNA. When supercoiled plasmid DNA is incubated with an active eukaryotic DNA topoisomerase I, DNA topoisomers were generated.

MATERIALS:

negatively supercoiled plasmid DNAs;

10X TBE buffer: 0.89 M Tris-borate, 20 mM EDTA, pH 8.0;

6X Loading Buffer : 30% Ficoll (type 400), 0,1% bromophenol blue, 0,1% xylene cyanol;

gel electrophoresis apparatus;

EtBr: 10 mg/ml dissolved in dH_2O.

1% agarose solution was prepared, and before casting the gel the solution was slowly cooled. The gel was set and after its polymerization, the comb was

removed and inserted in the gel electrophoresis apparatus with 1X TBE. 6X loading buffer was added to DNA sample and after the loading a voltage of 140 volts for 5 hours was set. A buffer recirculation with a peristaltic pump allowed a uniform and more stable migration.

Gel was stained in 1-2 L dH_2O containing 0.5 μg/ml EthBr for 30 minutes, and destained for 20 minutes in dH_2O to improve visualization of the DNA bands. EtBr stained DNA was visualized directly with a UV transilluminator.

3.21 DNA Top1p *In vitro* activity assay

MATERIALS:

10X Topoisomerase reaction buffer;

1-2 M KCl to a final KCl concentration of interest;

positevely/negatevely DNA plasmid substrate (300 ng);

purified topoisomerase enzyme;

dH_2O

96- wells plate;

Phenol:Chloroform:Isoamyl Alcohol 25:24:1 saturated with 10mM Tris pH8.0, 1 mM EDTA Sigma®.

All reagents excepted the enzyme were added in the reaction mix and 27μl for each sample were aliquoted. Then 3μl of the previously diluted protein were added and incubated at 37^0C for 1 hour. Each fraction was already diluted 1:2 glycerol after purification step and same concentration was used in this *in vitro* assay.

Then samples were treated with 1:1 w/v phenol:chloroform then vortexed for 30 seconds and centrifuged for 3 min at 14000 rpm. The visible lower phase of each sample was discarded by micro-pipetting. To the remaining volume samples 6X loading buffer were added, then loaded in a 1% agarose gel and run in 2X TBE for 4 hours at 140 volts.

3.22 DNA Cleavage assays

MATERIALS:

pBlueScriptAK3-1;

AseI (5 μl, 10U/μl , New England Biolabs);

NE Buffer 3: 100 mM NaCl, 50 mM Tris-HCl, 10mM $MgCl_2$, 1mM ditiotreitol pH 7,9;

SspI (5 μl, 10U/μl , New England Biolabs);

NE Buffer SspI: 100 mM NaCl, 50 mM Tris-HCl, 10 mM $MgCl_2$, 0,025% TritonX-100 pH 7.5;

T7 DNA polymerase (13U/μl Sequenase from USB);

Acrylamide solution: 40% acrilamide:bis-acrylamide;

10% ammonium persulfate;

10X TBE buffer;

6X Loading buffer: 30% Ficoll (type 400), 0,1% bromophenol blue, 0.1% xylene cyanol;

3 M NH_4OAc;

100% Ethanol;

Deoxyribonucleotides: 100mM solutions of dCTP, dGTP, dTTP;

α^{32}P-dATP;

Phenol:Chloroform:Isoamyl Alcohol 25:24:1 saturated with 10mM Tris pH8.0, 1 mM EDTA Sigma®;

10X G-Buffer: 20 mM Tris, pH 7,5, 10 mM $MgCl_2$, 0,1 mM EDTA, 50 mM KCl, 50 μg/ml gelatine;

10% SDS;

Proteinase K: 20 mg/ml in dH_2O;

DMSO SigmaAldrich®;

Camptothecin: 4 mg/ml dissolved in DMSO;

Sample buffer: 38% formamide, 8 mM EDTA, 2 mg/ml bromophenol blue, 2 mg/ml xylene cyanol;

Acrylamyde/Urea gel mix: 7,6% acrylamide, 0,4% bis-acrylamide, 7 M Urea, 0,1 M Tris-Borate, pH 8, 2 mM EDTA;

Fixer: 10% acetic acid, 10% methanol.

Linear substrate preparation

10 μg of pBlueScriptAK3-1 plasmid was digested by AseI enzyme for 120 min at 37°C, in buffer NE 3 solution. Then ends were treated with 10 units of T7 Sequenase, 1,25 mM nucleotides, 50 μCi of ^{32}P-dATP for 15 minutes at 37°C. DNA was processed with an equal volume of phenol:chloroform and precipitated with 1/10 volume of 3 M sodium acetate and 3 volumes of 100% ethanol overnight at -20°C.

After centrifugation at 14000 rpm for 30 minutes, pellet was washed with 70% ethanol.

When it was dry, 43 μl of dH_2O, 5 μl of 10X NE buffer SspI, 2 μl of SspI enzyme were added and resuspended. Incubation was set at 37°C for 120 min.

DNA was then precipitated overnight and pellet again resuspended in 30 μl gel loading buffer and dH_2O.

DNA was loaded in 5% non denaturing polyacrylamide gel and electrophoresed in 1X TBE at 300 Volts for 2,5 hours.

Radiolabeled band corresponding to a 900 bp fragments was extracted and incubated with 1 ml of 3M sodium acetate at 37°C in gently shaking overnight. Then DNA was precipited overnight and pellet was resuspended in dH_2O to a final concentration about 50000 cpm/μl measured by β-counter.

Cleavage reaction

DNA cleavage reaction was prepared with DNA topoisomerase I mixed with single-end labelled DNA substrate (5000 cpm) and 5 μl 10X G buffer in a 50μl final volume. Rections were performed at 50 mM KCl in presence of DMSO or 50 μM CPT. Proteins were treated with DTT 10 mM before adding the substrate. Incubation of the reactions was set to 37°C for 30 min and stopped at 75°C for 10 min with 5 μl of 10% SDS to trap the covalent complex. 1μl of proteinase K (5mg/ml) were added to allow digestion of covalently attached protein with an incubation at 37°C for 15 min. Then DNA was ethanol precipitated, pellet was then dissolved in 200 μl of 1X TE buffer and repeated once the precipitation.

Finally pellet was resuspended in 6 μl of the formamide containing sample buffer and incubated at 95^0C for 5 min to denature the DNA fragment [29] [140] [141].
DNA cleavage products were resolved in a 8% denaturing polyacrylamide gel, run at 100 Watts for 1,5h and visualized with a PhosphorImager.

3.23 Time course activity assay

MATERIALS:
negatively/positively supercoiled plasmid DNAs;
10X TBE buffer: 0.89 M Tris-borate, 20 mM EDTA, pH 8.0;
6X Loading Buffer: 30% Ficoll (type 400), 0,1% bromophenol blue, 0,1% xylene cyanol;
a gel electrophoresis apparatus;
EtBr: 10 mg/ml dissolved in dH_2O.

A reaction mix was prepared considering 27μl for each sample reaction. In order DNA of interest 300ng, KCl in proper concentration to reach the interested salt condition, topoisomerase 1X reaction buffer, dH_2O were added. Finally equal concentration of enzymes, 3μl in volume for each reaction, were suspended. The assay was carried out at 37^0C, 30 μl aliquots were produced at 15"- 30"seconds– 1' – 2'- 4'-8'-16'-30' minutes. The reactions were stopped by adding SDS 2,5% w/v. Samples were then loaded on 2% agarose gel [142] and analyzed.

3.24 Double DNA topoisomerization assay

MATERIALS:
10X Topoisomerase reaction buffer;
1-2 M KCl to a final KCl concentration of interest;
300 ng negatevely/positevely supercoiled DNA plasmids;
dH_2O to a final volume of 30 μl;

6X Loading Buffer: 30% Ficoll (type 400), 0,1% bromophenol blue, 0,1% xylene cyanol;
10% SDS;
EtBr: 10 mg/ml dissolved in dH_2O.

Similarly to *in vitro* activity assay, reaction mix were prepared, and incubated at 37^0C for 30 min. Then half volume aliquot was taken, 300 ng of a different DNA plasmid were added to the rest of the sample volume. Second step reaction was incubated at 37^0C for other 30 min. All reactions were stopped by the addition of 2,5% SDS and 1X sample loading buffer. Finally, samples were loaded on 2% agarose gels and analyzed after incubation in EtBr.

3.25 Molecular Dynamics simulations (MD)

The starting coordinates were extracted from those of DNA topoisomerase I obtained from x-ray diffraction (PDB entry 1A36) [17]. The spatial environment and stereochemical regularization of the structures were produced by the Powell minimization method implemented in the SYBYL program (Tripos Inc., St. Louis, MO). The mutant was obtained by changing the residue R-434 into alanine. Models were built for mutant and wild type and the molecular mechanics were carried out on a Silicon Graphics O_2 R5000 SC using the version 6.2 of the SYBYL program. The system topology was generated using the AMBER leap module and the AMBER95 all atom force field. The system was simulated in periodic boundary conditions, a cutoff radius of 9Å for the non-bonded interactions was used and the neighbor pair list was updated every 10 steps. Electrostatic interactions were calculated with the Particle Mesh Ewald method. The SHAKE algorithm was used to constrain all bond lengths involving hydrogen atoms [149]. To better quantify the mobility of the mutated residue, MD conformations were superimposed over the three-dimensional structure of the DNA-Top1 covalent complex.

4. RESULTS

4.1 Expression and purification of hTop1p, htop1 P431G, htop1 R434A, htop1 R434C, htop1 W205C.

Proteins were purified from galactose induced EKY3 cells, transformed with YCpGAL1-TOP1, YCpGAL1-top1P431G, YCpGAL1-top1R434A, YCpGAL1-top1R434C and YCpGAL1-top1W205C.

The specific activity was measured for each sample with a plasmid DNA relaxation assay. The results are shown in figure 4.1.

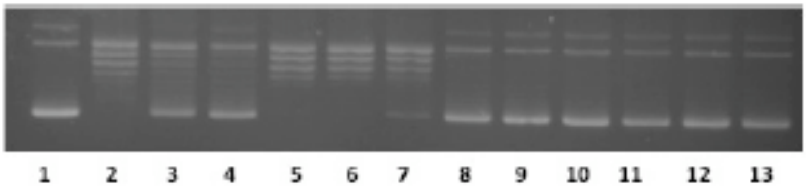

Fig. 4.1: Relaxation assay of yeast cell extracts. Control sample (lane1), hTop1p (lane 2–3), htop1 P431G (lane 4-5-6), htop1 R434A (lane 7-8), htop1 R434C (lane 9-10-11), htop1 W205C (lane 12-13).

No relaxation activity was associated in lane 1-8-9-10-11-12-13. As expected the control sample (lane 1) indicates the DNA substrate and no enzyme is added in the reaction mix, while relaxation activity was observed in lane 2-5-6-7 and in a lower manner in sample 3 and 4. Aliquots showing maximum ability to relax the DNA substrate were selected and analyzed by SDS-PAGE and Western Blot procedures.

4.2 Colloidal coumassie staining and western blot analysis

After protein purifications the biochemical features of hTop1p, and mutants htop1P434G, htop1R434A were analyzed with a 10% SDS polyacrylamide gel and proteins visualized by colloidal coomassie staining (Fig. 4.2).

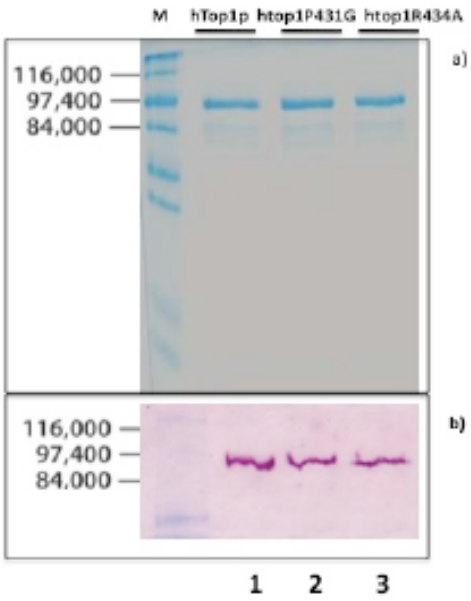

Fig.4.2: Equal amounts of wild type hTop1p (lane1), and mutants htop1P434G (lane2), htop1R434A (lane3) were analyzed by SDS-PAGE and visualized by colloidal coumassie staining **a)** and western blot analysis **b)**. The marker (M) is representend at the right of the figure.

As reported a single band is shown for each sample at the expected size, approximately 90 KDa as indicated by the marker.

These results were also confirmed with Western Blot analysis using the specific antibody recognizing the FLAG epitope engeneered in the human topo I vector and reporting high purified enzymes.

4.3 *In vivo* drug yeast sensitivity assay

In order to reach informations about viability and CPT citotoxicity, hTOP1, htop1P431G, htop1R434A and htop1R434C proteins were expressed in yeast strains top1Δ (EKY3) under the inducible promoter of galactose GAL1 on a single copy *ARS/CEN* plasmid (fig. 4.3 a), as also reported in "materials and methods". EKY3 yeast strain, deleted of the endogenous topoisomerase, is CPT resistant [141], therefore expression of exogenous enzyme is necessary to valuate CPT sensitivity.

As shown in figure 4.3 b-c yeast cells expressing each of the DNA topoisomerase construct were viable when plated into selective solid media added with 2% dextrose. In this condition there was no expression of exogenous DNA topoisomerase. In presence of galactose in selective media,

Gal1 promotor induced the expression of different Top1p mutants. The wild type grew normally on control plates and showed lethality when plated in presence of CPT (in all concentrations used b-c). Tyr723 mutant mutated to Phe (Y723F) exhibited a slow growing phenotype (fig.4.3 b) and CPT had no effect on these cells. Protein can only bind the Top1-DNA but is defective in DNA cleavage. Probably the over expression of the inactive protein interferes with the biological process. Furthermore YCP50 the vector control, and T729E a known CPT resistant [129] mutants are used as positive control (fig. 4.3 b). EKY3 strains expressing htop1W205C showed a partial resistance phenotype to the drug while mutations at P431 and R434 reported a not viable phenotype in presence of 0,5-1 μg/ml CPT.

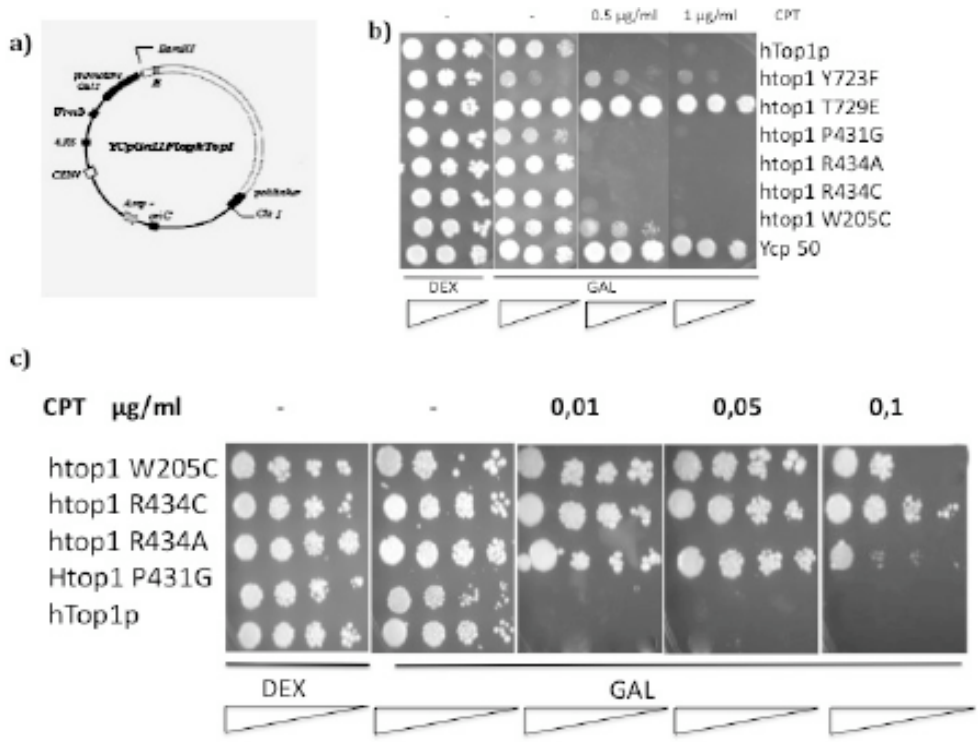

Fig.4.3: *In vivo* drug yeast sensitivity assay Exponential cultures of EKY3 (*top1Δ) cells transformed with* YCpGAL1-hTOP1 plasmid a) and with *vector control YCp50, YCpGAL1-htop1Pro431Gly,* hTop1Arg434Ala, hTop1Arg434Cys and hTop1Trp205Cys*, YCpGAL1-htop1Tyr723Phe [a known slow grow mutant] and YCpGAL1-htop1Tyr723Glu [a known positive control mutant for CPT resistant] b)* were serially 10-fold diluted and spotted onto SC-uracil plates supplemented with dextrose (Dex) or galactose (Gal) and as indicated CPT concentration (high drug dose). c) An altered CPT sensitivity was shown by htop1W205C and R434 mutants when expressed in yeast in presence of low CPT doseCell viability was assessed following incubation at 30^0C

To further investigate these first results, the effect of the expression of the single mutated proteins (P431G, R434A, R434C, W205C) on cell viability and CPT citotoxicity were assayed at lower 0,5 μg/ml drug doses. As reported in figure 4.3 c, substitutions at R434A, R434C, W205C showed a vital phenotype and a camptothecin resistance to concentration below 0,1 μg/ml CPT. While expression of htop1P431G protein confirmed a lethal phenotype in presence of the drug also at lower CPT concentrations (fig. 4.3 b-c).

Single mutation at R434 substituted by the alanine could interfere with the correct closure of the enzyme, modifying the right positioning around the DNA and or pertubating the CPT interation in the pocket structure.

4.4 DNA Cleavage Assay

Investigating CPT sensitivity for each mutant, the stability of the covalent complex formation was analyzed (fig. 4.4).

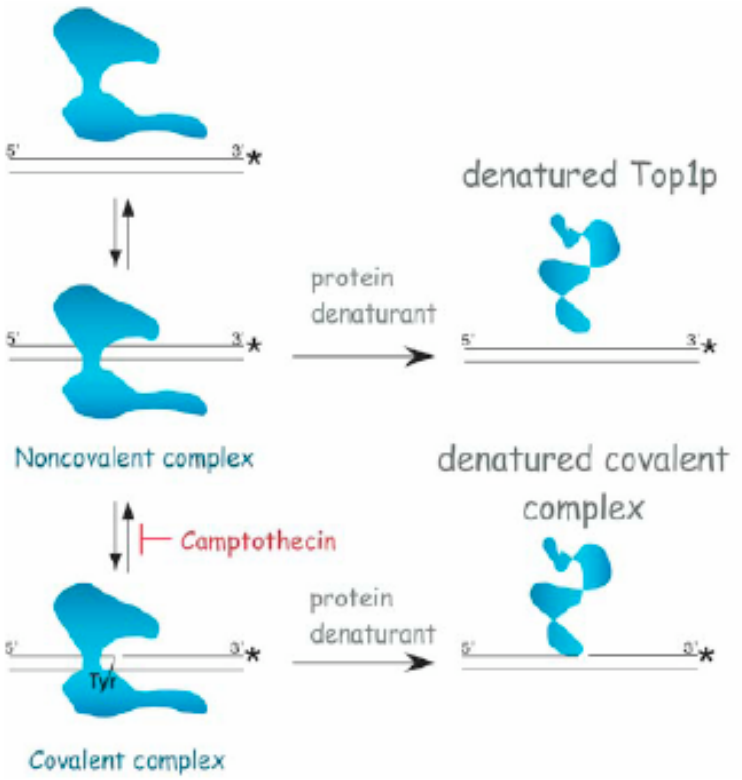

Fig. 4.4 DNA cleavage assay: Top1 cleaves the single strand of the DNA by forming a reversibile phosphotyrosyl linkage. CPT inhibits the resolution of this Top1-DNA complex, increasing the stability of these covalent intermediates.

Equal concentrations of hTop1p, htop1P431G, htop1R434A, htop1R434C and htop1W205C proteins were incubated with a single 900 bp ^{32}P-end-labeled DNA fragment in absence or presence of CPT for 30 minutes at 37^{0}C(Fig. 4.4.1). Then reactions were stopped by addition of 1% SDS allowing the trapping of the cleavable complexes. Cleaved DNA fragments were resolved in a denaturing polyacrylamide gel as reported in "matherials and metods" section.

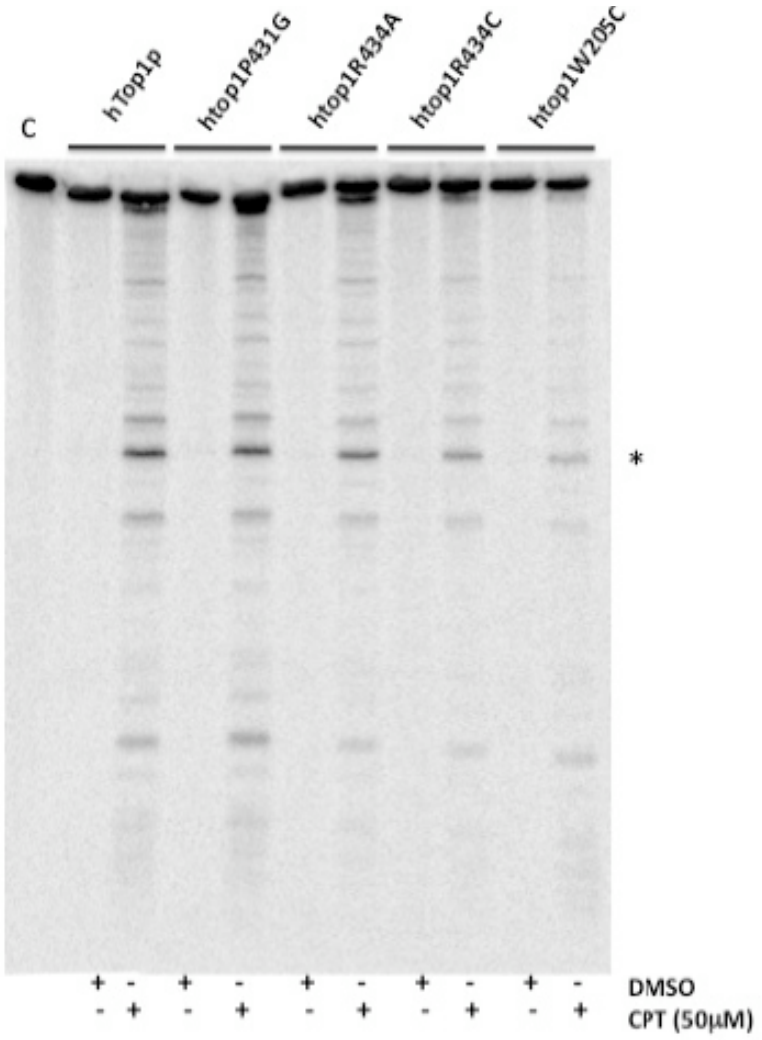

Fig. 4.4.1: DNA Cleavage Assay Equal concentrations and activities of purified hTop1 proteins were incubated with a single 3' ^{32}P-end-labeled 900 pb DNA fragment, in presence of the inhibitor DMSO or 50 μM CPT. Reactions were incubated for 10 min at 37 ^{0}C and stopped with 1 SDS % to trap the covalent complex, then DNA cleavage product were resolved in 8% denaturing polyacrilamide gel and visualized with a PhosphorImager. C indicates the control sample with no enzyme in the reaction. The asterisk reported the position of a high affinity cleavage site.

Therefore, cleaved DNA fragments distribution give information about the contribution of a single mutation on the covalent enzyme-DNA intermediates and if or not was CPT induced. When hTop1 protein was incubated in absence of CPT, no cleavage of the labeled DNA strand was detected

However, when the same protein was exposed to the drug, a dramatic increase in cleaved DNA fragments was observed. Same result was reported for htop1P431G suggesting that this mutant is not resistant to CPT *in vitro*. For what concerns htop1R434A, htop1R434C and htop1W205C a decreasing in covalent complex formations were observed in presence of the drug. The extent of cleavage correlates with *in vivo* drug resistance of the R434 and W205 mutants, showing a reduction of cleavable complex formation.

Mutations analyzed at the *hinge* region are responsible for the alteration in the binding of the protein with the DNA and drug interaction.

4.5 2D gel assay: positive and negative supercoiled plasmids.

Positive supercoiled DNA substrates were generated and assayed for next experiments. As already reported in "Materials and Methods" an enzymatic approach was used to obtain positive supercoils.

To compare the relaxation of positively and negatevely supercoiled plasmids by purified proteins of interest a 2D gel assay was carried on as reported in figure 4.5.

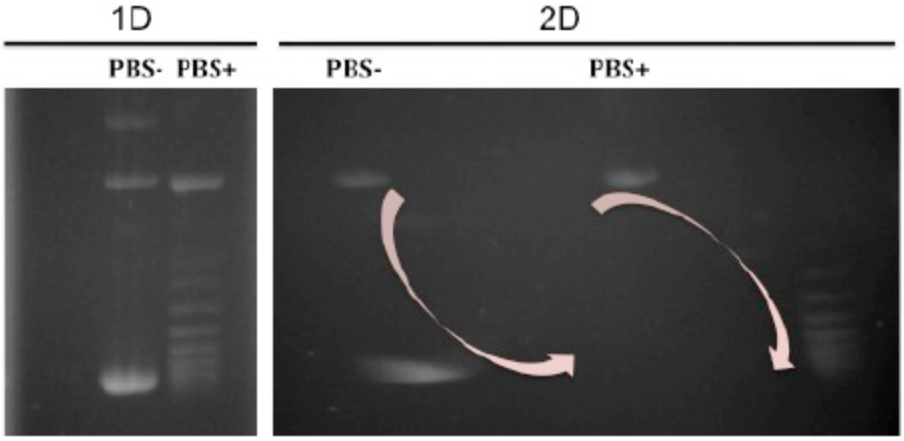

Fig. 4.5: 2D gel assay of a 3000 Kbp DNA plasmid. Topoisomers were electrophoresed without intercalator during first dimension (1D left side) and with a low intercalator concentration during the second dimension (2D right side of the figure). The intercalator in 2D differently separated negative topoisomers from positive ones as showed by pink arrows.

Positively substrate was prepared by incubating negatively pBS plasmid with reverse gyrase, where negatively supercoiled substrate was obtained by *Escherichia coli* expression and purification, organism that naturally maintains all DNA in an under-wound state. 2D gel allowed to appreciate different topoisomers of a negative or a positive substrate, as reported in "materials and methods". The intercalator ethidium bromide used in an appropriate concentration in the second dimension reduced the twist of the DNA (untwist the duplex) and consequently altered the gel velocity of supercoiled topoisomers. The intercalator binds with different affinity the negative and positive topoisomers. In particolar positive supercoiled topoisomers bind ethidium bromide with less efficiency respect the negative ones. The different binding properties induce the separation of the two-topoisomer species that migrate in the second dimension as an arc.
In figure 4.5 both supercoiled DNA species are shown. During the experimental setup 300 ng of both supercoiled PBS DNAs were spectrophotometrically measured and digested with HindIII, therefore linearized in order to make sure that equal amounts of substrates were used. Furthermore positively supercoiled plasmids bound ethidium bromide less efficiently and were less stained than negatively substrate.

4.6 *In vitro activity assay*

hTop1p activity was assayed in DNA relaxation catalyzed reaction. Equal concentrations of purified hTop1, htop1P434G, htop1R434A, htop1R434C and htop1W205C proteins were incubated with negatevely (fig. 4.6 a) and positevely (fig. 4.6 b) supercoiled PBS plasmid DNA at the indicated KCl concentrations.
The different ionic strenght conditions allowed to performe the relaxation assay and evaluating the affinity rate of each mutant for the double helix.
It's well-known that high salt concentration inhibits topoisomerase catalyzed relaxation by reducing the binding with the DNA.

Reactions were incubated at 37^{0}C for 30 minutes and stopped with 1% SDS. Resulting products were resolved in 1% agarose gel as reported in the figure 4.5, stained with ethidium bromide and visualized with a BioRad Gel doc system.

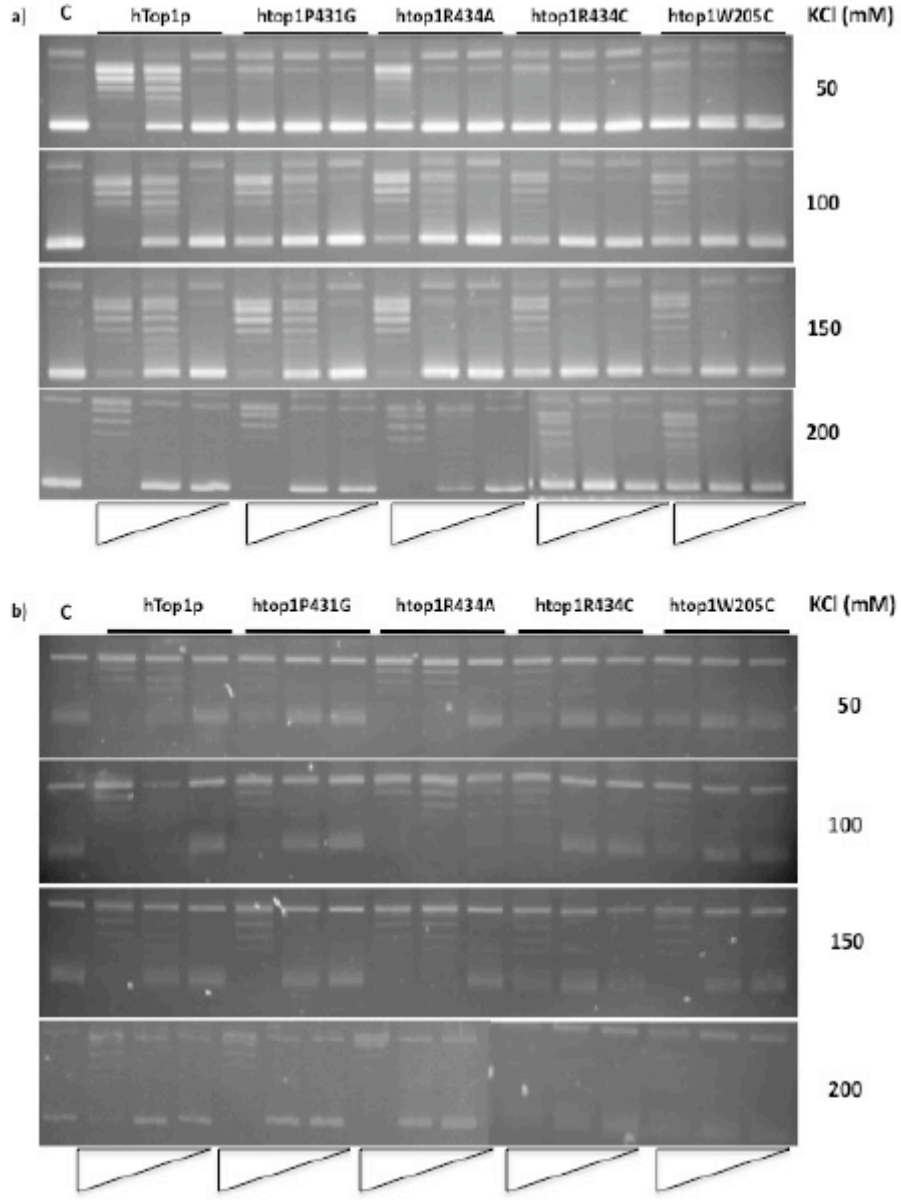

Fig.4.6: ***In vitro activity assay*** Limited amount of purified hTop1p, hTop1Pro431Gly, hTop1Arg434Ala, hTop1Arg434Cys and hTop1Trp205Cys were serially 10-fold diluted and incubated in DNA relaxation assays with 300 ng negatively supercoiled plasmid DNA **a)** and positively supercoiled plasmid DNA **b)** at different ionic strenght (from 50to 200 mM KCl). Following incubation at 37°C for 30 min, the reaction products were resolved in 1% agarose gels and visualized after staining with ethidium bromide. C indicates no enzyme control.

Therefore to investigate if mutations could alter the catalytic reaction of the enzyme the specific activity was tested 10-fold serially diluted. For what concerns negative supercoiled DNA substrate (fig.4.6 a), wild-type enzyme as expected shows the optimal activity at 150mM KCl, while a reduction is detectable for htop1R434A, htop1R434C and htop1W205C. Same behaviour was observed for htop1R434A at lower salt concentration (50 mM KCl) while no relaxation activity is detected for htop1P431G, htop1R434C and htop1W205C at all.

At high ionic strenght condition (200 mM KCl) htop1R434A protein is the only showing the higher relaxation activity, the supercoiled amount decreased also at 1/10 dilution.

These results suggest a difference in activity when alanine or cysteine, were used as substitution of R434.

Incubation with positive supercoiled PBS plasmid DNA showed that wild-type enzyme confirmed is optimum relaxation activity at 150 mM KCl, but if compared to htop1R434A protein, a higher relaxation activity is reported.

Similar behaviour was detected at 100 mM KCl, 1/100 diluted, where R434A mutation enhanced its relaxation activity.

At lower ionic strenght (50 mM KCl) htop1pR434A relaxed better than wild-type, this was supported by 1/10 dilution results. No significant activity was detected for other mutants at the same salt condition. At higher ionic strenght (200 mM KCl) the only relaxation activity was reported for hTOP1p, htop1P431G and htop1R434A proteins, in this case mutants showed an increased catalytic activity.

4.7 *In vitro* activity assay at high ionic strenght condition

In order to assess the condition in which mutants relax supercoiled DNA, in figure 4.7 is reported the *in vitro* activity relaxation for the most interesting, htop1P431G and htop1R434 proteins compared with the wild type. This assay was carried on also at 250 mM KCl.

As already reported mutation at R434 position with an alanine affected the relaxation activity more than wild-type and htop1P431G protein, and in a

wider range of KCl concentration. Dashed red line in the figure 4.7 showed a costant relaxation activity from 150 mM to 250 mM KCl, after incubation with both negative (fig. 4.7 a) and positive (fig. 4.7 b) DNA substrate. Instead relaxation activity of wild-type protein was appreciated until 200 mM KCl.

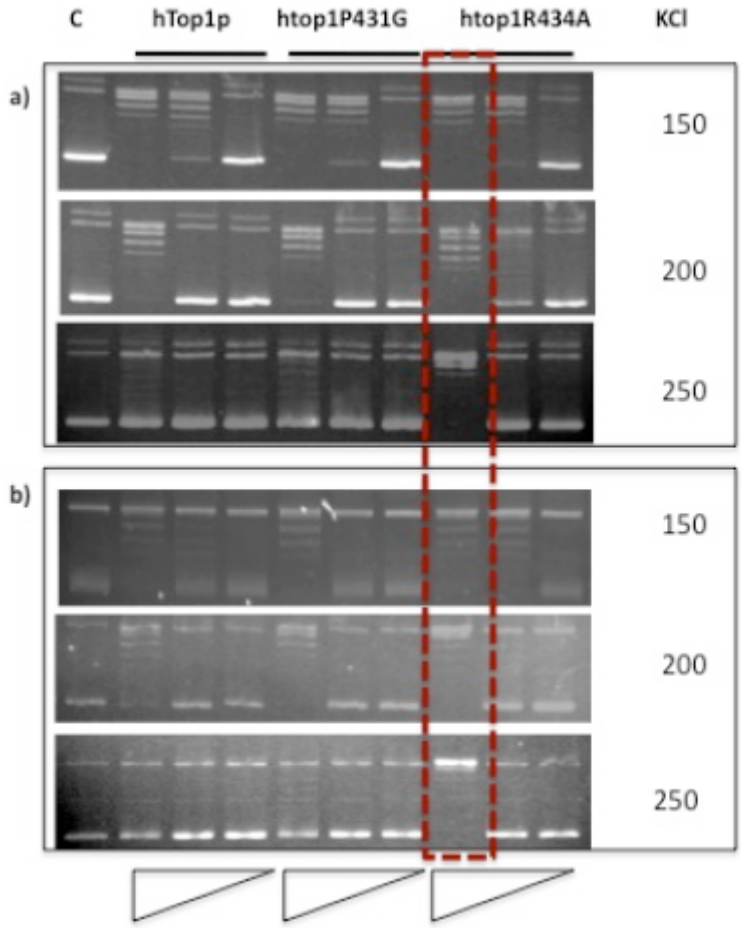

Fig.4.7: ***In vitro activity assay*** of purified hTop1p, hTop1Pro431Gly, hTop1Arg434Ala, serially 10-fold diluted a) b), incubated in DNA relaxation assays with negatively supercoiled plasmid DNA a) and positively supercoiled plasmid DNA b) The reactions were tested in presence of the indicated KCl. Following incubation at 37°C for 30 min, the reaction products were resolved in 1% agarose gels and visualized after staining with ethidium bromide. C indicates no enzyme control. Dashed lines in red show the continued hTop1Arg434Ala activity in relaxing DNA.

Supported by these results, the salt concentration used in the *in vitro* activity assay, was extended until 1000 mM, as reported in figure 4.7.1.

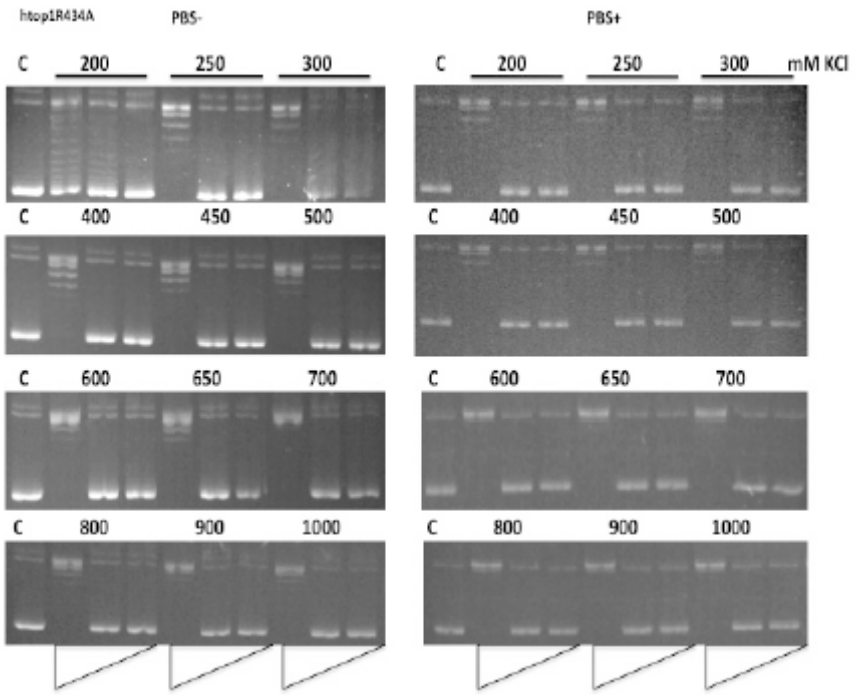

Fig.4.7.1: Relaxation activity of htop1R434A at high ionic strenght condition with positive (left side) **and negative** (right side of the figure) **supercoiled DNA.** Purified protein, serially 10-fold diluted was tested in presence of the indicated KCl concentrations in a range from 200mM to 1000mM. Following incubation at 37°C for 30 min, the reaction products were resolved in 1% agarose gels and visualized after staining with ethidium bromide. C indicates no enzyme control.

Positively and negatively supercoiled DNAs were incubated with equal amount of the purified htop1R434A protein and compared. The ionic strength range from 200 mM to 1000 mM KCl was used as a variable condition in the reaction mixture. Relaxation activity was observable in all experiments in 1/1 enzyme dilutions, both for negative and positive substrates. All control samples represented the supercoiled plasmid DNA where no enzyme incubation occured.

The same assay was also performed with 5-fold diluted proteins, comparing htop1R434A with htop1R434C enzyme activities at high ionic strength conditions (fig. 4.7.2).

This allowed to investigate the crucial role of the mutated residue and the specificity deriving from the alanine or cysteine amino acid at the 434 position.

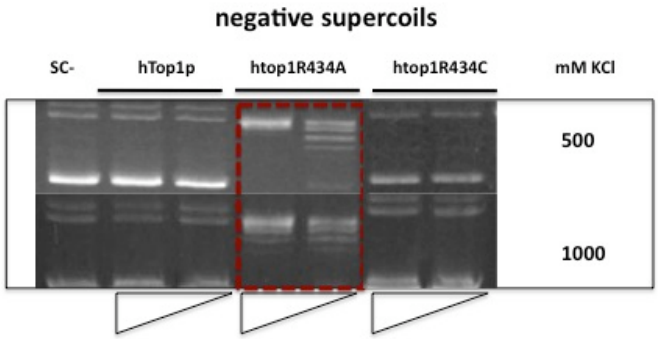

Fig.4.7.2: Comparison between relaxation activity of htop1R434A and htop1R434C. Purified proteins, 5-fold diluted were tested in presence of the indicated KCl concentrations from 500mM to 1000mM with negatively supercoiled DNA (SC-). Following incubation at 37°C for 30 min, the reaction products were resolved in 1% agarose gels and visualized after staining with ethidium bromide. C indicates no enzyme control.

4.8 Time course activity assay

In order to appreciate differences in the catalytic process for both wild-type and mutant proteins, a time course activity assay was performed. At fixed times: 15 , 30 seconds, 1, 2, 4, 8, 16 minutes reactions were stopped by the addition of 1% SDS. This assay is similar to the *in vitro* activity one, supercoiled plasmid DNA was incubated with enzyme at 37^0C, then aliquots were collected at the indicated times.

Experiment was set up incubating both excess and limited amount of hTop1 protein in the reaction (fig. 4.8).

Time course assay was carried on in optimal KCl condition (150 mM) in a 4-molar excess of DNA substrate (limited amount of protein), and in 4-molar excess of protein (limited amount of DNA).

As expected in presence of protein excess, wild-type enzyme performed the complete relaxation, one or more enzymes were probably bound to a single DNA molecule.

Same behaviour is observable for both negative and positive substrate DNA, 15 seconds were sufficient to relax supercoils.

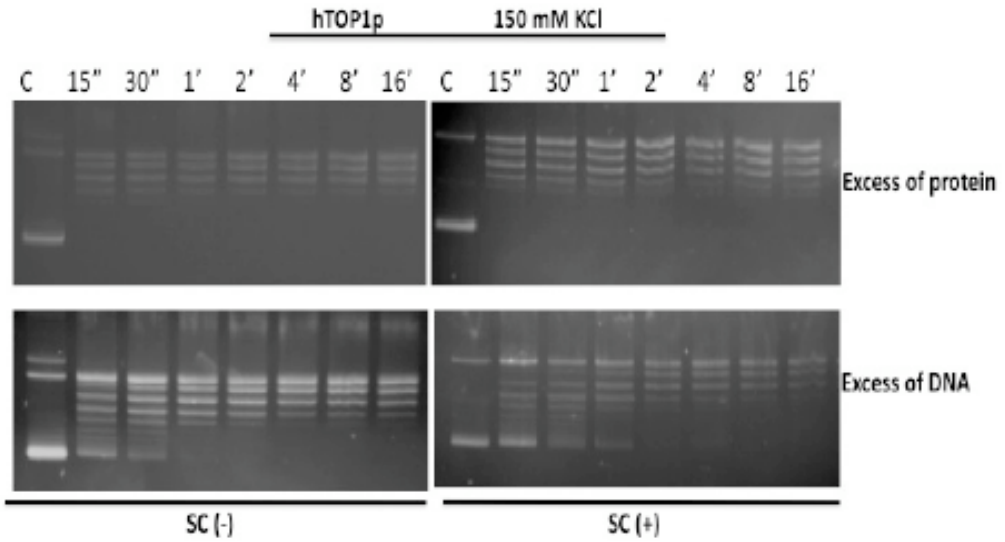

Fig. 4.8: Time course *in vitro* activity, excess and limited amount of purified wild-type enzyme was used to set up the assay. Reactions were incubated with negatively (SC-) and positively (SC+) supercoiled DNA at 37 ^{0}C and then stopped at the indicated times at the top.

In excess of plasmid DNA, hTop1 protein relaxed the negative substrate almost to completion after 1 minute, and after 2 minutes in presence of positive supercoiled DNA.

This suggests that association/dissociation of the enzyme is the rate limiting step of the relaxation. In this condition it's possible to appreciate enzyme activity: dissociating from a relaxed plasmid and binding a new supercoiled substrate.

4.8.1 Time course activity assay with excess of proteins

The activity of purified enzymes at shorter times was also reported for other mutants in protein excess.

As reported in figure 4.8.1 hTop1p, htop1P431G, htop1R434A, htop1R434C, htop1W205C proteins were incubated with negative supercoils (SC-) and 150 mM KCl at 37^{0}C and analyzed after stopping reactions at indicated times.

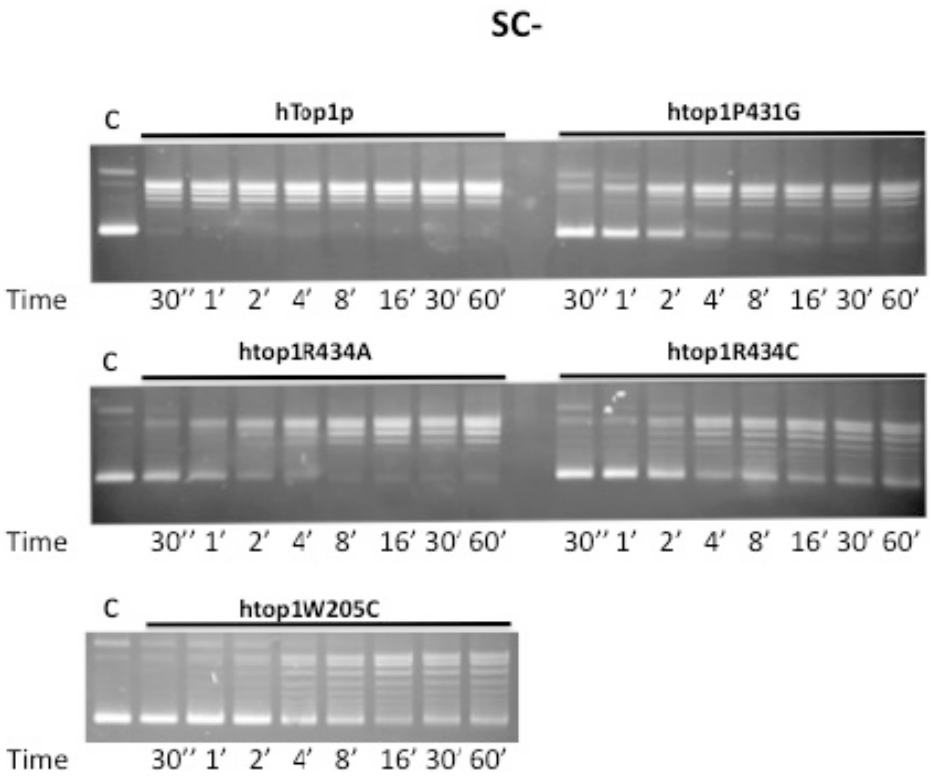

Fig. 4.8.1: Time course relaxation assay with excess of proteins. Purified wild-type, htop1P431G, htop1R434A, htop1R434C and htop1W205C proteins were tested and collected at fixed time as reported up of the figure. C representes the control for the reactions where no enzyme incubation occurs. DNA relaxation was asseyed in a 4-molar excess of protein and incubated with PBS negatively (SC-) supercoiled DNA.

In this condition the enzyme dissociation rate from the substrate is no longer the limiting step between the wild type and mutants. Only hTop1p relaxed completely supercoiled DNA after 30 seconds. Moreover, among purified mutants the most active was htop1R434A, after 8 minutes performed the complete relaxation, but then, also htop1P431G showed same activity. Instead less activity was observed for htop1R434C and htop1W205C proteins, which didn't reach the supercoiled relaxation also after 60 minutes (fig. 4.8.1).

4.8.2 Time course activity assay with limited amount of proteins

Limited amount of hTop1, htop1P431G and htop1R434A proteins were incubated with negatevely (SC-) and positevely (SC+) supercoiled with 150 mM KCl, at 37^0C as reported in figure 4.8.2.

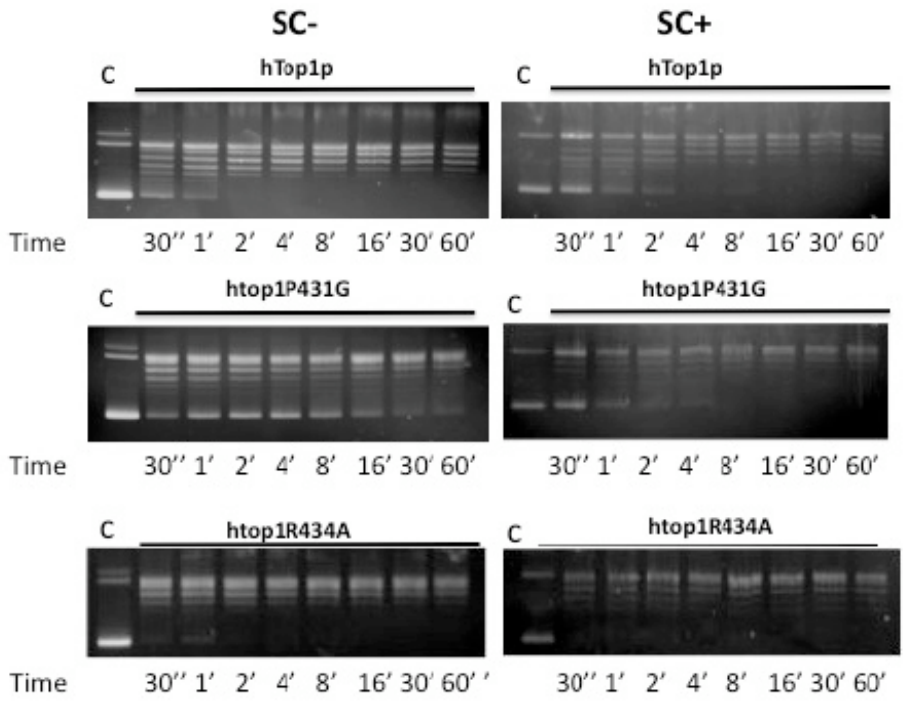

Figure 4.8.2: Time course relaxation assay with limited amount of proteins. Purified wild-type, htop1P431G and htop1R434A proteins were tested and collected at fixed time as reported up of the figure. C representes the control for the reaction, where no enzyme incubation occurs. DNA relaxation was followed in a 4-molar excess of PBS negatively (SC-) and positively (SC+) supercoiled DNA.

As demonstrated, the association/dissociation is rate limiting for DNA relaxation and is possible to appreciate the disappearing in the supercoiled during time. htop1R43A protein is faster in realeasing supercoiled, after 2 minutes is able to complete relaxation of negatevely supercoiled if compare to the wild type and mutant with the proline residue. The mutant obtained from R434A substitution, showed also a faster ability in relaxing positevely than negatevely supercoiled DNA if compared to other enzymes as reported in figure 4.8.2. After 30 seconds the complete relaxation of positevely substrate was observed.

4.9 Double DNA relaxation activity

It has been demonstrated that hTop1p activity exhibited a salt optimum around 150 mM and deviations from this suggest an increased or decreased (if > 150 mM KCl) DNA binding affinity.

Nevertheless htop1R434A protein exhibited a relaxation activity in a wider range of KCl concentration, from 150 mM to 1000 mM. In order to better understand how htop1R434A protein catalyzes the relaxation activity also at high salt concentration, a double DNA assay was performed as described in "materials and methods". The *in vitro* activity assay was modified by the addition of a second step to the process.

First protein was incubated with AK31, supercoiled plasmid DNA for 30 min at 37^0C, then an half aliquot was collected and stopped. Then, to the rest of the mixture an appropriate amount of PBS supercoiled DNA was added and incubated for other 30 min at 37^0C (fig. 4.9-1).

This was also assayed for wild-type protein and in reversable condition: first PBS then Ak31 DNA substrate were added for the incubation (fig.4.9-2), moreover negative (Fig 4.9 a) and positive (fig. 4.9 b) supercoiled DNA for both assays was also tested. Processivity and distributivity for both enzymes were tested at low (50mM), optimal (150mM) and high (500 and 1000 mM) salt concentration, as reported in figure 4.9.

As expected wild type showed processive behaviour at 150 mM, distributive at 50 mM and no relaxation activity was observed at 500 mM and 1000 mM KCl. Otherwise htop1R434A protein showed to be distributive starting at 50mM KCl and becoming more processivity as salt concentration increased. This was supported by the visible and continous relaxation activity during the two steps reaction. The addition of the second DNA substrate even if Ak31 or PBS for first, didn't interfere with the topoisomerase mutant activity, suggesting different way in which interaction with DNA could occured.

At high salt condition and in the second step of incubation and both DNAs are present in the mixture, the activity appeared very processive and no supercoiled was detected. Moreover when positively supercoiled substrates were used, no appreciable differences were observed compared with the negative plasmid DNAs.

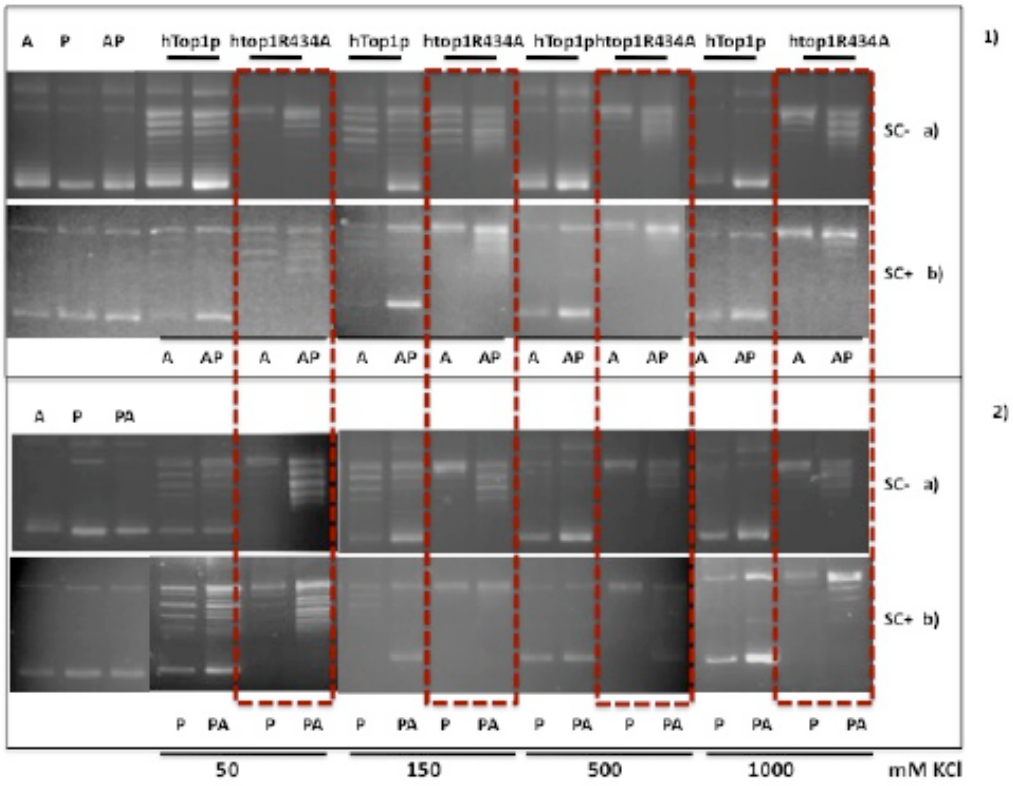

Fig.4.9: Double DNA relaxation activity: purified hTop1p and hTop1Arg434Ala were incubated in two steps DNA relaxation assays with two negatively supercoiled plasmids DNA a) and positively supercoiled plasmids DNA b) at the indicated KCl concentration. First three columns indicate control DNA with no enzyme for each reaction, A stands for AK31, P for PBS and AP when both DNAs were used. 1) First step: reactions were incubated with AK31, following incubation at 37°C for 30 min aliquots were collected. Second step: addition to the reaction of an equal amount of DNA PBS and incubation at 37°C for 30 min. 2) The addition of two DNA were reversed, firstly PBS, then AK31 were used. The reaction products were resolved in 1% agarose gels and visualized after staining with ethidium bromide. Dashed lines in red show the continued hTop1Arg434Ala activity in relaxing DNA.

In addition to these results, this experiment was also tested with a negative and a positive supercoiled substrate mixed together in the reaction (fig. 4.9.1 b) and compared with the previous results (fig. 4.9.1 a). Data were shown at low and high salt conditions.

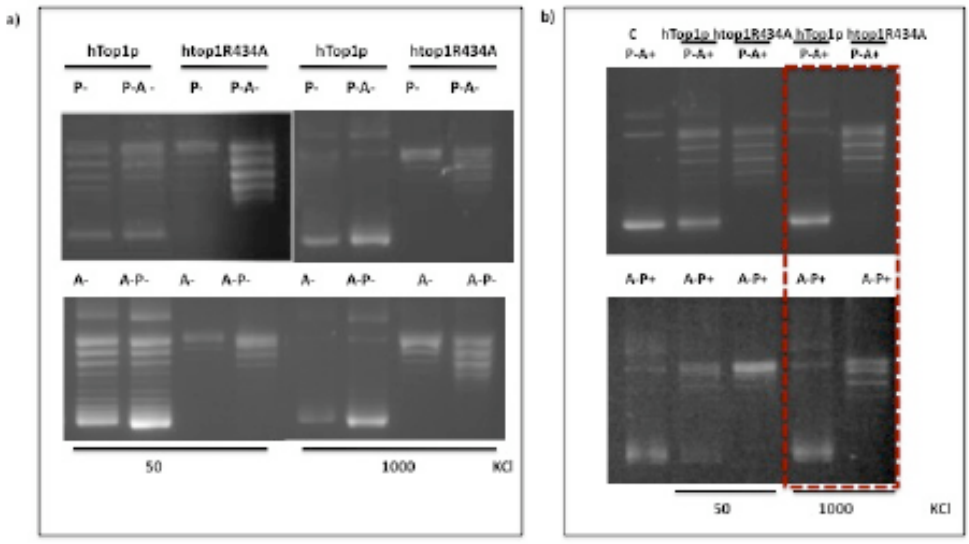

Fig.4.9.1: Comparison beetween double DNA relaxation activity with negatevely supercoiled DNA substrate a) and the same procedure reaction using firstly a negatively DNA supercoiled then a positively one, as indicated b) Assays were reported at 50 and 1000mM KCl and in reversable condition. A stands for AK31, P for PBS and (-) when negatively supercoiled DNA and (+) when positively supercoiled DNA were used. C indicates no enzyme control. The reaction products were resolved in 1% agarose gels and visualized after staining with ethidium bromide. Dashed line in red shows the continued hTop1Arg434Ala activity in relaxing DNA.

No differences were observable for the relaxation activity, the switch from a negative to a positive supercoiled, and the opposite reaction, didn't change the results.

Wild-type protein relaxed supercoiled DNA only at 50 mM of salt concentration, while mutant interacted with all kind of substrates and conditions.

4.10 Molecular Dynamics simulations (MD)

In order to investigate the possible structural properties underlined by the experimental data for the R434A mutation, a simulative approache was also performed. Since the overall structure is maintained through-out the simulation time, the secondary structures of each amino acid residue for both wild type and htop1R434A protein were obtained and fully maintained (fig. 4.10).

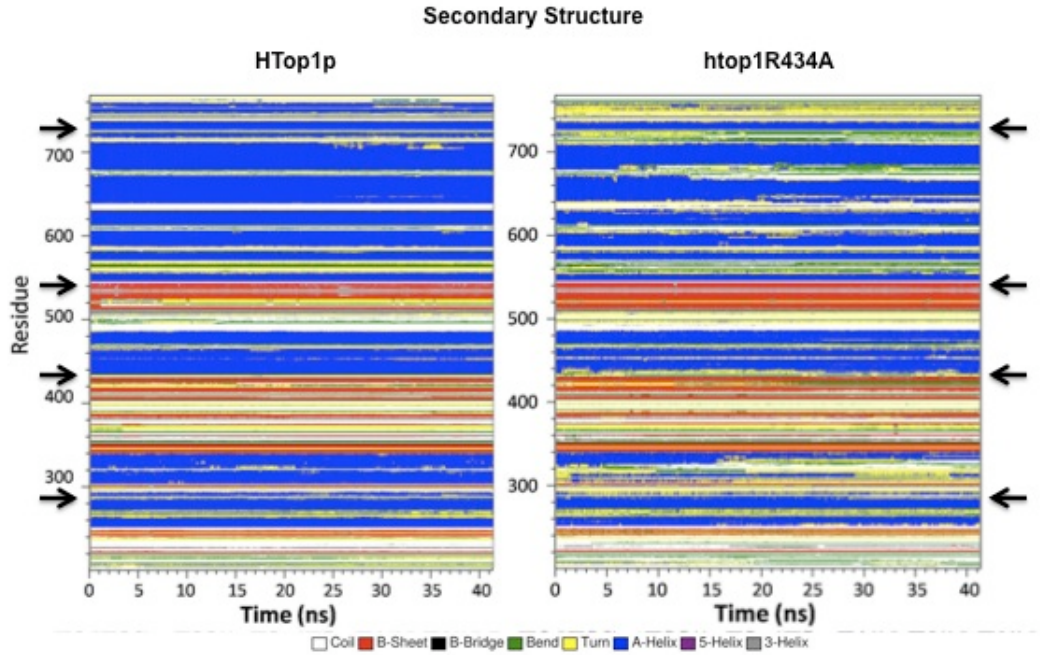

Fig. 4.10 HTop1p and htop1R434A secondary structures as a function of time. Secondary structures for Wild type (left side) and mutated htop1R434A (right side) proteins are reported. α-helix, 3.10 helix, random coil, β-sheet, turn and bend are represented in blue, grey, white, red, yellow, green respectively, as shown. Black arrows indicate relevant variations between protein domains.

As reported in the figure 4.10 is possible to visualize several variations (black arrows) between the two secondary structures. These are observed at the level of the N-terminal domain (around 700 residue), but also around 540 – 434 positions and below 300 residues. Moreover root mean square fluctuations (rmsf) as a function of residue was measured, and revealing a different behaviour for wild type and mutated protein (fig. 4.10.1). This method allows to valuate the conformational space visited by each residue during time.

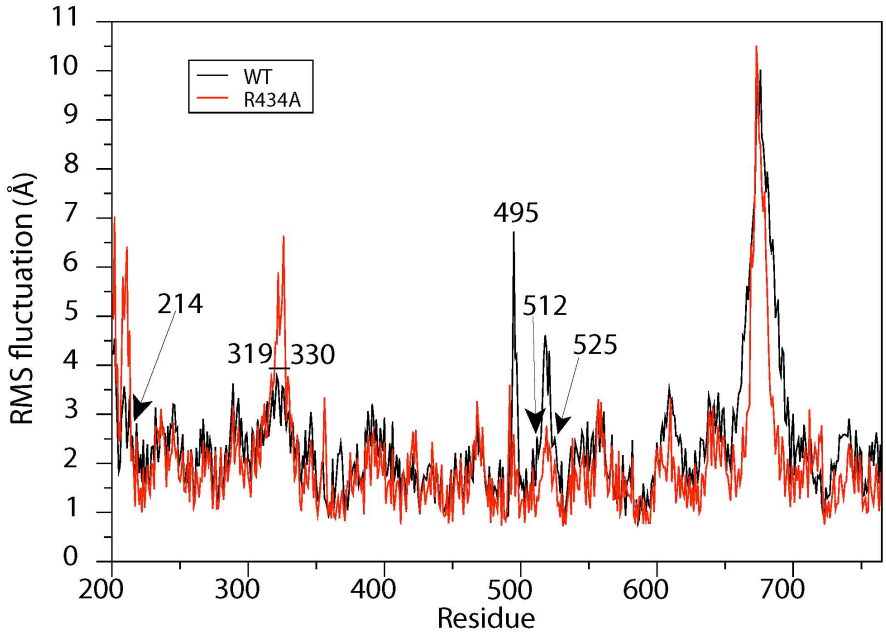

Fig. 4.10.1 Root mean square fluctuations (rmsf) as a function of residues Wild type and htop1R434A proteins are represented in black and red respectively. Arrows indicate the most important deviations between the two samples.

The mutated protein showed differences around the N-terminal domain (214 residue); the subdomain I (319-330 residues) and the subdomain III (512-525 residues) if compared to the wild type.

The simulation model also showed a large conformational change in the "nose cone" region and on the tip of the linker domain. This is quite interesting since these two regions are supposed to regulate the velocity of DNA relaxation.

5. DISCUSSION AND CONCLUSIONS

DNA topoisomerases are not only fascinating examples of natural selection but also important tools for clinical therapy [149]. Thanks to their action different topological state of DNA molecule are controlled.

The analysis presented in this work has been focused on this direction, investigating functional and structural contribute of some residues located in the flexible *hinge* (429-436 residues) region and surrounding domains. Single mutated proteins (P431G, R434A, R434C, W205C) were studied, it has already been reported interactions between the Trp-205 and His-346 and Gly-437 at the level of the *hinge* [24]. Moreover according to Sari and Andricioei analyses, in 2005, the strechting movements of this region reported a contribute to the negative supercoils relaxation. Carrying on the *in vitro* time course activity assay hTopIB mutants were incubated with both positive and negative supercoiled and a stronger affinity of R434A and P431G mutants for positive substrate was reported if compared to the negative supercoils relaxation. The reactions were performed considering the association/dissociation as rate limiting for reaction and limited amounts of proteins were used. Other mutants (W205C and R434C) didn't show a better performance in relaxing DNA than the wild type enzyme, probably affinity in binding DNA was affected due to mutations.

What is well-known from crystal structures analyses of hTopoIB bound to DNA is that there are no sufficient space for a free DNA rotation and different domains have to interacted one or more time, thus high flexibility of the structure is required to allow DNA binding and the strand rotation. The aminoacidic substitution of arginine with an alanine supposed to be more smoothly and elongation of the α-helix of the *hinge* could occured. Moreover a glycine mutating in a proline increased the strechting and flexibility in the region where is located. Experiments were conducted in a range of ionic strenght, assuring a folded protein during the *in vitro* topoisomerizzation

process and valuating the rate of affinity for the DNA substrate. What is well-know from literature is that an optimal salt concentration for wild-type purified protein is 150 mM KCl, in this condition a distributive catalyzed reaction is observed, while at both higher (>150mM KCl) and lower (50 mM KCl) ionic strenght the processivity of the event can be appreciated. As expected in the experiments shown, wild-type exerts the most relaxation at 150 mM KCl, and this was also reported for *htop1P431G, htop1R434C* and *htop1W205C* mutants, then their activities stopped at 250 mM KCl. During a processive reaction, protein is capable to completely relax the substrate without dissociating from it. The results are in agreement with this but the only exception is observed for *htop1R434A* mutant that still relax to higher 250 mM of salt concentration. The high salt concentration should inhibits topoisomerase catalytic activity, but *htop1R434A* relaxed both positive and negative supercoils in a range from 50mM to 1000mM of ionic strenght. Investigating distinct strand rotation mechanisms for both supercoiled signs, htop1R43A protein reported a faster ability in releasing positive substrate than negative compared to the wild-type and other mutants. Indeed *htop1P431G* mutant showed a preferential activity for positive than negative DNA molecule. For both mutation R434A and P431G the different affinity for positive than negative substrate has to be identified in the structural modifications occured at the *hinge* level. Other mutations showing a decreased in the ability to bind DNA, confirm the key role of the 434 and 431 residues in the strand rotation mechanism. The greater affinity for DNA molecule has been investigated with a multiple assay, where purified htop1R434A protein was firstly incubated for 30 minutes with a type DNA, then half an aliquot was collected and to the rest of the tube mix a second DNA smallest in size was added and incubation stopped again after 30 minutes. A visible and continous relaxation activity during the two step reactions was reported. This suggests that R434A mutant is able to dissociate from the first DNA and to bind the new one, added in the mixture, no

supercoiled substrate was detected in all reactions analyzed.

Since human DNA topoisomerase IB is also a specific target of the most clinically use, chemoterapeutic agent, these mutants were also investigated for the cytotoxic mechanism mediated by camptothecin (CPT).

From one side the cleavage equilibrium assay, in presence of 50 mM CPT, suggests a clear camptothecin resistance of the htop1W205C protein, and same pattern of cleavable complex formations was observed for wild-type and *htop1P431G* mutant, but on the other hand both mutations at 434 residue showed a decreasing in the cleavable complex if compared to the wild-type. It could be hypothesized that positions R434 and W205 are strongly affected by the drug interaction, thus *in vivo* analyses carryed in a wide range of camptothecin concentrations, from 5 μg/ml to 0.01 μg/ml allowed to investigate the functional poisoning of the human DNA topoisomerase IB. Interestingly wild-type and Pro431Gly mutated yeast cells showed a lethal phenotype after drug treathment, while mutated protein reporting W205C, R434A and R434C substitutions, reported a CPT resistance to very low doses, below 0.1 μg/ml. These data were supported by the cleavage equilibrium results where the camptothecin resistance was appreciated for the R434A and W205C mutated residues. From a genetically backgrounds, from tumor cells to yeast strains deleted for such a important checkpoint or DNA repair pathway, it has been reported any kind of predition correlated between Top1 protein levels and drug response [149] but camptothecin resistance observed *in vivo* viability assay for mutated *htop1R434A* and *htop1W205C* is strictly in agreement with single molecule experiments in yeast provided the Top1 positive supercoils accumulation after drug treathment. Moreover it's supported by the ability of *htop1R434A* mutant to relax faster positive substrate.

Indeed modeling simulation analyses indicated a long range communications between different topoisomerase domains. The single mutation reported at R434 residue altered the linker domain and nose cone helices when a

dynamic simulation is performed. The secondary structure data confirmed this long-effect communication due to structural changings at the level of key protein region during DNA rotation.

Far to consider the molecular simulation a defined tridimentional structure, it is quite interesting to observe that the major conformational changes occur in the two region that are supposed to be very important in the control of strand rotation. The biochemical data of the R434A mutant such as high ionic strength optimum and the ability to relax faster posituve supercoils, are in reasonable agreement with the altered structures.

All these data suggest that the *hinge* region could be indeed a topological sensor correlating the linker with the N-terminal domains during the strand rotation mechanism.

6. REFERENCES

[1] Boles TC, White JH, Cozzarelli NR. Structure of plectonemically supecoiled DNA. (1990) *J Mol Biol.* Jun 20; **213**(4):931-51;

[2] Mirkin SM. DNA Topology: Fundamentals. (2001) *Nature Publishing Group,* www.els.net;

[3] Bliska JB, Cozzarelli NR. Use of site-specific recombination as a probe of DNA structure and metabolism in vivo (1987) *J Mol Biol* Mar 20; **194**(2):205-18;

[4] Zacharias W, Jawoski A, Larson JE, Wells RD. The B- to Z-DNA equilibrium in vivo is pertubed by biological processes. (1988) *Proc Natl Acad Sci U.S.A.* Oct;**85**(19):7069-73;

[5] McClellan JA, Boublikova P, Palecek E, Lilley DM. Superhelical torsion in cellular DNA responds directly to environmental and genetic factors. (1990) *Proc Natl Acad Sci U.S.A* Nov;**87**(21):8373-7;

[6] Dayn A, Malkhosyan S, duzhy D, Lyamichev V, Panchenko Y, Mirkin S. Formation of (dA-dT)n cruciforms in Escherichia coli cells under different environmental conditions. (1991) *J. Bacteriol.* Apr;**173**(8):2658-64;

[7] Glaubiger D, Hearst JE. Effect of superhelical structure on the secondary structure of DNA rings (1967) *Biopolymers*. **5**(8):691-6;

[8] Wang JC. Variation of the average rotation angle of the DNA helix and the superhelical turns of covalently closed cyclic lambda DNA. (1969) *J Mol Biol.* Jul 14;**43**(1):25-39;

[9] Depew DE, Wang JC. Conformational fluctuations of DNA helix. (1975). *Proc Natl Acad Sci U.S.A.* Nov;**72**(11):4275-9;

[10] Keller W. Determination of the number of superhelical turns in simian virus 40 DNA by gel electrophoresis. (1975) *Proc Natl Acad Sci U.S.A.* Dec;72(12):4876-80;

[11] Wang JC Interaction between DNA and an Escherichia coli protein omega (1971) *J Mol Biol* Feb 14;**55**(3):523-33;

[12] Bidnenko V, Ehrlich SD, Janniere L In vivo relations between pAMbeta1-encoded type I topoisomerase and plasmid replication (1998) *Mol Microbiol* Jun;**28**(5):1005-16;

[13] Champoux JJ. DNA topoisomerases: structure, function and mechanism (2001). *Annu Rev Biochem* **70**:369-413;

[14] Timsit Y. Local sensing of global DNA topology: from crossover geometry

to type II topoisomerase processivity. (2011). *Nucleic Acids Res*. Nov 1;39(**20**):8665-76;

[15] Wang JC. Cellular roles of DNA topoisomerases: a molecular perspective. (2002). *Nat Rev. Mol. Cell. Biol.* Jun;3(**6**):430-40;

[16] Redinbo MR, Champoux JJ, Hol WG. Structural insight into the function of type IB topoisomerases. (1999), *J Mol Biol* 292(**3**):685-96;

[17] Redinbo MR, Stewart L, Kuhn P, Champoux JJ, Hol WG. Crystal structures of human topoisomerase I in covalent and noncovalent complexes with DNA. (1998). *Science* 279(**5356**):1504-13;

[18] Mo YY, Wang C, Beck WT. A novel nuclear localization signal in human DNA topoisomerase I (2000). *J Biol Chem* 275(**52**):41107-13;

[19] Bharti AK, Olson MO, Kufe DW, Rubin EH. Identification of a nucleolin binding site in human topoisomerase I (1996). *J Biol Chem* 271(**4**):1993-7;

[20] Stewart L, Ireton GC, Parker LH, Madden KR, Champoux JJ. Biochemical and biophysical analyses of recombinant forms of human topoisomerase I. (1996). *J Biol Chem* 271(**13**):7593-601;

[21] Palle K, Pattarello L, van der Merwe M, Losasso C, Benedetti P, Bjornsti MA. Disulfide cross-links reveal conserved features of DNA topoisomerase I architecture and a role for the N terminus in clamp closure (2008). *J Biol Chem* 283(**41**):27767-75;

[22] Haluska P Jr, Rubin EH. A role for the amino terminus of human topoisomerase I (1998). *Adv Enzyme Regul* **38**:253-62;

[23] Leppard JB, Champoux JJ. Human DNA topoisomerase I: relaxation, roles, and damage control (2005). *Chromosoma* 114(**2**):75-85;

[24] Redinbo MR, Campoux JJ, Hol WG., Novel insights into catalytic mechanism from a crystal structure of human topoisomerase I in complex with DNA. (2000) *Biochemistry* 39(**23**):6832-40;

[25] Chillemi G, Fiorani P, Benedetti P, Desideri A. Protein concerted motions in the DNA-human topoisomerase I complex. (2003) *Nucleic Acids Res.* 31(**5**):1525-35;

[26] Chrencik JE, Staker BL, Burgin AB, Pourquier P, Pommier Y, Stewart L, Redinbo MR. Mechanisms of camptothecin resistance by human topoisomerase I mutations (2004) *J Mol Biol,* 339(**4**):773-84;

[27] Stewart L, Ireton GC, Champoux JJ. Reconstitution of human topoisomerase I by fragment complementation (1997), *J Mol Biol,* 269(**3**):355-72;

[28] Stewart L, Ireton GC, Champoux JJ. A functional linker in human topoisomerase I is required for maximum sensitivity to camptothecin in a DNA relaxation assay (1999). *J Biol Chem* 274(**46**):32950-60;

[29] Fiorani P, Amatruda JF, Silvestri A, Butler RH, Bjornsti MA, Benedetti P. Domain interactions affecting human DNA topoisomerase I catalysis and camptohecin sensitivity. (1999) *Mol Pharmacol* 56(**6**):1105-15;

[30] Fiorani P, Bruselles A, Falconi M, Chillemi G, Desideri A, Benedetti P. Single mutation in the linker domain confers protein flexibility and camptothecin resistance to human topoisomerase I. (2003) *J Biol Chem* 278(**44**):43268-75;

[31] Losasso C, Cretaio E, Palle K, Pattarello L, Bjornsti MA, Benedetti P. Alterations in linker flexibility suppress DNA topoisomerase I mutant-induced cell lethality. (2007) *J Biol Chem* ;282(**13**):9855-64;

[32] Chillemi G, Castrignanò T, Desideri A. Structure and hydration of the DNA-human topoisomerase I covalent complex (2001) *Biophys J* 81(**1**):490-500;

[33] Stewart L, Redinbo MR, Qiu X, Hol WG, Champoux JJ. A model for the mechanism of human topoisomerase I (1998), *Science* 279(**5356**):1534-41;

[34] Champoux JJ DNA topoisomerase I-mediated nicking of circular duplex DNA (2001) *Methods Mol Biol* **95**:81-7;

[35] Koster DA, Croquette V, Dekker C, Shuman S, Dekker NH, Friction and torque govern the relaxation of DNA supercoils by eukaryotic topoisomerase IB (2005), *Nature*, 434(**7033**):671-4;

[36] Confalonieri F, Elle C, Nadal M, de La Tour C, Forterre P, Duguet M. Reverse gyrase: a helicase-like domain and a type I topoisomerase in the same polypeptide (1993), *Proc Natl Acad Sci U.S.A.* 90(**10**):4753-7;

[37] Shibata T, Nakasu S, Yasui K, Kikuchi A, Intrinsic DNA-dependent ATPase activity of reverse gyrase (1987) *J Biol Chem,* 262(**22**):10419-21;

[38] Jaxel C, Bouthier de la Tour C, Duguet M, Nadal M. Reverse gyrase gene from Sulfolobus shibatae B12: gene structure, transcription unit and comparative sequence analysis of the two domains. (1996) *Nucleic Acids Res* 24(**23**):4668-75;

[39] Nadal M, Mirambeau G, Forterre P, Reiter W-D, Duguet M, Positively supercoiled DNA in a virus-like particle of an archaebacterium, (1986) *Nature* **321**:256-258;

[40] Nadal M. Reverse gyrase: An insight into the role of DNA-topoisomerases

(2007) *Biochemie* 89(**4**):447-55;

[41] Bouthier de la Tour C, Portemer C, Huber R, Forterre P, Duguet M Reverse gyrase in thermophilic eubacteria (1991) *J Bacteriol,* 173(**12**):3921-3;

[42] Jaxel C, Nadal M, Mirambeau G, Forterre P, Takahashi M, Duguet M, Reverse gyrase binding to DNA alters the double helix structure and produces single-strand cleavage in the absence of ATP (1989) *EMBO J* 8(**10**):3135-9;

[43] Rodriguez AC, Stock D Crystal structure of reverse gyrase: insights into the positive supercoiling of DNA. (2002) *EMBO J* 21(**3**):418-26;

[44] Dèclais AC, Marsault J, Confalonieri F, de La Tour CB, Duguet M, Reverse gyrase, the two domains intimately cooperate to promote positive supercoiling. (2000) *J Biol Chem,* 275(**26**):19498-504;

[45] Capp C, Qian Y, Sage H, Huber H, Hsieh TS, Separate and combined biochemical activities of the subunits of a naturally split reverse gyrase (2010) *J Biol Chem* 285(**51**):39637-45;

[46] Lòpez-Garcia P, Forterre P, Control of DNA topology during thermal stress in hyperthermophilic archaea: DNA topoisomerase levels, activities and induced thermotolerance during heat and shock in Sulfolobus (1999), *Mol Microbiol* 33(**4**):766-77;

[47] Christensen MO, Krokowski RM, Barthelmes HU, Hock R, Boege F, Mielke C, Distinct effects of topoisomerase I and RNA polymerase I inhibitors suggest a dual mechanism of nucleolar/nucleoplasmic partitioning of topoisomerase I (2004) *J Biol Chem* 279(**21**):21873-82;

[48] Leppard JB, Champoux JJ Human DNA topoisomerase I: relaxation, roles, and damage control (2005) *Chromosoma* 114(**2**):75-85;

[49] Mao Y, Mehl IR, Muller MT, Subnuclear distribution of topoisomerase I is linked to ongoing transcription and p53 status (2002) *Proc Natl Acad Sci U.S.A.* 99(**3**):1235-40;

[50] Søe K, Dianov G, Nasheuer H,P, Bohr V,A, Grosse F, Stevnsner T, A human topoisomerase I cleavage complex is recognized by an additional human topoisomerase I molecule *in vitro* (2001) *Nucleic Acids Res,* 29(**15**): 3195–3203;

[51] Søe K, Hartmann H, Schlott B, Stevnsner T, Grosse F The tumor suppressor protein p53 stimulates the formation of the human topoisomerase I double cleavage complex in vitro (2002) *Oncogene* 21(**43**):6614-23;

[52] Christensen MO, Barthelmes HU, Boege F, Mielke C, The N-terminal domain anchors human topoisomerase I at fibrillar centers of nucleoli and nucleolar organizer regions of mitotic chromosomes (2002) *J Biol Chem* 277(**39**):35932-8;

[53] Shaiu WL, Hsieh TS Targeting to transcriptionally active loci by the hydrophilic N-terminal domain of Drosophila DNA topoisomerase I (1998) *Mol Cell Biol* 18(**7**):4358-67;

[54] Bermejo R, Doksani Y, Capra T, Katou YM, Tanaka H, Shirahige K, Foiani M, Top1- and Top2-mediated topological transitions at replication forks ensure fork progression and stability and prevent DNA damage checkpoint activation (2007) *Genes Dev* 21(**15**):1921-36;

[55] Abdurashidova G, Radulescu S, Sandoval O, Zahariev S, Danailov MB, Demidovich A, Santamaria L, Biamonti G, Riva S, Falaschi A. Functional interactions of DNA topoisomerases with a human replication origin (2007) *EMBO J* 26(**4**):998-1009;

[56] Falaschi A, Abdurashidova G, Sandoval O, Radulescu S, Biamonti G, Riva Molecular and structural transactions at human DNA replication origins (2007) S. *Cell Cycle*. 6(**14**):1705-12;

[57] Park H, Sternglanz R, Identification and characterization of the genes for two topoisomerase I-interacting proteins from Saccharomyces cerevisiae. (1999) *Yeast* 15(**1**):35-41;

[58] Khopde S, Roy R, Simmons DT. The binding of topoisomerase I to T antigen enhances the synthesis of RNA-DNA primers during simian virus 40 DNA replication, (2008) *Biochemistry* 47(**36**):9653-60;

[59] Arlt MF, Glover TW Inhibition of topoisomerase I prevents chromosome breakage at common fragile sites (2010) *DNA Repair (Amst)* 9(**6**):678-89;

[60] Clower RV, Hu Y, Melendy T. Papillomavirus E2 protein interacts with and stimulates human topoisomerase I (2006) *Virology* 348(**1**):13-8;

[61] Hu Y, Clower RV, Melendy T. Cellular topoisomerase I modulates origin binding by bovine papillomavirus type 1 E1 (2006) *J Virol* 80(**9**):4363-71;

[62] Liu LF, Wang JC. Supercoiling of the DNA template during transcription *Proc Natl Acad Sci U.S.A.* (1987) 84(**20**):7024-7;

[63] Tsao YP, Wu HY, Liu LF. Transcription-driven supercoiling of DNA: direct biochemical evidence from in vitro studies. (1989) *Cell* 56(**1**):111-8;

[64] Avemann K, Knipper R, Koller T, Sogo JM. Camptothecin, a specific inhibitor of type I DNA topoisomerase, induces DNA breakage at replication forks (1988) *Mol Cell Biol* 8(**8**):3026-34;

[65] Wang JC. DNA topoisomerases. (1996) *Annu Rev Biochem* **65**:635-92;

[66] McClendon AK, Rodriguez AC, Osheroff N. Human topoisomerase IIalpha rapidly relaxes positively supercoiled DNA: implications for enzyme action ahead of replication forks. (2005) *J Biol Chem* 280(**47**):39337-45;

[67] Salceda J, Fernàndez X, Roca J. Topoisomerase II, not topoisomerase I, is the proficient relaxase of nucleosomal DNA. (2006). *EMBO J* 25(**11**):2575-83;

[68] Lebel M, Spillare EA, Harris CC, Leder P. The Werner syndrome gene product co-purifies with the DNA replication cmplex and interacts with PCNA and topoisomerase I. (1999). *J Biol Chem* 274(**53**):37795-9;

[69] Brill SJ, Sternglanz R. Transcription-dependent DNA supercoiling in yeast DNA topoisomerase mutants. (1988) *Cell* 54(**3**):403-11;

[70] Merino A, Madden KR, Lane WS, Champoux JJ, Reinberg D. DNA topoisomerase I is involved in both repression and activation of transcription. (1993) *Nature* 365(**6443**):227-32;

[71] Rossi F, Labourier E, Fornè T, Divita G, Derancourt J, Riou JF, Antoine E, Cathala G, Brunel C, Tazi J. Specific phosphorylation of SR proteins by mammalian DNA topoisomerase I. (1996) *Nature* 381(**6577**):80-2;

[72] Pommier Y, Kerrigan D, Hartman KD, Glazer RI. Phosphorylation of mammalian DNA topoisomerase I and activation by protein kinase C. (1990) *J Biol Chem* 265(**16**):9418-22;

[73] Yu D, Khan E, Khaleque MA, Lee J, Laco G, Kohlhagen G, Kharbanda S, Cheng YC, Pommier Y, Bharti A. Phosphorylation of DNA topoisomerase I by the c-Abl tyrosine kinase confers camptothecin sensitivity. (2004) *J Biol Chem* 279(**50**):51851-61;

[74] Anderson RD, Berger NA. International Commission for Protection Against Environmental Mutagens and Carcnogens. Mutagenicity and carcinogenicity of topoisomerase-interactive agents. (1994) *Mutat Res* 309(**1**):109-42;

[75] Rosenstein BS, Subramanian D, Muller MT. The involvement of topoisomerase I in the induction of DNA-protein crosslink's and DNA single-strand breaks in cells of ultraviolet irradiated human and frog cell lines. (1997) *Radiat Res,* 148(**6**):575-9;

[76] Bullock P, Champoux JJ, Botchan M. Association of crossover points with topoisomerase I cleavage sites: a model for nonhomologous recombination. (1985) *Science*, 230(**4728**):954-8;

[77] Zhu J, Schiestl RH. Human topoisomerase I mediates illegitimate

recombination leading to DNA insertion into the ribosomal DNA locus in Saccharomyces cerevisiae. (2004). *Mol Genet Genomics* 271(**3**):347-58;

[78] Pourquier P, Pilon AA, Kohlhagen G, Mazumder A, Sharma A, Pommier Y. Trapping of mammalian topoisomerase I and recombination's induced by damaged DNA containing nicks or gaps. Importance of DNA end phosphorylation and camptothecin effects. (1997). *J Biol Chem* 272(**42**):26441-7;

[79] Castano IB, Brzoska PM, Sadoff BU, Chen H, Christman MF. Mitotic chromosome condensation in the rDNA requires TRF4 and DNA topoisomerase I in Saccharomyces cerevisiae. (1996) *Genes Dev* 10(**20**):2564-76;

[80] Losada A, Hirano T. Biology in pictures. New light on sticky sisters. (2000) *Curr Biol* 10(**17**):R615;

[81] Chen AY, Yu C, Gatto B, Liu LF. DNA minor groove-binding ligands: a different class of mammalian DNA topoisomerase I inhibitors. (1993) *Proc Natl Acad Sci U.S.A.* 90(**17**):8131-5;

[82] Hsiang YH, Hertzberg R, Hecht S, Liu LF. Camptothecin induces protein-linked DNA breaks via mammalian DNA topoisomerase I. (1985) *J Biol Chem* 260(**27**):14873-8;

[83] Muggia FM, Creaven PJ, Hansen HH, Cohen MH, Selawry OS. Phase I clinical trial of weekly and daily treatment with camptothecin (NSC-100880): correlation with preniclinical studies. (1972) *Cancer Chemother Rep* 56(**4**):515-21;

[84] Gottlieb JA, Guarino AM, Call JB, Oliviero VT, Block JB. Preliminary pharmacologic and clinical evaluation of camptothecin sodium (NSC-100880). (1970) *Cancer Chemother Rep* 54(**6**):461-70;

[85] Drawl MN, Agama K, Wakelin LP, Pommier Y, Griffith R. Exploring DNA topoisomerase I ligand space in search of novel anticancer agents. (2011). *Plos one* 6(**9**):e25150;

[86] Eng WK, Faucette L, Johnson RK, Sternglanz R. Evidence that DNA topoisomerase I is necessary for the cytotoxic effects of camptothecin. (1988) *Mol Pharmacol* 34(**6**):755-60;

[87] Wang JC. DNA topoisomerase. New break for archaeal enzyme. (1997). *Nature* 386(**6623**):329-331;

[88] Kingsbury WD, Boehm JC, Jakas DR, Holden KG, Hecht SM, Gallagher G, Caranfa MJ, McCabe FL, Faucette LF, Johnson RK et al. Synthesis of water-soluble (aminoalkyl)camptothecin analogues: inhibition of topoisomerase I and antitumor activity. (1991) *J Med Chem* 34(**1**):98-107;

[89] Pommier Y, Barcelo JM, Rao VA, Sordet O, Jobson AG, Thibaut L, Miao ZH, Seiler JA, Zhang H, Marchand C, Agama K, Nitiss JL, Redon C. Repair of topoisomerase I-mediated DNA damage (2006) *Prog Nucleic Acid Res Mol Biol* **81**:179-229;

[90] Priel E, Showalter SD, Blair DG Inhibition of human immunodeficiency virus (HIV-1) replication in vitro by noncytotoxic doses of camptothecin, a topoisomerase I inhibitor. (1991) *AIDS Res Hum Retroviruses* 7(**1**):65-72;

[91] Pommier Y, Redon C, Rao VA, Seiler JA, Sordet O, Takemura H, Antony S, Meng L, Liao Z, Kohlhangen G, Zhang H, Kohn KW. Repair of and checkpoint response to topoisomerase I-mediated DNA damage. (2003) *Mutat Res* 532(**1-2**):173-203;

[92] Horwitz SB, Chang CK, Grollman AP. Studies on camptothecin. I. Effects of nucleic acid and protein synthesis (1971) *Mol Pharmacol* 7(**6**):632-44;

[93] Holm C, Covey JM, Kerrigan D, Pommier Y. Differential requirement of DNA replication for the cytotoxicity of DNA topoisomerase I and II inhibitors in Chinese hamster DC3F cells. (1989) *Cancer Res* 49(**22**):6365-8;

[94] Staker BL, Feese MD, Cushman M, Pommier Y, Zembower D, Stewart L, Burgin AB, Structure of three classes of anticancer agents bound to the human topoisomerase I-DNA covalent complex. (2005) *J Med Chem* 48(**7**):2336-45;

[95] Adams VR, Burke TG Camptothecin in cancer therapy. Cancer Drug Discovery&Development (2005) *Humana Press*;

[96] Pommier Y, Topoisomerase I inhibitors: camptothecins and beyond. *Nat Rev Cancer* (2006) 6(**10**):789-802;

[97] Marchand C, Antony S, Kohn KW, Cushman M, Ioanoviciu A, Staker BL, Burgin AB, Stewart L, Pommier Y. A novel norindenoisoquinoline structure reveals a common interfacial inhibitor paradigm for ternary trapping of the topoisomerase I-DNA covalent complex. (2006) *Mol Cancer Ther* 5(**2**):287-95;

[98] Pommier Y, Pourquier P, Urasaki Y, Wu J, Laco GS. Topoisomerase I inhibitors: selectivity and cellular resistance. (1999) *Drug Resist Updat* 2(**5**):307-318;

[99] Goldwasser F, Shimizu T, Jackman J, Hoki Y, O'ConnorPM, Kohn KW, Pommier Y. Correlations between S and G2 arrest and the cytotoxicity of camptothecin in human colon carcinoma cells. (1996) *Cancer Res* 56(**19**):4430-7;

[100] Hsiang YH, Lihou MG, Liu LF. Arrest of replication forks by drug-stabilized topoisomerase I-DNA cleavable complexes as a mechanism of cell killing by camptothecin. (1989) *Cancer Res* 49(**18**):5077-82;

[101] Hsiang YH, Liu LF, Wall ME, Wani MC, Nicholas AW, Manikumar G, Kirschenbaum S, Silber R, Potmesil M. DNA topoisomerase I-mediated DNA cleavage and cytotoxicity of camptothecin analogues. (1989) *Cancer Res* 49(**16**):4385-9;

[102] Zhou Y, Gwadry FG, Reinhold WC, Miller LD, Scherf U, Liu ET, Kohn KW, Pommier Y, Weinstein JN. Transcriptional regulation of mitotic genes by camptothecin-induced DNA damage: microarray analysis of dose- and time-dependent effects. (2002) *Cancer Res* 62(**6**):1688-95;

[103] Nitiss JL, Wang JC. Mechanism of cell killing by drugs that trap covalent complexes between DNA topoisomerases and DNA. (1996) *Mol Pharmacol* 50(**5**):1095-102;

[104] Strumberg D, Pilon AA, Smith M, Hickey R, Malkas L, Pommier Y. Conversion of topoisomerase I cleavage complexes on the leading strand of ribosomal DNA into 5'-phosphorylated DNA double-strand breaks by replication runoff. (2000) *Mol Cell Biol* 20(**11**):3977-87;

[105] Shao RG, Cao CX, Zhang H, Kohn KW, Marc SW, Pommier Y Replication-mediated DNA damage by camptothecin induces phosphorylation of RPA by DNA-dependent protein kinase and dissociates RPA:DNA-PK complexes. (1999) *The EMBO Journal* **18**, 1397 – 1406;

[106] Simbulan-Rosenthal CM, Rosenthal DS, Boulares AH, Hickey RJ, Malkas LH, Coll JM, Smulson ME. Regulation of the expression or recruitment of components of the DNA synthesome by poly(ADP-ribose) polymerase. (1998) *Biochemistry* 37(**26**):9363-70;

[107] Staron K, Kowalska-Loth B, Nieznanski K, Szumiel I. Phosphorylation of topoisomerase I in L5178Y-S cells is associated with poly(ADP-ribose) metabolism. (1996) *Carcinogenesis* 17(**3**):383-7;

[108] Plo I, Liao ZY, Barcelò JM, Kohlhangen G, Caldecott KW, Weinfeld M, Pommier Y. Association of XRCC1 and tyrosyl DNA phosphodiesterase (Tdp1) for the repair of topoisomerase I-mediated DNA lesions. (2003). *DNA Repair (Amst)* 2(**10**):1087-100;

[109] Pommier Y, Jenkins J, Kohlhagen G, Leteurtre F. DNA recombinase activity of eukaryotic DNA topoisomerase I: effects of camptothecin and other inhibitors. (1995) *Mutat Res* 337(**2**):135-45;

[110] Cheng C, Shuman S. Recombinogenic flap ligation pathway for intrinsic repair of topoisomerase IB-induced double-strand breaks. (2000) *Mol Cell Biol* 20(**21**):8059-68;

[111] Sordet O, Khan QA, Kohn KW, Pommier Y. Apoptosis induced by topoisomerase inhibitors. (2003). *Curr Med Chem Anticancer Agents* 3(**4**):271-90;

[112] Goldwasser F, Bae I, Valenti M, Torres K, Pommier Y. Topoisomerase I-related parameters and camptothecin activity in the colon carcinoma cell lines from the National Cancer Institute anticancer screen. (1995) *Cancer Res* 55(**10**):2116-21;

[113] Beidler DR, Cheng YC. Camptothecin induction of a time- and concentration –dependent decrease of topoisomerase I and its implication in camptothecin activity. (1995). *Mol Pharmacol* 47(**5**):907-14;

[114] Desai SD, Liu LF, Vazquez-Abad D, D'Arpa P. Ubiquitin-dependent destruction of topoisomerase I is stimulated by the antitumor drug camptothecin. (1997) *J Biol Chem* 272(**39**):24159-64;

[115] Fu Q, Kim SW, Chen HX, Grill S, Cheng YC. Degradation of topoisomerase I inhibitors is dependent on inhibitor structure but independet of cell death. (1999) *Mol Pharmacol* 55(**4**):677-83;

[116] Mao Y, Desai SD, Liu LF. SUMO-1 conjugation to human DNA topoisomerase II isozymes. (2000) *J Biol Chem* 275(**34**):26066-73;

[117] Mao Y, Sun M, Desai SD, Liu LF. SUMO-1 conjugation to topoisomerase I: A possible repair response to topoisomerase-mediated DNA damage (2000). *Proc Natl Acad Sci U.S.A.* 97(**8**):4046-51;

[118] Desai SD, Mao Y, Sun M, Li TK, Wu J, Liu LF. Ubiquitin, SUMO-1, and UCRP in camptothecin sensitivity and resistance. (2000) *Ann N Y Acad Sci* 922:306-8;

[119] Mo YY, Yu Y, Shen Z, Bech WT. Nucleolar delocalization of human topoisomerase I in response to topotecan correlates with sumoylation of the protein. (2002) *J Biol Chem* 277(**4**):2958-64;

[120] Ma J, Maliepaard M, Nooter K, Loos WJ, Kolker HJ, Verweij J, Stoter G, Schellens JH. Reduced cellular accumulation of topotecan: a novel mechanism of resistance in human ovarian cancer cell line. (1998). *Br J Cancer* 77(**10**):1645-52;

[121] Goto T, Wang JC. Cloning of yeast TOP1, the gene encoding DNA topoisomerase I, and construction of mutants defective in both DNA topoisomerase I and DNA topoisomerase II. (1985) *Proc Natl Acad Sci U.S.A.* 82(**21**):7178-82;

[122] van Waardenburg RCAM and Bjornsti M.A. Biochemical and genetic analyses of DNA topoisomerase I-mediated DNA damage (2005) *Ed. T. Burke. Humana Press* "Camptothecin in cancer therapy";

[123] Nitiss J, Wang JC. DNA topoisomerase-targeting untitumor drugs can be studied in yeast (1988). *Proc Natl Acad Sci U.S.A.* 85(**20**):7501-5;
[124] Bjornsti MA, Benedetti P, Vigilanti GA, Wang JC. Expression of human DNA topoisomerase I in yeast cells lacking yeast DNA topoisomerase I: restoration of sensitivity of the cells to the antitumor drug camptothecin. (1989) *Cancer Res* 49(**22**):6318-23;

[125] Alsner J, Svejstrup JQ, Kieldsen E, Sørensen BS, Westergaard O. Identification of an N-terminal domain of eukaryotic DNA topoisomerase I dispensable for catalytic activity but essential for in vivo function. (1992) *J Biol Chem* 267(**18**):12408-11;

[126] Colley WC, van der Merwe M, Vance JR, Burgin AB Jr, Bjornsti MA. Substitution of conserved residues within the active site alters the cleavage religation equilibrium of DNA topoisomerase I. (2004) *J Biol Chem* 279(**52**):54069-78;

[127] Staker BL, Hjerrild K, Feese MD, Behnke CA, Burgin AB Jr, Stewart L. The mechanism of topoisomerase I poisoning by camptothecin analog. (2002) *Proc Natl Acad Sci U.S.A.* 99(**24**):15387-92;

[128] Kubota N, Kanzawa F, Nishio K, Takeda Y, Ohmori T, Fujiwara Y, Terashima Y, Saijo N. Detection of topoisomerase I gene point mutation in CPT-11 resistant lung cancer cell line (1992) *Biochem Biophys Res Commun*. Oct 30;188(**2**):571-7;

[129] Losasso C, Cretaio E, Fiorani P, D'Annessa I, Chillemi G, Benedetti P. A single mutation in the 729 residue modulates human DNA topoisomerase IB DNA binding and drug resistance. (2008) *Nucleic Acids Res* 36(**17**):5635-44;

[130] Chillemi G, Fiorani P, Castelli S, Bruselles A, Benedetti P, Desideri A. Effect on DNA relaxation of the single Thr718Ala mutation in human topoisomeraseI: a functional and molecular dynamics study, *Nucleic Acids Res*. (2005), 33(**10**):3339-50;

[131] Koster DA, Palle K, Bot ES, Bjornsti MA, Dekker NH, Antitumour drugs impede DNA uncoiling by topoisomerase I (2007) *Nature* 448(**7150**):213-7;

[132] Sari L, Andricioaei I. Rotation of DNA around intact strand in human topoisomerase I implies distinct mechanisms for positive and negative supercoil relaxation (2005) *Nucleic Acids Res.* 33(**20**):6621-34;

[133] Chillemi G, Redinbo M, Bruselles A, Desideri A. Role of the linker domain and the 203-214 N-terminal residues in the human topoisomerase I DNA complex dynamics. (2004) *Biophys J* 87(**6**):4087-97;

[134] Frøhlich RF, Veigaard C, Andersen FF, McClendon AK, Gentry AC, Andersen AH, Osheroff N, Stevnsner T, Knudsen BR; Tryptophane-205 of human topoisomerase I is essential for camptothecin inhibition of negative but not positive supercoil removal. (2007) *Nucleic Acids Res.* 35(**18**):6170-80;
[135] Woo MH, Losasso C, Guo H, Pattarello L, Benedetti P, Bjornsti MA. Locking the DNA topoisomerase I protein clamp inhibits DNA rotation and induces cell lethality (2003) *Proc Natl Acad Sci U S A.* 100(**24**):13767-72;

[136] Bjornsti MA, Wang JC. Expression of yeast DNA topoisomerase I can complement a conditional-lethal DNA topoisomerase I mutation in Escherichia coli. (1987) *Proc Natl Acad Sci U S A.* 84(**24**):8971-5;

[137] Dyballa N, Metzger S. Fast and sensitive colloidal coomassie G-250 staining for proteins in polyacrylamide gels. (2009) *J Vis Exp* (**30**). pii: 1431. doi: 10.3791/1431;

[138] Valenti A, Perugino G, D'Amaro A, Cacace A, Napoli A, Rossi M, Ciaramella M. Dissection of reverse gyrase activities: insight into the evolution of a thermostable molecular machine (2008) *Nucleic Acids Research* 36(**14**):4587-4597;

[139] Clarke JD. DNA Topoisomerases: Methods and Protocols (2009) *Humana Press*;

[140] Knab AM, Fertala J, Bjornsti MA. A camptothecin-resistant DNA topoisomerase I mutant exhibit altered sensitivities to other DNA topoisomerase poisons. (1995). *J Biol Chem*, 270(**11**):6141-8;

[141] Knab AM, Fertala J, Bjornsti MA. Mechanism of camptothecin resistance in yeast DNA topoisomerase I mutants. (1993) *J Biol Chem,* 268(**30**):22322-30;

[142] Lisby M, Olesen JR, Skouboe C, Krogh BO, Straub T, Boege F, Velmurugan S, Martensen PM, Andersen AH, Jayaram M, Westergaard O, Knudsen BR. Residues within the N-terminal domain of human topoisomerase I play a direct role in relaxation. (2001) *J Biol Chem* 276(**23**):20220-7;

[143] Kauh EA, Bjornsti MA. SCT1 mutants suppress the camptothecin sensitivity of yeast cells expressing wild-type DNA topoisomerase I. (1995) *Proc Natl Acad Sci U. S. A.* 92(**14**):6299-303;

[144] Tobey RA. Effects of cytosine arabinoside, daunomycin, mithramycin, azacytidine, adriamycin, and camptothecin on mammalian cell cycle traverse. (1972). *Cancer Res* 32(**12**):2720-5;

[145] D'Arpa P, Beardmore C, Liu LF. Involvement of nucleic acid synthesis in

cell killing mechanisms of topoisomerase poisons. (1990) *Cancer Res* 50(**21**):6919-24;

[146] Fiorani P, Tesauro C, Mancini G, Chillemi G, D'Annessa I, Graziani G, Tentori L, Muzi A, Desideri A. Evidence of the crucial role of the linker domain on the catalytic activity of human topoisomerase I by experimental and simulative characterization of the Lys681Ala mutant. (2009) *Nucleic Acids Res* 37(**20**):6849-58;

[147] Megonigal MD, Fertala J, Bjornsti MA. Alterations in the catalytic activity of yeast DNA topoisomerase I result in cell cycle arrest and cell death. (1997). *J Biol Chem* 272(**19**):12801-8;

[148] Pommier Y. DNA Topoisomerases and Cancer (2011) *Humana Press*;

[149] Fiorani P, Bruselles A, Falconi M, Chillemi G, Desideri A, Benedetti P. Single mutation in the linker domain confers protein flexibility and camptothecin resistance to Human Topoisomerase I (2003) *J Biol Chem* 278(**44**):43268-75.